

THE BRICKS WE LAY: PURSUING A PLAGUE GENOME FROM
FIRST PANDEMIC TURKEY AND THE REALITIES OF ANCIENT
DNA

THE BRICKS WE LAY: PURSUING A PLAGUE GENOME FROM FIRST
PANDEMIC TURKEY AND THE REALITIES OF ANCIENT DNA

By REN DELA CRUZ MANALO, Hon. B.Sc.

A Thesis Submitted to the School of Graduate Studies in Partial Fulfilment of
the Requirements for the Degree Master of Arts

McMaster University MASTER OF ARTS (2024) Hamilton, Ontario
(Anthropology)

TITLE: The Bricks We Lay: Pursuing a Plague Genome from First Pandemic
Turkey and the Realities of Ancient DNA

AUTHOR: Ren Dela Cruz Manalo. H. B.Sc. (University of Toronto)

SUPERVISOR: Dr. Hendrik Poinar

NUMBER OF PAGES: ix, 137

Abstract

Conclusive genomic and historical analysis of the first plague pandemic is remarkably diminutive due to a lack of associated archaeological evidence. Genomic research has established the presence of *Yersinia pestis* in Central Asia during the late 2nd century, as well as in England, France, Germany, and Spain in the 6th through 8th centuries. Considering the state of the scholarship that uses written sources to construct plague's history, the first pandemic's debated transmission from Central Asia towards the Mediterranean, demands further scientific analysis and careful interdisciplinary contextualization. As stressed in the historiography, a central region in the history of the first plague pandemic is Turkey, though there is not yet any genomic evidence that places first-pandemic plague there.

This study analyzed 134 human teeth from sites in northern and northwestern Turkey in efforts to derive the first Northeastern Mediterranean *Y. pestis* genome for the first plague pandemic.

The study successfully identified one individual who died with detectable levels of *Yersinia pestis* in their bloodstream; this individual will later undergo enrichment to increase the pathogenic portion of the extract. One individual demonstrated significant levels of *hepatitis B virus* and other individuals had detectable levels of *Mycobacterium tuberculosis*. All the remains yielded very little endogenous content indicating poor overall preservation.

Plague studies have been historically defined by a system created to generate and answer primarily Eurocentric questions. Although a single novel genome from Turkey cannot completely answer the many debates associated with the first plague pandemic, it does alter the geography of current *Y. pestis* discoveries which remain restricted to western European sites. It would also serve to highlight the necessity for a wider geographic sampling range and more interdisciplinary analysis. This study also comments on the understated realities of ancient DNA and the necessity for a push in ethical decision-making in the field.

Acknowledgements

First, I would like to extend my gratitude to my supervisor, Dr. Hendrik Poinar, for his guidance and continuous support over the last two years. Thank you for granting me the opportunity to traverse such a ground-breaking field and building my confidence as both a student and a researcher. I would also like to thank my committee member, Dr. Timothy Newfield, for helping us contextualize our findings with new perspectives. Your knowledge of the first pandemic and its associated histories have been invaluable throughout this project. I would also like to extend my sincere thanks to Dr. Nükhet Varlik for being my third reader for this thesis.

This thesis would not have been possible without the continuous help from the members of the Poinar Lab. Thanks to Adiya, MH, and Jess for their encouragement and conversation in 412. Special thanks as well to Tess and Sina, who were always able to help trouble-shoot lab results with me. This thesis would have taken much longer without your expertise. I would also like to give special thanks to Mel, who spent long hours in-lab with me and pointed me in the right direction when I had questions. An especially warm thank you to Rav, who patiently trained me in-lab and with bioinformatics. Your knowledge of the field inspired me to work harder and your comments on the necessity of ethics opened my eyes to the need for change.

Thank you to the Anthro grad peeps, who encouraged me to write this thesis and finish all the quail eggs during our hotpot get-togethers. Thank you to members of Anthrohouse 1.0 for helping me find a place to call home in Hamilton: to Victoria for their uplifting conversation, discussions, and sourdough; to Toast, the best orange cat, for allowing me to know the importance of a lint roller; to Bob (Anthrohouse by association) for the welcome distractions and boundless reassurance; and to Kay, who has been a pillar of support, laughs, and friendship since the very beginning of this graduate journey.

Thank you to Ma, Tay, and Lorraine, as always, for your continued support and confidence. And to Lord Shiro Farquaad Jonathan Philip Horatio Perry Poot Royce III, thank you for always being available to listen and snuggle even when you would rather be taken out for walks.

Table of Contents

Abstract	ii
Acknowledgements	iii
List of Figures	vi
List of Tables	vii
List of Abbreviations and Symbols	viii
Declaration of Academic Achievement	ix
Chapter 1: Introduction	1
1.1 Introduction	1
1.2 <i>Yersinia pestis</i> and the Historical Plague Pandemics.....	2
1.3 Ancient DNA	5
1.4 The First Plague Pandemic: Current Genomes	8
1.4.1 <i>Aschheim, Germany</i>	10
1.4.2 <i>Altenerding, Germany</i>	10
1.4.3 <i>Edix Hill, United Kingdom</i>	11
1.4.4 <i>Lunel-Viel Quartier centrale, France</i>	12
1.4.5 <i>Saint-Doulchard Le Pressoir, France</i>	13
1.4.6 <i>Dittenheim, Germany</i>	14
1.4.7 <i>Petting, Germany</i>	14
1.4.8 <i>Unterthürheim, Germany</i>	14
1.4.9 <i>Valencia, Plaça de Almoína, Spain</i>	15
1.4.10 <i>Tian Shan Mountains, Kyrgyzstan</i>	15
1.5 The First Plague Pandemic: Current Debates	16
1.5.1 <i>Maximalist and Minimalist Platforms</i>	16
1.5.2 <i>Origins</i>	18
1.5.3 <i>Biasing Catastrophe</i>	19
1.6 Research Objectives.....	19
1.7 References	20
Chapter 2: Historical Background	27
2.1 The Ancient Mediterranean and Histories of the First Plague Pandemic	27
2.1.1 <i>Plague Historians</i>	27
2.1.2 <i>Waves of Plague in First Pandemic Histories</i>	32
2.2 Historical Sites in Study.....	35
2.2.1 <i>İznik Roman Theatre</i>	35
2.2.2 <i>Haydarpaşa Train Station</i>	36
2.2.3 <i>İznik Hisardere Necropolis</i>	36
2.2.4 <i>Ayasuluk</i>	37
2.2.5 <i>Agora of Smyrna</i>	38
2.2.6 <i>Metropolis</i>	39
2.2.7 <i>Perinthos</i>	39
2.2.8 <i>Priene</i>	40
2.2.9 <i>Kadıkalesi</i>	41
2.3 Silivri District Necropolis (BOTAŞ Excavation)	42
2.4 References	42
Chapter 3: Methods and Results	48
3.1 Introduction.....	48
3.2 Samples	48
3.2.1 <i>Sample Size</i>	48
3.2.2 <i>Ethics Approval</i>	51
3.3 Laboratory Procedures	52
3.3.1 <i>Subsampling</i>	52

3.3.2 aDNA Extraction	53
3.3.3 Inhibition Testing	55
3.3.4 PCR Assay	56
3.3.5 Double-stranded Library Preparation, aDNA Quantification, and Indexing.....	56
3.3.6 Pooling and Shotgun Sequencing.....	57
3.3.7 Radiocarbon Dating.....	57
3.4 Bioinformatic Analysis	58
3.4.1 Quality Control	58
3.4.2 Mapping to Reference Genomes	58
3.4.3 Pathogenic Confirmation and Visualization	59
3.5 Results: Historic Sites Sample Set	61
3.5.1 Preliminary <i>pla</i> Screening	61
3.5.2 Shotgun Data Analysis	62
3.5.3 Estimated Dates.....	68
3.6 Results: Silivri Excavation Sample Set.....	71
3.6.1 Preliminary <i>pla</i> Screening	71
3.6.2 Shotgun Data Analysis	74
3.6.3 Estimated Dates.....	78
3.7 References	80
Chapter 4: Discussion and Analysis	83
4.1 Historical Sites and Silivri Excavation Sample Sets.....	83
4.2 Positive Plague Sample.....	89
4.2.1 Preliminary Pathogenic Confirmation.....	89
4.2.2 Significance in First Pandemic Studies.....	98
4.3 Limitations of aDNA	98
4.4 References	102
Chapter 5: Conclusions and Future Directions	105
5.1 Summary	105
5.1.1 Ancient DNA: Realistic Expectations.....	105
5.1.2 Rejecting Eurocentrism in First Pandemic Studies.....	109
5.2 Future Research.....	116
5.3 References	118
Supplemental Tables and Figures	119

List of Figures

Chapter 3: Methods and Results	48
Figure 3.1 (a-c): Site Estimates.....	50
Figure 3.2 (a-b): Two methods of extraction.....	55
Figure 3.3 (a-b): Initial <i>pla</i> Screen of TFP39.....	62
Figure 3.4 (a-b): TFP13 mapped to the masked human reference genome hg38 (min35, MQ30).....	63
Figure 3.5 (a-d): TFP13 mapped to the <i>M. tuberculosis</i> reference genome (min35, MQ30).....	65
Figure 3.6 (a-d): TFP50 mapped to the <i>M. tuberculosis</i> reference genome (min35, MQ30).....	66
Figure 3.7 (a-d): TFP39 mapped to the hepatitis B virus reference genome.....	67
Figure 3.8 (a-d): TFP39 mapped to the hepatitis B virus genome X65257.1.....	68
Figure 3.9 (a-h): Calibrated radiocarbon dates for the Historical Sites sample set.....	71
Figure 3.10: Subsampling photos of tooth belonging to individual BFP39.....	72
Figure 3.11: <i>pla</i> Screening Amplification and Melt Curves for BFP39 extracts.....	73
Figure 3.12 (a-b): BFP55 mapped to the masked human reference genome hg38 (min35, MQ30).....	74
Figure 3.13 (a-d): BFP18 mapped to the <i>M. tuberculosis</i> reference genome (min35, MQ30).....	76
Figure 3.14 (a-d): BFP55 mapped to the <i>M. tuberculosis</i> reference genome (min35, MQ30).....	77
Figure 3.15 (a-d): BFP61 mapped to the <i>M. tuberculosis</i> reference genome (min35, MQ30).....	78
Figure 3.16 (a-c): Calibrated radiocarbon dates for the Silivri Excavation sample set.....	79
Chapter 4: Discussion and Analysis	83
Figure 4.1: Percentage of Endogenous Reads of Individuals Excavated in Turkey, Denmark, and the UK....	85
Figure 4.2: CS-BFP39 mapped to the <i>Y. pestis</i> reference genome (min35, MQ30).....	91
Figure 4.3 (a-d): ME-BFP39 mapped to the <i>Y. pestis</i> reference genome (min35, MQ30).....	92
Figure 4.4 (a-d): CS-BFP39 mapped to the <i>Y. pestis</i> reference genome (min30, MQ30).....	92
Figure 4.5 (a-d): ME-BFP39 mapped to the <i>Y. pestis</i> reference genome (min30, MQ30).....	93
Figure 4.6 (a-b): CS-BFP39 mapped to the masked human reference genome hg38 (min35, MQ30).....	94
Figure 4.7 (a-b): ME-BFP39 mapped to the masked human reference genome hg38 (min35, MQ30).....	95
Figure 4.8 (a-b): CS-BFP39 mapped to the masked human reference genome hg38 (min30, MQ30).....	95
Figure 4.9 (a-b): ME-BFP39 mapped to the masked human reference genome hg38 (min30, MQ30).....	96
Figure 4.10 (a-b): Krona visualization plots for BFP39 extracts showing the proportion of reads in the <i>Yersinia</i> genus.....	97
Chapter 5: Conclusions and Future Directions	105
Figure 5.1: Workflow of the proposed resin-casting subsampling method.....	113
Figure 5.2 (a-d): Experimentation with the resin-casting method.....	114
Supplemental Tables and Figures	119
Figure S5.1: TFP39 mapped to the masked human reference genome hg38 (min35, MQ30).....	129
Figure S5.2: TFP50 mapped to the masked human reference genome hg38 (min35, MQ30).....	130
Figure S5.3: BFP18 mapped to the masked human reference genome hg38 (min35, MQ30).....	130
Figure S5.4: BFP61 mapped to the masked human reference genome hg38 (min35, MQ30).....	131
Figure S5.5: Krona plot of TFP14 showing the proportion of reads in the <i>Yersinia</i> genus.....	132
Figure S5.6: Krona plot of TFP58 showing the proportion of virus reads. A.....	132
Figure S5.7: Krona plot of TFP06 showing the proportion of virus reads.....	133
Figure S5.8: Krona plot of TFP13 showing proportion of reads in the <i>M. tuberculosis</i> complex.....	133
Figure S5.9: Krona plot of TFP50 showing proportion of reads in the <i>M. tuberculosis</i> complex.....	134
Figure S5.10: Krona plot of TFP39 showing proportion of virus reads.....	134
Figure S5.11: Krona plot of CS-BFP39 showing proportion of reads in the <i>Yersinia</i> genus.....	135
Figure S5.12: Krona plot of ME-BFP39 showing proportion of reads in the <i>Yersinia</i> genus.....	135
Figure S5.13: Krona plot of BFP18 showing proportion of reads in the <i>M. tuberculosis</i> complex.....	136
Figure S5.14: Krona plot of BFP55 showing proportion of reads in the <i>M. tuberculosis</i> complex.....	136
Figure S5.15: Krona plot of BFP61 showing proportion of reads in the <i>M. tuberculosis</i> complex.....	137

List of Tables

Chapter 3: Methods and Results	48
Table 3.1: Number of Human Teeth Analyzed Per Site.	51
Table 3.2: Summary of Extracts with Evidence of Pathogens.....	60
Table 3.3: Cycle Amplification and Melt Peak values for BFP39 extracts.	73
Table 3.4: Summary of BFP39 Extracts.	73
Supplemental Tables and Figures	119
Table S5.1: Overview of samples processed from historical sites in Turkey.	120
Table S5.2: Overview of samples processed from the Silivri District Necropolis.	122
Table S5.3: Bioinformatic overview of samples from historical sites and the Silivri District Necropolis.....	125
Table S5.4: Endogenous content of remains from second pandemic Denmark.	127
Table S5.5: Endogenous content of remains from second pandemic UK.....	128

List of Abbreviations and Symbols

aDNA – ancient DNA

BLAST – Basic Local Alignment Search Tool

bwa – Burrows-Wheeler aligner

DNA – deoxyribonucleic acid

GIS – geographic information system(s)

HTML – Hypertext Markup Language

MQ – Mapping Quality

PCR – polymerase chain reaction

pla – plasminogen activator gene

qPCR – quantitative polymerase chain reaction

RNA – ribonucleic acid

rRNA – ribosomal RNA

SNP – single nucleotide polymorphism

Declaration of Academic Achievement

I, Ren Claire Dela Cruz Manalo, declare this thesis to be my own work. No part of this document has been published, submitted for publication, or submitted for a degree at another institution.

The archaeological sample set was provided by Dr. Vedat Onar (Istanbul University). Radiocarbon dating was conducted by the W. M. Keck Carbon Cycle Accelerator Mass Spectrometer (KCCAMS) Facility at the University of California, Irvine. I conducted all laboratory work for the sample sets included in this thesis with guidance from Ravneet Sidhu, Melanie Kuch, Dr. Sina Baleka, and Dr. Hendrik Poinar. I performed bioinformatic analysis with assistance from Ravneet Sidhu and Tess Wilson. Endogenous content of this sample set was compared to unpublished work conducted by Ravneet Sidhu and Katherine Eaton in the McMaster Ancient DNA Centre. Animal remains for methodological testing was provided by Christine Cluney in the department of Anthropology at McMaster University. The structure of this thesis was designed in consultation with my committee, Dr. Hendrik Poinar (McMaster University) and Dr. Timothy Newfield (Georgetown University), who contributed to its drafts. Dr. Nükhet Varlık (Rutgers University) served as the third reader for this thesis.

Chapter 1: Introduction

1.1 Introduction

The bacterium *Yersinia pestis* has been identified as the primary cause of each of the historical plague pandemics (Yersin, 1894; Bos *et al.*, 2011; Wagner *et al.*, 2014; Spyrou *et al.*, 2019). Until quite recently, evidence for ancient and medieval plague outbreaks was strictly derived from written and archeological sources. However, with recent advancements in targeted enrichment coupled with high-throughput sequencing methods over the last 15 years, it has become possible to not only recover ancient pathogen DNA, but also to effectively reconstruct plague genomes (Duchene *et al.*, 2020). Compared to subsequent plague pandemics, evidence attributable to the first plague pandemic, which historically began in the 6th century CE and continued until at least the 8th century CE, is relatively scarce (Stathakopoulos 2004; Morony 2007). As such, modern academic scholarship on the first plague pandemic offers more hypotheses than facts and tends to rely on assumptions, some of which have come to fuel intergenerational debates about the origins, cause(s), and demographic impact of late antique plague. Over recent years, genomic evidence has become instrumental to some of these debates. Yet, at the time of writing, all published first plague pandemic genomes have been recovered from European locations with a single basal genome from Central Asia, with possibly none corresponding directly to historical accounts of plague. One narrative primarily involves repeated ‘waves’ of plague spreading westward from Central Asia where recent genomes have been retrieved, seeding reservoirs in Europe from which subsequent outbreaks emerged. Yet another narrative has the first pandemic emerging from East Africa after having arrived there earlier from Central Asia (Sarris 2002, Green 2015; Harper 2017; Newfield 2018; Keller,

Spyrou, and McCormick *et al.*, 2019; Sarris 2022). This diversity of opinion on such a seemingly elementary component of the pandemic's history underscores that more data are very much needed. To help settle debates about the origins and early geography of the first pandemic, this thesis hopes to contribute to our integration of current historical, archaeological, and genomic evidence by presenting evidence for *Y. pestis* in late antiquity.

1.2 *Yersinia pestis* and the Historical Plague Pandemics

As mentioned, *Y. pestis* is the causative agent of plague, an infectious zoonotic disease that typically results in the swelling of lymph nodes due to rapid bacterial replication. Plague is primarily a disease of sylvatic rodents and typically transmitted by fleas to other rodents. Examples of modern susceptible rodent populations include rats, marmots, and prairie dogs, though other animals such as mice, guinea pigs, dogs, and camels have also served as sources in modern outbreaks (Barbieri *et al.*, 2021). The sylvatic cycle in rodents mainly consists of enzootic cycles, though may transform into epizootic and zoonotic cycles through spillover events (Cui and Song, 2016; Vallès *et al.*, 2020). The enzootic cycle of plague involves the natural cycle of a pathogen within its reservoir; in the case of plague, the amount of *Y. pestis* is low to prevent rodent population die-off and involves the cycling of the bacterium, fleas, and rodents. Epizootic cycles occur when there is a greater than average number of infected hosts within a population. These cycles can then lead to zoonoses where infections are able to cross species (from rodents to humans in the case of bubonic plague) through a spillover event, where a highly infected host population interacts and infects a population of a new species (Cui and Song, 2016).

To better understand how rodent reservoirs may have proliferated outbreaks in past pandemics, we can look at the relationships between fleas and their hosts in modern rodent populations. Previous research on modern rodent populations has established that flea abundance can be affected by changes in precipitation and/or host abundance as well as increases in temperature (Salkeld and Stapp, 2008). In their study of flea abundance and prairie dogs in the United States, Salkeld and Stapp (2008) found that flea abundance in burrows increased during disease outbreaks, likely due to a larger number of fleas being unable to find a suitable living host. In the same study, they proposed that, as their mammalian hosts die-off, fleas may be able to act as reservoirs in burrows as they wait to infect new hosts. More recently, primarily following the articulation of first and second plague pandemic *Y. pestis* lineages, it has been argued that the bacterium integrated itself into the local wildlife following the Justinianic Plague and Black Death (Carmichael 2014; Varlik 2020; Slavin 2021; Newfield 2022). Some interdisciplinary analyses have sought to disprove this theory. Using georeferenced historical outbreaks and dendro-based paleoclimatology, Schmid and colleagues (2015) attempted to uncover the drivers of plague spillovers that reached Europe following the Black Death. Their study did not recover evidence to support a climate-sensitive plague reservoir in medieval Europe but lent further support to the idea that plague was repeatedly introduced to Europe from eastern regions. In place of a contemporary European rodent reservoir, the authors hypothesize that the climate-driven recurrent waves of plague were caused by black rats in urban centres and temperature-affected flea abundances, comparing more to waves of plague in 19th and 20th century India with its various modes of transmission without relying on a permanent reservoir. In wake of genomic evidence for the

maintenance of plague in the wider Euro-Mediterranean region, the push for long-distance imports appears to be waning; recent second pandemic studies, however, have utilized interdisciplinary approaches to investigate the persistence of the pathogen in Europe, highlighting the benefit of considering archaeological, climatic, and ecological factors in a holistic approach to science (Guellil *et al.*, 2020; Bramanti *et al.*, 2021).

The three most common forms of plague are bubonic, pneumonic, and septicemic, though meningial plague, gastrointestinal plague, and pharyngeal plague have also been described (Barbieri *et al.*, 2021). Notably, only pneumonic plague and plague transmitted by human ectoparasites are capable of human-human transmission. Crucially, genomic techniques are currently unable to distinguish between the forms of plague. Furthermore, as previously mentioned, there are three documented historical plague pandemics. The first plague pandemic began with the Plague of Justinian from 541-544/9 CE and lasted well into the 8th century. The second plague pandemic was introduced to the Mediterranean region and Europe in the infamous Black Death of 1346-1353 and historically continued until the end of the 19th century, at least in the central and eastern Mediterranean (Cohn, 2008; Varlık, 2020; Poinar, 2022). The third plague pandemic enters historical records in Yunnan, China in the mid-nineteenth century and persists today. It is important to note that the century-long gap between the historical second and third pandemics stems from a Eurocentric perspective heavily privileges written sources; this is in addition to the prevalent but erroneous idea that the second pandemic concluded with the 1720-1722 plague of Marseille.

Plague persists today, of course, has been seen in numerous countries on multiple continents including the western United States, Uganda, China, the Democratic Republic of Congo, Peru, Vietnam, and Madagascar (Demeure *et al.*, 2019). Furthermore, as third-pandemic strains are derived from those of the second plague pandemic, it can be argued that we are still genetically living in the second pandemic, with the third pandemic being a misnomer (Poinar, 2022; Eaton *et al.*, 2023). Thus, as genetic technologies improve, it is evidently clear that the traditional and widespread notion of there being three historical plagues needs revisiting. Similarly, as stated by numerous researchers, it is clear that constant contextualization and re-visitation is required in plague studies to conclusively incorporate genomes and genetic insights into histories of past plagues.

1.3 Ancient DNA

Ancient DNA (aDNA) is DNA retrieved from ancient biological material (remains, plants, soil, etc.). In the past, analyzing DNA from these sources was next to impossible due to the rapid degradation of the organic material (Duchêne *et al.*, 2020). The relatively recent ability to retrieve genetic information from ancient samples through advancements in aDNA techniques has been able to settle some long-standing debates. Over time, DNA molecules in remains fragment into extremely small pieces and may undergo chemical changes preventing the use of traditional DNA recovery methods. Most aDNA studies utilize material found in ancient bones and teeth due to their durability and low water content, contributing to preservation of cells (Ludes and Keyser, 2016). Plague studies particularly use teeth since *Y. pestis* is preserved in the pulp cavity and the outer layers of the tooth partially protect it from environmental

contamination. Additionally, the matrices of both bone and tissues (namely dentin) consist of hydroxyapatite which is capable of binding double-stranded DNA, increasing preservation. Chapter 4 expands on how changes in the climate and geography of regions in Turkey contribute to varying levels of preservation of remains in archaeological sites. In anthropological analyses, DNA has been used to identify sex when skeletal morphology is inconclusive due to the age of individuals. Additionally, DNA has been used in kinship analyses to determine genetic links between individuals as well as paleopathology to study pathogen-causing diseases in ancient remains; the latter of which is notable as many human diseases do not leave evidence on bones (Ludes and Keyser, 2016).

The field of ancient DNA was officially initiated in 1984, during an extraction of fragments from an extinct species of zebra (Higuchi *et al.*, 1984). Notably, this experiment used bacterial cloning (a long and arduous process) and was only able to generate data from large DNA fragments. This experiment was followed by the first aDNA PCR amplifications in 1988, and the first aDNA extractions from bone in 1990 (Orlando *et al.*, 2021). Dental pulp was first used to extract pathogenic aDNA of *Y. pestis* near the turn of the millennium (Drancourt *et al.*, 1998). Then, next-generation sequencing (NGS) was first utilized in 2006 on ancient remains and was instrumental in the expansion of aDNA due to its ability to sequence large amounts of genetic information in a short amount of time (Poinar *et al.*, 2006; Arning and Wilson, 2020; Orlando *et al.*, 2021). The development of targeted enrichment in 2007 further pushed the boundaries of aDNA as specific regions of a genome of interest were able to be amplified (Okou *et al.*, 2007). Using these high-throughput sequencing techniques, the first bacterial paleogenome of *Y. pestis* was retrieved in 2011 (Bos *et al.*, 2011). Other

diseases investigated using techniques in ancient DNA include malaria, leprosy, and tuberculosis (Duchêne *et al.*, 2020).

Bioinformatically, it is crucial to classify the identity of sequencing reads and authenticate if the DNA being analyzed truly is ancient. First, to increase the quality of data being analyzed, adapter sequences must be removed or trimmed from the raw reads. The total proportion of reads aligning to a pathogen of interest is considered in proportion to *all* trimmed and merged reads in a sample. A greater proportion of pathogen DNA relative to all other taxa would support the classification and validity of that pathogen. Issues can arise when, as is too often seen in studies of ancient pathogens, very few reads map to the genome at all. This may occur when the sample is not well-preserved or if an issue occurred during sample/library preparation or sequencing. Here, we would expect a very low proportion of target DNA compared to all reads, a rough or spiky deamination profile as the program analyzing fragment misincorporation struggles to make sense of very little data, and fluctuating fragment lengths (Hider *et al.*, 2022). This issue can be addressed through targeted enrichment, as it can increase the total number of mapped reads specific to a region of interest. Despite the leaps in progress we have seen in recent years, results retrieved through aDNA analysis are not absolute. Particularly, we should be very aware of the biases often introduced during each step of processing. Subsequent chapters of this thesis are dedicated to discussing these biases, how the preservation of samples may affect the quality of our results, and how the preservation of samples may have hindered robust studies of the first pandemic. The final chapter in particular overviews the realities of ancient DNA, and detail what I have seen, felt, and experienced as an incoming researcher into the field.

1.4 The First Plague Pandemic: Current Genomes

The first draft genomes attributed to the Justinianic Plague were published in 2014 (Wagner *et al.*, 2014). Genomes from individuals buried in the Aschheim-Bajuwarenring cemetery in Germany generated novel branches on the phylogenetic tree of *Y. pestis*. These branches revealed no known connections to subsequent pandemics or modern strains, concluding that the first and second plague pandemics were independent of one another (Wagner *et al.*, 2014). Subsequent reanalysis of the genome from individual A120 posited that several substitutions in the original study were false positives (Feldman *et al.*, 2016), though these conclusions have been questioned; as few genomes and known mutations currently exist for the first pandemic, careful revising and challenging of past findings using more advanced technology is a necessity.

A higher coverage genome was later recovered from an individual buried in a nearby cemetery in Altenerding, Germany. Notably, after factoring false-positive SNP calling, individuals AE1175 and A120 were posited to be genetically identical (Feldman *et al.*, 2016). Both genomes from Aschheim and Altenerding are remarkable not only because of their novelty but also because of the lack of historical records mentioning plague in 6th or 7th century Germany, effectively expanding the geography of the working narrative of the first pandemic. Interestingly, the genome from Altenerding was genetically identical to genomes subsequently retrieved from Dittenheim, Germany (DIT003) and Unterthürheim, Germany (UNT003 and UNT004). Genomes (PET004 and VAL001) were also recovered from individuals in Petting, Germany and Valencia, Spain, respectively; notably, a polytomy is hypothesized to have resulted in a divergence from the Altenerding genome to the

Petting, Valencia, and French genomes (Keller, Spyrou, and Scheib *et al.*, 2019).

Namely, several strains from 5th to 9th century France were also recovered. On the basis that all three were linked to the same overall strain, the low-coverage reads of individuals LVC001, LVC005, and LVC006 from Lunel-Viel were combined to create the genome known as LVC_Merged (Keller, Spyrou, and Scheib *et al.*, 2019). Several genomes were also retrieved from Saint-Doulchard and LSD001, LSD020, and LSD023 were added to published phylogenies (Keller, Spyrou, and Scheib *et al.*, 2019; Eaton *et al.*, 2023). Notably, the genomes from France have a common chromosomal deletion as well as a deletion on the pMT1 plasmid (Keller, Spyrou, and Scheib *et al.*, 2019).

Additionally, genomes were retrieved from individuals EDI001, EDI003, and EDI004 buried at Edix Hill in the United Kingdom (Keller, Spyrou, and Scheib *et al.*, 2019; Guellil *et al.*, 2022). Currently, the most recently published first pandemic genome is YP-EDI064 and is noteworthy because of a possible co-infection with *Haemophilus influenzae*, a bacterial infection typically affecting children (Guellil *et al.*, 2022). Although records exist defending the existence of plague in England in the seventh century, plague is scarcely identified as having been present at Edix Hill, or in England generally, in the sixth century (Keller, Spyrou, and Scheib *et al.*, 2019).

Strikingly, a genome (DA101) retrieved from an individual buried in the Tian Shan Mountains in Kyrgyzstan with the gene mutations required to support pathogenic transmission through fleas was recovered in 2018 (Damgaard *et al.*, 2018). DA101 has been used to defend, problematically in the eyes of some scholars, the hypothesis that plague was brought to Europe from Central Asia, whether via Silk Roads or through migrations of Central Asian populations (Damgaard *et al.*, 2018). As

a single genome itself is unable to unequivocally settle debates on the origin of the first pandemic, subsequent studies are required to bridge the gaps between the centuries as well as between regions.

1.4.1 Aschheim, Germany

In 2014, the first draft genomes attributed to the Justinianic Plague were published, where teeth from two individuals (A120 and A76) from the Aschheim-Bajuwarenring cemetery in Germany were analyzed. Notably, the genomes were able to generate novel branches on the phylogenetic tree of *Y. pestis*, concluding that the First Plague Pandemic and the subsequent Second Pandemic were independent of one another (Feldman et al., 2016). As pandemics are hypothesized to have multiple replication cycles and affect mutation rates of infectious agents, the increase in mutation rate of the Aschheim genomes have been used to support the hypothesis that the strains were linked to the Justinianic plague outbreak. Subsequent reanalysis of the genome from individual A120 found that several substitutions in the original study were instances of DNA damage due to sequencing errors, reiterating the necessity of questioning past conclusions with advanced technology (Feldman et al., 2016).

1.4.2 Altenerding, Germany

A higher coverage genome was recovered in 2016 from an adult individual (AE1175) buried in Altenerding, Germany. After factoring in the false positive SNPs of the previous *Y. pestis* genome, AE1175 and A120 were found to be genetically identical; AE1175 has thus been primarily utilized over A120 in subsequent phylogenetic analyses (Feldman et al., 2016). Despite the lack of historical records mentioning

plague in sixth-century Germany, the Aschheim and Altenerding genomes expand the working narrative of the First Plague Pandemic at the time of their respective publications. In a subsequent study, a 14.8 kb deletion on the pMT1 plasmid coding for 21 hypothetical proteins was also found (Keller, Spyrou, and Scheib *et al.*, 2019).

1.4.3 Edix Hill, United Kingdom

As first outlined by Keller and colleagues in 2019, Edix Hill is described as having served as an Anglo-Saxon burial site, which appears to have been in use from the early 6th to 7th centuries (Keller, Spyrou, and Scheib *et al.*, 2019; Malim *et al.*, 1998). The site is also linked to a wider Roman network, near roads connecting to the Roman settlements Duroliponte, Londinium, and Lindum Colonia. Though records exist detailing the presence of plague in and around Edix Hill in the 7th century, the same cannot be said for the 6th century and thus cannot corroborate recovered genomes (Keller, Spyrou, and Scheib *et al.*, 2019). Multiple individuals from this site tested positive for *Y. pestis* with varying effectiveness. Individuals EDI001.A, EDI003, and EDI004 were positively screened for plague and found to have genetically identical SNP profiles. As the study chose to only map one quality genome per site in efforts to minimize errors in SNP alignment, only EDI001.A was used for phylogenetic analysis (Keller, Spyrou, and Scheib *et al.*, 2019).

The most recent Edix Hill genome YP-EDI064 has been found to be genetically similar to EDI001.A, plausibly differing in only two SNP positions hypothesized to be caused by erroneous mapping; consideration of both SNP profiles suggest they are either identical to each other or the latter has been derived from the former (Guellil *et al.*, 2022). Notably, YP-EDI064 is significant due to its possible co-

infection with *Haemophilus influenzae*. Convincing premodern cases of co-infection involving plague are quite rare. One example in recent literature involves *Treponema pallidum pertenue* (yaws) in a 15th-century plague victim (Giffin et al., 2020).

Another study of Bronze Age individuals in Hagios Charalambos cave in Crete studied *Y. pestis* and *Salmonella enterica* genomes in separate individuals (Neumann et al., 2020). Importantly, similar cases of co-occurrence of plague with other pathogens in the historical and archaeological record can rarely be established. For instance, the effect of co-infections is perplexing due to how fast plague can result in death and because coevality is difficult to defend (Guellil et al, 2022).

1.4.4 Lunel-Viel Quartier centrale, France

Located at the intersection of two popular Roman roads, the site is thought to have been active in late antiquity (Keller, Spyrou, and Scheib *et al.*, 2019). Three plague-positive individuals were recovered, though their individual coverages were too low to be analyzed individually. On the basis that all three were linked to an identical overall strain, the *Y. pestis* reads of individuals LVC001, LVC005, and LVC006 were combined to create the genome known as LVC_Merged. Interestingly, this genome, along with genomes from Saint-Doulchard Le Pressoir, presented 7 non-synonymous SNPs; among them was the phosphoenolpyruvate carboxylase gene *ppc* known for Yops (*Yersinia* outer membrane proteins) infiltration into host cells. Furthermore, LVC_Merged was discovered to have a 12.9 kb chromosomal deletion resulting in issues with arabinose metabolism; these issues with the arabinose operon are hypothesized to help render the strain avirulent, though there is no evidence for this as

of yet (Keller, Spyrou, and Scheib *et al.*, 2019).

1.4.5 Saint-Doulchard Le Pressoir, France

The area, excavated in 2007, consists of many burials dated to between the 7th and 12th centuries (Keller, Spyrou, and Scheib *et al.*, 2019). However, ancient burial mounds and remnants of a Roman villa have also hinted at possible earlier occupation, dating to the 6th to 4th centuries BCE. In 571, contemporary narrator Gregory of Tours notes the presence of plague in Bourges, a town nearby Le Pressoir. This predates the first pandemic genomes retrieved at this site, as they are dated to around two hundred years after his account (Keller, Spyrou, and Scheib *et al.*, 2019).

A 2019 study was able to discern two high-quality genomes in LSD001.A and LSD023 (Keller, Spyrou, and Scheib *et al.*, 2019). Although the LSD020.A genome was not included in the 2019 paper, it was, in place of the LSD023.A genome, included in the 2023 study conducted by Eaton and colleagues (Eaton *et al.*, 2023); this switch can be attributed to varying selection criteria between the studies. Furthermore, LSD001.A and LSD023.A had the same seven non-synonymous mutations as LVC_Merged, though had a unique substitution in the *lacY* gene. LSD001.A and LSD023.A differed through their 4 and 3 unique SNPs, respectively. In the same study, a 12.9 kb chromosomal deletion and 14.8 kb deletion on the pMT1 plasmid outlined previously were also found, differentiating them from the Altenerding and Dittenheim genomes (Keller, Spyrou, and Scheib *et al.*, 2019).

1.4.6 Dittenheim, Germany

Though many of its burials are linked to the early medieval period, Dittenheim is near the Roman Limes and recorded to have been in use between the 6th and 7th centuries (Keller et al., 2019). The SNP profile of a genome from individual DIT003 was found to be identical to the one in Altenerding as well as two from the site in Unterthürheim (Keller, Spyrou, and Scheib *et al.*, 2019). The study also found a lack of a 14.8kb deletion on the pMT1 plasmid coding for hypothetical proteins. Despite being otherwise genetically identical, this deletion was posited as being more common and is present in the genomes from the Unterthürheim, Saint-Doulchard Le Pressoir, and Lunel-Viel Quartier centrale (Keller, Spyrou, and Scheib *et al.*, 2019).

1.4.7 Petting, Germany

Petting is hypothesized to have been associated with the Roman city of Iuvavum during the late antique period (Keller, Spyrou, and Scheib *et al.*, 2019). Interestingly, due to its position within the Roman province *Noricum ripense* and separation from *Raetia secunda* by the River Inn, rivers themselves are hypothesized to have served as physical barriers to plague. The *Y. pestis* genome retrieved from individual PET004 notably had two unique SNPs — one of them a non-synonymous SNP for hypothetical protein YPO3510 (Keller, Spyrou, and Scheib *et al.*, 2019).

1.4.8 Unterthürheim, Germany

The cemetery is notable for its proximity to Roman constructs such as roads *Via Iuxta Danuvium* and *Via Claudia Augusta*, the Roman fort *Submuntorium*, and what was likely an Imperial Roman settlement (Keller, Spyrou, and Scheib *et al.*, 2019;

McCormick, 2016). Two plague genomes were retrieved from the site (UNT003 and UNT004). As mentioned, Keller and colleagues (2019) mapped only one quality genome per site in efforts to minimize errors in SNP alignment, though the plague SNP profiles from both individuals were identical to the genomes from Altenerding and Dittenheim. In accordance with these genomes, UNT003 and UNT004 both lacked a 14.8kb deletion on the pMT1 plasmid coding for hypothetical proteins, distinguishing it from the genomes from Unterthürheim and those from France.

1.4.9 Valencia, Plaça de Almoína, Spain

Valencia was likely active for a significantly long period between the 5th to 7th centuries and had evidence of pre-Roman architecture (Keller, Spyrou, and Scheib *et al.*, 2019; McCormick, 2016). As the remains within the cemetery appear to have been heavily disturbed at the time of excavation at the end of the 20th century, the sex and age of the individual linked to the *Y. pestis* genome (VAL001) could not be identified. The genome has 3 unique SNPs in its profile; notably, the genes *tyrP* (a virulence factor in mice), and YPO1985 (likely also a virulence factor) were found to have non-synonymous SNPs. A polytomy was also hypothesized to have resulted in its divergence from the Altenerding genome, similar to the Petting and French genomes (Keller, Spyrou, and Scheib *et al.*, 2019).

1.4.10 Tian Sian Mountains, Kyrgyzstan

The Uch-Kurbu burial site is associated by some scholars with the movement of the Northern Huns during the Great Migrations of Peoples between the 2nd and 5th centuries (Damgaard *et al.*, 2018). Specifically, it is found on a floodplain terrace

above the Tosor River in accordance with other nomadic burials. The Uch-kurbu burial ground is also characterized by its peculiar archaeological lack of pots and presence of organized burial (contrasting typical scattered burial mounds); notably, this was also seen around the Issyk-Kul basin (Damgaard et al., 2018). Historical records have speculated Issyk-Kul to be the first epidemic site of the second pandemic (Dols, 1974; Norris, 1977; Slavin, 2019). Genomic evidence from cemeteries within the basin was recently recovered, though its identity as the true source of the Black Death is contested (Spyrou *et al.*, 2022).

Of 140 individuals, only 2 (DA101 and DA147) were of high-enough quality for downstream analysis. The genome of individual DA101 was of significantly higher quality than DA147, allowing for more definitive genomic and phylogenetic analysis. Additionally, the *ymt* gene was detected in DA101, differentiating it from the Bronze-age strains and showing evidence of mutations required to support transmission through fleas. The positioning of the genome on the *Y. pestis* phylogeny has been used to defend the problematic hypothesis that plague was brought to Europe from Central Asia over the centuries via the Silk Road (Damgaard et al., 2018).

1.5 The First Plague Pandemic: Current Debates

1.5.1 Maximalist and Minimalist Platforms

The central argument in the interdisciplinary subfield of first pandemic studies is the population mortality of the Justinianic Plague and subsequent plague outbreaks. The impact of the Justinianic Plague's mortality has been contested in waves over decades (see Durliat 1989; Sarris, 2002). The demographic impact of the first pandemic was recently debated with no clear result emerging from the disagreement

(Mordechai and Eisenberg, 2019; Mordechai *et al.*, 2019; Eisenberg and Mordechai, 2020; Sessa, 2019; Faure, 2021; Schoolman, 2022; Batterman, 2024). Some researchers question the claim that the Justinianic Plague killed tens of millions (perhaps a quarter to a half of the Mediterranean population) as has been thought for generations (see literature surveyed in Stathakopoulos, 2016; Eisenberg and Mordechai 2019; Newfield, 2022). By quantitatively analyzing inscriptional, numismatic, palynological, and genomic data, an argument was waged that the population-scale mortality and significance of the Justinianic plague is now and has long been overexaggerated (Mordechai *et al.*, 2019). Countering this, some scholars have argued that these interdisciplinary approaches work to serve only a minimalist mindset. They find no place for quantitative methodologies and argue that historians should proceed with qualitative contextualization (Meier, 2020). To date, minimalist argumentation has been countered, successfully or not, several times (Meier 2020; McCormick, 2021; Sarris, 2022; Harper 2023), but again these rebuttals have focused largely on the quantitative methodologies employed in the handling of written sources. Underlying issues, however, remain, particularly in the assumptions underpinning maximalist histories where the First Plague Pandemic is claimed to kill tens of millions based on so-called ‘positivistic’ or literal readings of relatively few contemporary eye-witness sources and the smearing of the far better-documented Black Death into the history of the First Plague Pandemic. Though the discovery of novel genomes in Turkey cannot effectively attempt to end these long-held and often heated debates, it will undoubtedly reposition current scholarly knowledge while underlining the importance of interdisciplinarity in addressing it.

1.5.2 *Origins*

Another debate, one not exclusive to any of the plague pandemics, is on the “origins” of *Y. pestis* as well as the tracing of late antique plague’s chronology and geography in the Eastern hemisphere. As a considerably smaller amount of both historical and genomic evidence can be definitively attributed to the first pandemic than the second or third pandemics, the term “origins” has sparked intense debate. Unsurprisingly, there is more opportunity for divisive debates when the evidence is thinnest. Specifically, the problem primarily lies with the science’s inconsistencies with written historical evidence and within the evolving interpretations of the extant written material. As briefly outlined, past historical studies have posited that *Y. pestis* spread from Central Asia or Eastern Africa to Europe, relying on literal readings of sixth-century plague passages (as discussed in Sessa 2019; Newfield, 2022), some contemporary to the 540s, and some quite later (ex. Stathakopoulos, 2004; Sarris, 2002, 2022; Green 2015). Paleogenomic interpretations have followed historians’ leads (Wagner *et al.*, 2014; Damgaard *et al.*, 2018; Keller, Spyrou, and Scheib *et al.*, 2019). A minority of other studies have posited that the pandemic emerged closer to the plague-struck Mediterranean region, in Northern Africa or Southwest Asia (Stathakopoulos, 2003; Sallares, 2007; Newfield, 2018). More recently, based on the dating and phylogeny of the Edix Hill genomes, it has been suggested that the presence of plague was more complicated in the Euro-Mediterranean (Keller, Spyrou, and Scheib *et al.*, 2019; Guillil *et al.*, 2022). Again, even if new Mediterranean genomes are published and investigated alongside known histories of past pandemics, they will not be able to effectively resolve this debate. Nevertheless, their discovery may be able to integrate new perspectives and refine current working narratives.

1.5.3 Biasing Catastrophe

With the scarcity of uncontested evidence, the Black Death and the second plague pandemic has been used as a surrogate for the first pandemic (Newfield, 2022). When doing so, it is crucial to use caution to prevent forcing unproven models onto the first pandemic and generating definitive conclusions in attempts to end existing debates. Some first plague pandemic studies modelled after the Black Death have also been accused of seeking out catastrophe or having a catastrophe bias (Mordechai et al., 2019; Newfield, 2022). Here, a historical pandemic is only considered to be of interest when there is significant mass mortality; these notions have been argued to be influenced by the greater amount of second plague pandemic evidence; maximalist arguments have been criticized for often leaving out smaller, individual stories on the individual or community level. At the same time, there remains a real possibility that the evidence for significant late antique plague mortality, which minimalists are asking for, will be uncovered.

1.6 Research Objectives

The goals of this thesis are: *(i) to analyze late antique human remains from Turkey to improve current understanding of the geography and transmission of First-Pandemic plague in non-European contexts, (ii) to underline the importance of implementing interdisciplinary approaches to the study of infectious disease in the past, and (iii) to comment on the realities and expectations of ethically sourcing and analyzing ancient DNA.* Ancient remains from sites in northern and northwestern Turkey were screened for plague in efforts to derive the first Mediterranean genome for the first plague pandemic. As mentioned, genomic evidence attributed to the pandemic has been retrieved and published from sites in Germany, France, Spain, and

England. This evidence has been unable to be linked to genomes of the Black Death and subsequent plague outbreaks and are characterized as a genetic ‘dead-end’ in the phylogenetic tree of *Y. pestis* (Wagner *et al.*, 2014; Feldman *et al.*, 2016; Keller, Spyrou, and Scheib *et al.*, 2019). In addition, recent publications have addressed the importance of enhancing interdisciplinarity in understanding the plague pandemics (Green, 2022; Newfield, 2022; Poinar, 2022; Sarris, 2022). Strategically screening for *Y. pestis* in and around Anatolia is of interest as it is there that the bulk of the written and archaeological evidence for the first plague pandemic is located. Retrieving additional genomes from late antique individuals is significant as it will serve to expand the narrative of the first pandemic locally and globally, for which we are currently reliant on published genomic evidence from western Europe. In the same vein, researchers should prioritize considerate and active interaction with remains of the deceased, dedicating as much if not more attention to ethical approaches than the discovery of a novel genome. As stated, debates will remain unresolved until more first pandemic genomes are retrieved, published, and contextualized using methods that span multiple disciplines.

1.7 References

- Arning, N., & Wilson, D. J. (2020). The past, present and future of ancient bacterial DNA. *Microbial genomics*, 6(7), mgen000384. <https://doi.org/10.1099/mgen.0.000384>
- Batterman, T. (2024). The Pen Behind the Pathogen: *Yersinia pestis* and the Lombard Conquest in Paul the Deacon's *Historia Langobardorum*. *Journal of Late Antiquity* 17(1), 159-199. <https://doi.org/10.1353/jla.2024.a926284>.
- Bos, K. I., Schuenemann, V. J., Golding, G. B., Burbano, H. A., Waglechner, N., Coombes, B. K., McPhee, J. B., DeWitte, S. N., Meyer, M., Schmedes, S., Wood, J., Earn, D. J. D., Herring, D. A., Bauer, P., Poinar, H. N., & Krause, J. (2011). A draft genome of *Yersinia pestis* from victims of the Black Death.

Nature, 478(7370). <https://doi.org/10.1038/nature10549>

- Bramanti, B., Wu, Y., Yang, R., Cui, Y., & Stenseth, N. C. (2021). Assessing the origins of the European Plagues following the Black Death: A synthesis of genomic, historical, and ecological information. *Proceedings of the National Academy of Sciences of the United States of America*, 118(36), e2101940118. <https://doi.org/10.1073/pnas.2101940118>
- Cohn S. K., Jr (2008). Epidemiology of the Black Death and successive waves of plague. *Medical history. Supplement*, (27), 74–100.
- Cui, Y., Song, Y. (2016). Genome and Evolution of *Yersinia pestis*. In: Yang, R., Anisimov, A. (eds) *Yersinia pestis: Retrospective and Perspective*. Advances in Experimental Medicine and Biology, vol 918, pp. 171-192. Springer, Dordrecht. https://doi.org/10.1007/978-94-024-0890-4_6
- Damgaard, P. de B., Marchi, N., Rasmussen, S., Peyrot, M., Renaud, G., Korneliussen, T., Moreno-Mayar, J. V., Pedersen, M. W., Goldberg, A., Usmanova, E., Baimukhanov, N., Loman, V., Hedeager, L., Pedersen, A. G., Nielsen, K., Afanasiev, G., Akmatov, K., Aldashev, A., Alpaslan, A., ... Willerslev, E. (2018). 137 ancient human genomes from across the Eurasian steppes. *Nature*, 557(7705). <https://doi.org/10.1038/s41586-018-0094-2>
- Dols, M. W. (1974). Plague in Early Islamic History. *Journal of the American Oriental Society*, 94(3), 371–383. <https://doi.org/10.2307/600071>
- Drancourt, M., Aboudharam, G., Signoli, M., Dutour, O., & Raoult, D. (1998). Detection of 400-year-old *Yersinia pestis* DNA in human dental pulp: an approach to the diagnosis of ancient septicemia. *Proceedings of the National Academy of Sciences of the United States of America*, 95(21), 12637–12640. <https://doi.org/10.1073/pnas.95.21.12637>
- Durliat, J. (1989). La peste du VI^e siècle: pour un nouvel examen des sources byzantines. In: *Hommes et richesses dans l'empire byzantine Pt. 1* (pp. 107-119).
- Duchêne, S., Ho, S. Y. W., Carmichael, A. G., Holmes, E. C., & Poinar, H. (2020). The Recovery, Interpretation and Use of Ancient Pathogen Genomes. *Current biology: CB*, 30(19), R1215–R1231. <https://doi.org/10.1016/j.cub.2020.08.081>
- Duchene, S., Lemey, P., Stadler, T., Ho, S. Y. W., Duchene, D. A., Dhanasekaran, V., & Baele, G. (2020). Bayesian Evaluation of Temporal Signal in Measurably Evolving Populations. *Molecular Biology and Evolution*, 37(11), 3363–3379. <https://doi.org/10.1093/molbev/msaa163>
- Eisenberg, M., & Mordechai, L. (2019). The Justinianic Plague: An interdisciplinary review. *Byzantine and Modern Greek Studies*, 43(2), 156–180. <https://doi.org/10.1017/byz.2019.10>

- Eisenberg, M., & Mordechai, L. (2020). The Justinianic Plague and Global Pandemics: The Making of the Plague Concept. *The American Historical Review*, 125(5), 1632–1667. <https://doi.org/10.1093/ahr/rhaa510>
- Faure, E. (2021). Did the Justinianic Plague Truly Reach Frankish Europe around 543 AD? *Vox Patrum*, 78, 427–465.
- Feldman, M., Harbeck, M., Keller, M., Spyrou, M. A., Rott, A., Trautmann, B., Scholz, H. C., Pääffgen, B., Peters, J., McCormick, M., Bos, K., Herbig, A., & Krause, J. (2016). A High-Coverage *Yersinia pestis* Genome from a Sixth-Century Justinianic Plague Victim. *Molecular Biology and Evolution*, 33(11), 2911–2923. <https://doi.org/10.1093/molbev/msw170>
- Giffin, K., Lankapalli, A.K., Sabin, S. *et al.* A treponemal genome from an historic plague victim supports a recent emergence of yaws and its presence in 15th century Europe. *Sci Rep* 10, 9499 (2020). <https://doi.org/10.1038/s41598-020-66012-x>
- Green, M. (2015). Preface The Black Death and Ebola: On The Value Of Comparison. In M. Green & C. Symes (Ed.), *Pandemic Disease in the Medieval World: Rethinking the Black Death* (pp. ix-xx). Amsterdam: ARC Humanities Press. <https://doi.org/10.1515/9781942401018-002>
- Green, M. H. (2022). A New Definition of the Black Death: Genetic Findings and Historical Interpretations. *De Medio Aevo*, 11(2), 139–155. <https://doi.org/10.5209/dmae.83788>
- Guellil, M., Kersten, O., Namouchi, A., Luciani, S., Marota, I., Arcini, C. A., Iregren, E., Lindemann, R. A., Warfvinge, G., Bakanidze, L., Bitadze, L., Rubini, M., Zaio, P., Zaio, M., Neri, D., Stenseth, N. C., & Bramanti, B. (2020). A genomic and historical synthesis of plague in 18th century Eurasia. *Proceedings of the National Academy of Sciences of the United States of America*, 117(45), 28328–28335. <https://doi.org/10.1073/pnas.2009677117>
- Guellil, M., Keller, M., Dittmar, J. M., Inskip, S. A., Cessford, C., Solnik, A., Kivisild, T., Metspalu, M., Robb, J. E., & Scheib, C. L. (2022). An invasive *Haemophilus influenzae* serotype b infection in an Anglo-Saxon plague victim. *Genome Biology*, 23(1), 22. <https://doi.org/10.1186/s13059-021-02580-z>
- Harper, K. (2017). *The fate of Rome climate, disease, and the end of an empire*. Princeton University Press. <https://doi.org/10.1515/9781400888917>
- Harper, K. (2023). The First Plague Pandemic in Italy: The Written Evidence. *Speculum* 98(2), 369-420. <https://doi.org/10.1086/723937>
- Hider, J., Duggan, A. T., Klunk, J., Eaton, K., Long, G. S., Karpinski, E., Giuffra, V.,

- Ventura, L., Fornaciari, A., Fornaciari, G., Golding, G. B., Prowse, T. L., & Poinar, H. N. (2022). Examining pathogen DNA recovery across the remains of a 14th century Italian friar (Blessed Sante) infected with *Brucella melitensis*. *International journal of paleopathology*, 39, 20–34. <https://doi.org/10.1016/j.ijpp.2022.08.002>
- Higuchi, R., Bowman, B., Freiburger, M. *et al.* (1984). DNA sequences from the quagga, an extinct member of the horse family. *Nature* 312, 282–284. <https://doi.org/10.1038/312282a0>
- Keller, M., Spyrou, M. A., McCormick, M., Bos, K. I., Herbig, A., & Krause, J. (2019). Ancient *Yersinia pestis* genomes provide no evidence for the origins or spread of the Justinianic Plague. *BioRxiv*, 819698. <https://doi.org/10.1101/819698>
- Keller, M., Spyrou, M. A., Scheib, C. L., Neumann, G. U., Kröpelin, A., Haas-Gebhard, B., Paffgen, B., Haberstroh, J., Ribera i Lacomba, A., Raynaud, C., Cessford, C., Durand, R., Stadler, P., Nägele, K., Bates, J. S., Trautmann, B., Inskip, S. A., Peters, J., Robb, J. E., ... Krause, J. (2019). Ancient *Yersinia pestis* genomes from across Western Europe reveal early diversification during the First Pandemic (541–750). *Proceedings of the National Academy of Sciences of the United States of America*, 116(25), 12363–12372. <https://doi.org/10.1073/pnas.1820447116>
- Ludes, B., & Keyser, C. (2015). Anthropology: Role of DNA. In *Encyclopedia of Forensic and Legal Medicine* (Second Edition, pp. 207–212). Elsevier Ltd. <https://doi.org/10.1016/B978-0-12-800034-2.00030-6>
- Malim, T., & Hines, J. (1998). The Anglo-Saxon cemetery at Edix Hill (Barrington A), Cambridgeshire: excavations 1989-1991 and a summary catalogue of material from 19th century interventions. In *Council for British Archaeology Research Reports* (p. 112). Archaeology Data Service. <https://doi.org/10.5284/1081785>
- Meier, M. (2020). The ‘Justinianic Plague’ - Die ‚Justinianische Pest‘: An “Inconsequential Pandemic”? A Reply. *Medizinhistorisches Journal*, 55(2), 172–199.
- McCormick M. (2016). Tracking mass death during the fall of Rome’s empire (II): a first inventory, *Journal of Roman Archaeology*, 29, 1008–46.
- Mordechai, L., Eisenberg, M., Newfield, T. P., Izdebski, A., Kay, J. E., & Poinar, H. (2019). The Justinianic Plague: An Inconsequential pandemic? *Proceedings of the National Academy of Sciences of the United States of America*, 116(51), 25546–25554. <https://doi.org/10.1073/pnas.1903797116>
- Neumann, G. U., Skourtanioti, E., Burri, M., Nelson, E. A., Michel, M., Hiss, A.N., McGeorge, P. J. P., Betancourt, P. P., Spyrou, M. A., Krause, J., &

- Stockhammer, P. W. (2022). Ancient *Yersinia pestis* and *Salmonella enterica* genomes from Bronze Age Crete. *Current biology*: 32(16), 3641–3649. <https://doi.org/10.1016/j.cub.2022.06.094>
- Newfield, T.P. (2018). The Climate Downturn of 536–50. In: White, S., Pfister, C., Mauelshagen, F. (eds) *The Palgrave Handbook of Climate History*. Palgrave Macmillan, London. https://doi.org/10.1057/978-1-137-43020-5_32
- Newfield, T. P. (2022). One Plague for Another? Interdisciplinary Shortcomings in Plague Studies and the Place of the Black Death in Histories of the Justinianic Plague. *Studies in Late Antiquity*, 6(4), 575–626. <https://doi.org/10.1525/sla.2022.6.4.575>
- Norris, J. (1977). East or West? The Geographic Origin of the Black Death. *Bulletin of the History of Medicine*, 51(1), 1–24. <http://www.jstor.org/stable/44450388>
- Okou, D. T., Steinberg, K. M., Middle, C., Cutler, D. J., Albert, T. J., & Zwick, M. E. (2007). Microarray-based genomic selection for high-throughput resequencing. *Nature methods*, 4(11), 907–909. <https://doi.org/10.1038/nmeth1109>
- Orlando, L., Allaby, R., Skoglund, P. *et al.* (2021). Ancient DNA analysis. *Nat Rev Methods Primers* 1, 14. <https://doi.org/10.1038/s43586-020-00011-0>
- Poinar, H. N., Schwarz, C., Qi, J., Shapiro, B., Macphee, R. D., Buigues, B., Tikhonov, A., Huson, D. H., Tomsho, L. P., Auch, A., Rampp, M., Miller, W., & Schuster, S.C. (2006). Metagenomics to paleogenomics: large-scale sequencing of mammoth DNA. *Science (New York, N.Y.)*, 311(5759), 392–394. <https://doi.org/10.1126/science.1123360>
- Salkeld, D. J., & Stapp, P. (2008). Prevalence and abundance of fleas in black-tailed prairie dog burrows: implications for the transmission of plague (*Yersinia pestis*). *The Journal of parasitology*, 94(3), 616–621. <https://doi.org/10.1645/GE-1368.1>
- Sarris, P. (2002). The Justinianic plague: origins and effects. *Continuity and Change*, 17(2), 169–182. [doi:10.1017/S0268416002004137](https://doi.org/10.1017/S0268416002004137).
- Sarris, P. (2022). Viewpoint New Approaches to the ‘Plague of Justinian’. *Past & Present*, 254(1), 315–346. <https://doi.org/10.1093/pastj/gtab024>
- Schoolman, E. M. Reconceptualizing the Environmental History of Sixth-Century Italy and the Human-Driven Transformations of Its Landscapes. (2022). *Studies in Late Antiquity*, 6(4): 707–733. <https://doi.org/10.1525/sla.2022.6.4.707>
- Schmid, B. V., Büntgen, U., Easterday, W. R., Ginzler, C., Walløe, L., Bramanti, B.,

- & Stenseth, N. C. (2015). Climate-driven introduction of the Black Death and successive plague reintroductions into Europe. *Proceedings of the National Academy of Sciences of the United States of America*, *112*(10), 3020–3025. <https://doi.org/10.1073/pnas.1412887112>
- Sessa, K. (2019). The New Environmental Fall of Rome: A Methodological Consideration. *Journal of Late Antiquity*, *12*(1), 211–255. <https://doi.org/10.1353/jla.2019.0008>
- Slavin, P. (2019). Death by the Lake: Mortality Crisis in Early Fourteenth-Century Central Asia. *The Journal of Interdisciplinary History*, *50*(1), 59–90. https://doi.org/10.1162/jinh_a_01376
- Spyrou, M. A., Keller, M., Tukhbatova, R. I., Scheib, C. L., Nelson, E. A., Andrades Valtueña, A., Neumann, G. U., Walker, D., Alterauge, A., Carty, N., Cessford, C., Fetz, H., Gourvenec, M., Hartle, R., Henderson, M., von Heyking, K., Inskip, S. A., Kacki, S., Key, F. M., ... Krause, J. (2019). Phylogeography of the second plague pandemic revealed through analysis of historical *Yersinia pestis* genomes. *Nature Communications*, *10*(4470). <https://doi.org/10.1038/s41467-019-12154-0>
- Spyrou, M. A., Musralina, L., Gnechhi Ruscone, G. A., Kocher, A., Borbone, P.-G., Khartanovich, V. I., Buzhilova, A., Djansugurova, L., Bos, K. I., Kühnert, D., Haak, W., Slavin, P., & Krause, J. (2022). The source of the Black Death in fourteenth-century central Eurasia. *Nature (London)*, *606*(7915), 718–724. <https://doi.org/10.1038/s41586-022-04800-3>
- Vallès, X., Stenseth, N. C., Demeure, C., Horby, P., Mead, P. S., Cabanillas, O., Ratsitorahina, M., Rajerison, M., Andrianaivoarimanana, V., Ramasindrazana, B., Pizarro-Cerda, J., Scholz, H. C., Girod, R., Hinnebusch, B. J., Vigan-Womas, I., Fontanet, A., Wagner, D. M., Telfer, S., Yazdanpanah, Y., ... Baril, L. (2020). Human plague: An old scourge that needs new answers. *PLOS Neglected Tropical Diseases*, *14*(8), e0008251. <https://doi.org/10.1371/journal.pntd.0008251>
- Wagner, D. M., Klunk, J., Harbeck, M., Devault, A., Waglechner, N., Sahl, J. W., Enk, J., Birdsell, D. N., Kuch, M., Lumibao, C., Poinar, D., Pearson, T., Fourment, M., Golding, B., Riehm, J. M., Earn, D. J. D., DeWitte, S., Rouillard, J.-M., Grupe, G., ... Poinar, H. (2014b). *Yersinia pestis* and the Plague of Justinian 541–543 AD: A genomic analysis. *The Lancet Infectious Diseases*, *14*(4), 319–326. [https://doi.org/10.1016/S1473-3099\(13\)70323-2](https://doi.org/10.1016/S1473-3099(13)70323-2)
- Wagner, J. K., Colwell, C., Claw, K. G., Stone, A. C., Bolnick, D. A., Hawks, J., Brothers, K. B., & Garrison, N. A. (2020). Fostering Responsible Research on Ancient DNA. *American journal of human genetics*, *107*(2), 183–195. <https://doi.org/10.1016/j.ajhg.2020.06.017>

Yersin, Alexandre (1894). La peste bubonique à Hong-Kong. *Annales de l'Institut Pasteur* 8: 662–667.

Yue, R. P., Lee, H. F., & Wu, C. Y. (2016). Navigable rivers facilitated the spread and recurrence of plague in pre-industrial Europe. *Scientific reports*, 6, 34867. <https://doi.org/10.1038/srep34867>

Yue, R. P. H., Lee, H. F., & Wu, C. Y. H. (2017). Trade routes and plague transmission in pre-industrial Europe. *Scientific reports*, 7(1), 12973. <https://doi.org/10.1038/s41598-017-13481-2>

Chapter 2: Historical Background

2.1 The Ancient Mediterranean and Histories of the First Plague Pandemic

2.1.1 *Plague Historians*

Several notable late antique historians and writers are of particular significance to the Plague of Justinian and the first plague pandemic overall. Three of these writers are introduced here. Procopius of Caesarea, a major sixth-century authority on whom historians of late antiquity have long relied, is responsible for writing arguably the most widely read narrative of the pandemic in his lengthy account of the wars of Justinian I. Although Procopius is often regarded as the last of the great classical Greek historians (“Procopius of Caesarea,” 2004), little is known about his personal life, and nearly all that *is* known is found in his own writings. Procopius was born in Caesara around the end of the 5th century and was trained in law, noted to have advised Belisarius, a commander who was entrusted to battle the Persian army during Justinian’s reign. As a witness and narrator of the reign of Justinian I, Procopius lived through the Nika Riots, battles for the Vandal kingdom, and remarkably lived through the Plague of Justinian while at Constantinople in 542 AD. Throughout his life, he wrote numerous historical works including the *Wars*, the so-called *Secret History*, and the *Buildings* (“Procopius of Caesarea,” 2004).

In his commentary on Procopius’ *Wars of Justinian*, Kaldellis notes how the narrator has been the only one brave enough to write concurrently with the rule of Justinian I, even sometimes presenting dangerous criticisms of his rule (Prokopios, 2014). Furthermore, although *Wars* was intended for public circulation due to its relatively neutral, biographical purpose, Procopius’ *Secret History*, in contrast, was on

account of the severity of the criticisms present within it, published anonymously; it is evident that this book was not intended for as wide an audience. Nevertheless, notions towards Procopius' growing frustration of the reign of Justinian I is observable in the *Wars*, as historians note, due to the change of tone in its later chapters; Greatrex (2022) notes how Procopius' perspectives are difficult to analyze due to their apparent shifts as events unfold around him. Procopius' writing style has been praised for its clarity and relative simplicity, which in part accounts for why modern historians tend to read him with a positivist lens (Newfield, 2022). Procopius' use of the superlative in his writings, clearly demonstrates his ability and confidence, showing his clear and unyielding judgements (Greatrex, 2022). Predictably, this too may encourage us today to read his text at face value. His inability to determine the cause and severity of plague during his time may also be indicative of the plague's sheer magnitude. Conversely, it could be a product of his goals to write an account of the pandemic in the capital city. While Procopius himself has been noted to have influenced subsequent scholars, his passages on plague particularly imitate those of earlier writers, particularly Thucydides. In addition to other writers including Herodotos and Xenophon, Procopius adopts phrasing and expressions used by Thucydides, and even modelled his account of plague after Thucydides' account of the plague of Athens more than nine centuries prior (Prokopios, 2014). Considering these influences, researchers should be wary of reading plague passages, like Procopius', in a literal sense.

The first-hand account by John of Ephesus from his *Ecclesiastical History* has been lost to time, though it is in large part present in the third section of the Zuqnin Chronicle and the later work of Michael the Syrian. Written by an author whose

identity has only been proposed, the Zuqnin Chronicle describes a plague outbreak nearly two hundred years after John of Ephesus' original account (see Allen, 1979). A recent effort has been made to replace the classic attribution to Dionysius I of Tel-Mahre with attribution to the Zuqnin monastery. Namely, renowned Syriac scholar François Nau first proposed that the true author of a large portion of the text is Joshua the Stylite, a priest who may have resided in the Zuqnin monastery (Chronicler of Zuqnin, 1999). Though revealing the true identity of the Chronicler is no longer considered essential in plague histories, scholars have yet to reach a consensus at the time of writing.

The Zuqnin Chronicle is a compendium of events written in Northern Mesopotamia around the 8th century AD. Although the Chronicle is quick to note the many texts and authors it borrows (often directly copying them), there is no evidence of other authors using it as a reference, displaying how its uniqueness contributes to its significance as a historical text (Chronicler of Zuqnin, 1999). The style of the Chronicle itself has been criticized by scholars due to its frequent cuts and changes in tone, likely due to the many different texts and authors from which it borrows. Specifically, as listed by Witakowski's translation, the author borrows from the Chronicle of Eusebius, the Ecclesiastical History of Socrates Scholasticus, and as elaborated below, the *Ecclesiastical History* of John of Ephesus (Chronicler of Zuqnin, 1996). As a rough estimate, Harrak states that only 29% of the work is the author's own words (Chronicler of Zuqnin, 1999). John of Ephesus, among many other tales of his travels, witnessed the destruction and calamity driven by the Justinianic Plague first-hand. However, many of these stories and nearly the entirety of his *Ecclesiastical History*, has been lost to time. Witakowski's translation draws

attention to the emotion evident within this chapter, likely that of John who offers a sentimental, religious depiction of the plague; John also makes frequent Biblical references, true to his writing style and occupation (Chronicler of Zuqnin, 1996). It is critical to underline how this emotion can transcend both time and language.

Evagrius Scholasticus is also credited with a detailed account of the Plague of Justinian in the fourth book of his own *Historia Ecclesiastica*, though scholars have frequently noted the evident biases and literary devices found in his account. Evagrius was likely born in Epiphania, though this knowledge can only be deduced from his writings. From his own account, he contracted and survived the Justinianic Plague in the early 540s when he was a child. Evagrius went on to pursue a successful legal and scholastic career, earning praise from emperors Tiberius and Maurice (Evagrius Scholasticus, 2000). There is little evidence on Evagrius' personal life, though texts indicate that his first wife and several members of his family had died in subsequent plague outbreaks nearing the end of the sixth century (Allen, 1981). *Historia Ecclesiastica* is Evagrius' only extant work. A collection of six books, Evagrius focuses particularly on the city of Antioch following the works of Chronicler John Malalas (Evagrius Scholasticus, 2000). Although Evagrius has been seen to rely on Procopius' description of military battles (likely due to his lack of first-hand knowledge of them), he offers his own account of events with which he is familiar, such as his account of plague in Antioch from 591-592 AD. Whitby, in his notes of Evagrius' text, notes modern criticism of his use of Procopius' work in that there is clear and evident switching in tone and style, where an emphasis on military and administrative events are replaced with reflections on miracles and religious subtext (Evagrius Scholasticus, 2000).

Some historians, in their own analyses and interpretations, argue that words and phrases used by several historical plague narrators contribute to a “hysterical” narrative and “exaggerate” the significance of the First Plague Pandemic (Aberth, 2018). On the other hand, some researchers have also considered the lack of available plague narratives as indication that the mortality rate of the Justinianic Plague has been overestimated. For instance, Mordechai and colleagues (2019) critique the magnitude of the Justinianic plague by quantitatively analyzing the presence of numismatic and palynological evidence, burials, and genomic data. Overall, they present the argument that the lethality of the Plague of Justinian is overexaggerated in modern research. Meier (2020) directly challenges these results by critiquing their “unusual methodological approach.” He argues that a quantitative approach measuring written sources leaves little room for qualitative, holistic contextualization. Meier defends that the paper, in its efforts to counter a “maximalist approach” instead presents itself as a “minimalist approach” and that no quantitative methodology can ever be more beneficial than qualitative contextualization (Meier, 2020). Aberth (2018) furthers this argument by acknowledging that a lack of sources may instead be reflective of plague’s effect on physical production and dissemination of literary texts; once again, we must be aware that we can only analyze the stories that have survived over the centuries.

To further scholarly research on past plague pandemics, it is crucial that researchers re-visit original copies, translations, and context of first-hand accounts. As recently addressed by Newfield (2022), the sanctity of historical accounts as well as their reliability regarding current research must be put into consideration along with new evidence from other fields. Differences in translation can be described and

categorized both temporally and spatially with differences in language, playing a significant factor in modern interpretation of past historical events. Patterns and indications found within the plague accounts by Procopius, John of Ephesus, and the Chronicler of Zuqin, as well as Evagrius Scholasticus cannot and should not be uniformly transmitted throughout time and space; each account must be independently analyzed and placed into context before being compared to other accounts.

Furthermore, there has been a recent push for the implementation of interdisciplinarity approaches to the study of plague. However, given the speed at which novel scientific data is produced, integration into the accounts of these plague narrators and interdisciplinarity in general is “as deficient as it is common” (Newfield, 2022, p. 576). In his review of the ongoing and seemingly endless debate associated with the subject, Newfield (2022) describes how modern perception, values, and ideals associated with the mass mortality of the Black Death has affected attitudes and approaches to the Justinianic Plague. As such, we see the hidden preconceptions rooted in social context as suggested by Gilbert (2018), even in academic literature. Strict reliance and literal interpretation of historical written sources has been criticized as well; both scientists and historians share equal responsibility in seeking to integrate both approaches. Avoiding a goal of a catastrophe-causing plague “worthy” of the name as well as the notion of an inviolability of historical written sources addresses how future research should present itself.

2.1.2 Waves of Plague in First Pandemic Histories

The analysis of historical sources has posited a series of fourteen to thirty-five epidemic ‘waves’ of first pandemic plague between 541 and 750/751 CE

(Stathakopoulos 2004; Tsiamis *et al.*, 2011; Harper 2017; Keller *et al.*, 2019). The first epidemic wave, according to historical records, initially appeared in Pelusium around 541 CE and spread into the Byzantine provinces and beyond, persisting perhaps to 547 CE in some regions (McCormick 2021). Tsiamis and colleagues (2011) argue that a second wave began in 557 CE, beginning in Mesopotamia before declining in 560 CE and a third wave spreading into neighbouring provinces of Constantinople and Italy around 598 CE. A fourth began in 618 CE, characterized by human involvement with the Byzantine–Sasanian War and the shipment of grain, followed by another from 626 CE to around 639 CE in Palestine and Syria. A sixth wave spread throughout Mesopotamia and Italy in 646 CE, while outbreaks began in Egypt once again around 672 CE. Following this, a 698 CE epidemic in Constantinople marked the advent of the eighth wave, with another occurring from 704-706 CE mainly in Syria and Mesopotamia. Another wave occurred from 711 to 740 CE in the Mediterranean, while the eleventh simultaneously took place in Syria and Egypt from 713-714 CE. With the second siege of Constantinople in 718 CE, another wave affected both the Byzantine and the Umayyad armies. The thirteenth wave took place from 724-725 CE stretching from Egypt to Mesopotamia, preceding another from 732-735 CE. The fifteenth wave took place between 743-745 CE stretching from Egypt to Italy and Constantinople, before a final outbreak in Syria and Mesopotamia occurred from 748-750 CE (Tsiamis *et al.*, 2011). As clear-cut as this chronology may be, it is essential to underscore that the historical evidence is incomplete and that identifying ‘wave’ start and end points reliably is impossible with the evidence in hand; the debatable nature of the surviving evidence explains why tallies of first plague pandemics differ as much as they currently do.

Tsiamis and colleagues (2011) meticulously noted the frequency of the recorded outbreaks. They reveal that the regions of Syria and Mesopotamia had the highest frequency of outbreaks (19 and 13, respectively), followed by Italy and Constantinople (11 and 10, respectively). The authors found that Egypt, Mesopotamia, and Syria increased in frequency from the 6th to the 8th century, whereas outbreaks in Asia Minor, Italy, and Constantinople gradually decreased. Furthermore, epidemics in Palestine were present at the inception of the Justinianic Plague in 541/542 and spiked in the 7th century before decreasing in frequency by the mid-8th century. The greatest number of outbreaks occurred during the mid-6th century with a total of 31 recorded documents across all provinces (Tsiamis *et al.*, 2011). As mentioned, researchers are not yet certain if and how the frequencies of these outbreaks shed light on the survival of written sources and the presence of literate observers. Interestingly, there are, or so it appears, nine brief “plague-free” periods of time between the mid-6th to mid-8th century. However, once again, this assumption is based on a lack of mention of plague in historical records during these periods; as will be covered in later chapters, absence of evidence is not evidence of absence. Tsiamis and colleagues (2011) posit that the waves of the disease may be due to enzootic areas in the affected regions. The authors also note that natural disaster events (most notably earthquakes) have preceded the start of many of the waves (Tsiamis, 2018). Additionally, sequential volcanic eruptions within a decade preceding the inception of the Justinianic Plague generated a volcanic winter, of which was documented by plague narrators such as Procopius and Michael the Syrian (Gibbons, 2018). Crucially, however, scarce definitive knowledge of spatiotemporal variables such as temperature, climate, and precipitation has limited how well researchers may utilize climatological data to corroborate the

ancient narratives of plague contemporaries (Luterbacher *et al.*, 2020). Nevertheless, though more research should be dedicated to investigating them, environmental factors may indeed have impacted enzootic areas in and around the Mediterranean region prior to each outbreak, contributing to the epidemic waves.

2.2 Historical Sites in Study

2.2.1 İznik Roman Theatre

The İznik Roman Theatre is an ancient site located in Bursa province of Turkey built under Plinius during the reign of Emperor Trajan in the 2nd century CE. The theatre is hypothesized to have fit over 10,000-15,000 spectators though was never completed in its entirety (Meriç, 2018; “Iznik Roman Theater Excavation,” n.d; Özgümüş, 2008). Dokuz Eylul University carried out the excavation and restoration of the Roman Theater with permission from Turkey’s Ministry of Culture and Tourism (“Iznik Roman Theater Excavation,” n.d). The site is proposed to have initially been used for religious purposes, though its components were stripped for building materials in defense of raids in the 8th century, before being converted into cemetery plots in the 12th century (Alper *et al.*, 2022). It continued to stand during the late Byzantine and Ottoman occupations as deduced through dating of ceramic kilns found in the area. Other archaeological findings include Roman pottery dating between 368 CE and 557 CE, coins from the 4th century CE, as well as glass, lamps, and jewelry (Özgümüş, 2008; Meriç, 2018). Recent excavations resulted in the discovery of human remains (likely Byzantine soldiers) buried in groups of six to eight, though the definitive reason for these mass burials is currently unknown (Özgümüş, 2008).

2.2.2 Haydarpaşa Train Station

The Haydarpaşa train station was designed and constructed in the early 20th century, symbolizing the good relationship between the Ottoman Empire and imperial Germany at the time of its construction (“Archaeological remains,” 2018; Aslankaya and Ustundag, 2019). The exterior of the train station was severely affected by a fire in late 2010 (Aslankaya and Ustundag, 2019; Kosebay Erkan, 2013). Notably, the train station is located in the ancient city of Chalcedon (present-day Kadıköy) called “the town of the blind” due its settlers overlooking the more ideally placed Byzantium on the opposite side of the river (Long, 1856). Historically, Chalcedon was part of the ancient kingdom of Bithynia, before being brought under Roman rule. It survived attacks by Mithridates before being labelled a free city and was eventually used to build Constantinople under the Ottoman Empire (Long, 1856). Excavations underneath the railroad tracks and around the train station began in 2018. During these excavations, an intact skeleton was found archaeologically dated to around the 11th century. Various coins dating to the 5th and 6th centuries as well as jewelry were found at the site. Additionally, a fountain dated to the Byzantine Period was recovered, along with podiums attributed to the Hellenistic Period. (“Intact skeleton,” 2018).

2.2.3 İznik Hisardere Necropolis

The Hisardere Necropolis is an archaeological site within the Turkish village of Hisardere, located 1.5 km from İznik; the necropolis is linked to the ancient Greek city of Nicaea (Eraslan and Altin, 2021). Excavation is currently ongoing and is conducted by the Archeology Department of İzmir’s Dokuz Eylül University (“Mummified skeletons,” 2021). The university noted how the remarkably well-preserved material

culture highlights the site's significance to the understanding of burial customs in Nicaea, spanning the 2nd to 5th centuries (“İzник Hisardere Necropolis,” n.d.). Meriç and Dreyer (2021) investigated two sarcophagi dated to the Roman Period at the necropolis. Their investigation revealed that one of the sarcophagus housed an individual named Antigonos, who was interred wearing a wool shroud. A glass bottle from the 3rd century CE, a wooden pillow, and a bed were also retrieved. The second sarcophagus contained a mother and daughter according to its inscriptions, who were interred with shrouds of linen, wool, and silk; mosaics surrounding this sarcophagus were dated to the 4th to 5th century CE.

2.2.4 Ayasuluk

Ayasuluk is found in Selçuk within the province of İzmir and incorporates the historical site of Ephesus (Caner Yüksel, 2019). Previous names for the settlement include Theologus by Byzantine scholars and Altoluodo in Italian sources, before being called Ayasoluk or Ayasuluk and later Selçuk in the 20th century (Caner Yüksel, 2019). The earliest known settlement in this site was called Apasa and was likely a settlement of the Hittite Empire in the Late Bronze Age (Caner Yüksel, 2019). Pottery fragments and a section of a Late Bronze Age wall has been posited to mark the location of Apasa (Bryce, 2009 citing Büyükkolancı, 2000). After the death of Alexander the Great, the settlement became known as Ephesus under Demetrius I and was known as an important location in the history of early Christianity, namely through its construction of holy buildings such as the Church of St. Mary and the Basilica of John the Apostle (Tepgec and Gorgulu, 2022; Caner Yüksel, 2019). Ayasuluk replaced Ephesus by the Aydınids in the 14th and 15th centuries (Caner

Yüksel, 2019). In addition to the individuals analyzed in this study, recent archaeological excavations at Ayasuluk Hill have recovered human remains. Particularly, Tepgec and Gorgulu (2022) sought to determine the origins of soldiers in the city of Ephesus during the Wars of the Diadochi. The study posited that their mitochondrial haplogroups were of European origin.

2.2.5 Agora of Smyrna

The initial location of Smyrna existed from the Neolithic to the Chalcolithic Periods (Esroy, 2016). The location of the site was moved under the orders of Alexander the Great, though the commands were carried out by Antigonos and Lysimachus upon the former's death (Schmitz, 1857b; Esroy 1857b). Its proximity to the sea and harbour contributed to its success as a commercial city; as a central place for trade, its fertile lands were inhabited continuously from the Hellenistic to Ottoman and then Republican Periods (Schmitz, 1857b; Esroy, 2016). The agora (a public gathering space in ancient Greece) of Smyrna was restored by Marcus Aurelius after its destruction by an earthquake in 178 CE (Şahin & Taslialan, 2010). Smyrna has historically claimed to be the birthplace of Homer, and a temple and statue were created in his honour (Schmitz, 1857b). Excavations began in 1932 before being abandoned in 1941 and resuming in 1996 (Şahin & Taslialan, 2010). Archaeological findings include sculptures created using two types of marble likely made in the 5th century CE, though most sculptures were likely created and erected in the 2nd century CE (Şahin & Taslialan, 2010); these material findings corroborate reports of Smyrna's mastery of philosophy and architecture (Schmitz, 1857b; Şahin & Taslialan, 2010).

2.2.6 *Metropolis*

Metropolis is an ancient city located in the province of İzmir known as the “City of the Mother Goddess” (Aybek *et al.*, 2009). Archaeological excavations began in 1990, and evidence has been collected from the Classical, Hellenistic, Roman, Byzantine, and Ottoman periods (“Cult of Zeus,” 2015). Interestingly, excavations in 2015 uncovered inscribed columns and pieces of an altar that belonged to a sanctuary of Zeus Krezimos, a cult of Zeus (Aybek *et al.*, 2018). The term Krezimos is said to be related to the word “crescere” meaning “to grow” in Latin, linking the group as one who strived for the growth of Metropolis with Zeus’ intervention; the group plausibly began in the 2nd century BCE and continued into the Roman period (“Cult of Zeus,” 2015). inscriptions link the cult to ceremonial rituals associated with water and fertility, with columns listing the names of the cult’s priests (Aybek *et al.*, 2018). Similar inscriptions describing cults of Hera and Ares have also been revealed, though the exact locations of their sanctuaries have not yet been located (Aybek *et al.*, 2018). Restorations in 2021 have repaired mosaics revealing depictions of the Greek gods Eros and Dionysus, with the latter’s wife Ariadne. Archaeologists posit that, as Metropolis was known for its festivities and theatre, visitors would be welcomed with mosaics depicting Dionysus, the god of festivity and theater (“Mosaics Restored,” 2021). Additionally, Metropolis was also known for their production of wine (Schmitz, 1857a).

2.2.7 *Perinthos*

Founded in 602 BCE (with some reports dictating its founding date as 599 BCE), Perinthos was initially a Samian colony (Dyer, 1857; Sayar, 2021). Roman emperor

Diocletian renamed Perinthos to Herakleis in 286 CE, though the title Perinthos was used historically until the mid-15th century (Sayar, 2021; Gregory, 2005). Plutarch and Diodorus Siculus document the site's use as defence against attacks by Philip of Macedon. Perinthos also had an affinity for commerce with its converging roads; this splendour may explain the surviving numismatic evidence of large celebrations (Dyer, 1857). Procopius' *Buildings* mention that, prior to the flourishing and independence of Constantinople, Perinthos had been Europa's most important city (Gregory, 2005). Archaeological remains include that of an aqueduct and a church, the former denoted by Procopius to have been restored by Emperor Justinian I and latter rebuilt by the Byzantine emperor Maurice upon its destruction by the Pannonian Avars in 592 CE (Dyer, 1857; Gregory, 2005). Today, the city is part of the Marmara Ereğlisi municipality in Turkey.

2.2.8 Priene

Definitive information about Priene as a settlement before the 4th century BCE remains unknown, though it was likely already established during the Ionian Revolt in 494 BCE (Raeck *et al.*, 2012). The city became part of the Seleucid and later of the Ptolemaic Empires, before then being part of the Roman and Byzantine Empires; it was under the latter's rule that it served as a bishopric suffragan to the larger city of Ephesus before being renamed to Sampson (Raeck *et al.*, 2012; Thonemann, 2018). Bountiful pottery and material culture have complimented Priene's clear stratigraphy (Amicone *et al.*, 2022). Notable archaeological findings include Hellenistic carvings of documents on the Temple of Athena Polias (built with Alexander the Great as its benefactor) as well as its many intact ancient public buildings such as a theater and the

Hellenistic bouleuterion (Cook and Spawforth, 2012; Raeck, 2012; Amicone *et al.*, 2022). Other structures include the Temple of Asklepios and the Sanctuary of Demeter and Kore. Priene is believed to have been inhabited until around 1300 CE (Raeck, 2012).

2.2.9 Kadıkalesi

Kadıkalesi is a Byzantine castle located within the Kuşadası municipality in Turkey, encompassing what was the ancient site of Anaia (Miszczak *et al.*, 2016). The discovery of a bronze statue in 2002 hints that the site was inhabited since at least the early Bronze Age, specifically around the Hittite Empire; this coincides with a legend that Anaia was the name of an Amazon who was buried there (Cramer, 1832; Demir, 2011; Miszczak, 2016). Archaeological excavations have also been conducted, revealing six archaeological strata: the Late Chalcolithic Age, the Early Bronze Age, the Middle Bronze Age, the Late Bronze Age, the Ancient Greek and Roman Empires, and the Islam-Byzantine stage (Akdeniz, 2007 as cited in Demir, 2011). With retrieval and analysis of pottery shards characteristic of the 12th to 13th centuries, Kadıkalesi was also posited to be a fortress used to defend Anaia in the late Byzantine period (Kirmizi *et al.*, 2015). The study by Kirmizi and colleagues (2015) also used the non-destructive methods of Raman spectroscopy and scanning electron microscopy to hypothesize the use of the ancient pigment *Naples yellow*; this is a notable finding due to how the pigment was scarcely seen in pottery between the establishment of the Roman Empire and the Renaissance.

2.3 Silivri District Necropolis (BOTAŞ Excavation)

The construction of a natural gas pipeline in the district of Silivri in Turkey (roughly 76 km from Istanbul) uncovered an ancient necropolis. The excavation of the site was conducted by the Istanbul Archaeological Museums and uncovered a total of 130 graves. An ancient water channel was determined to have extended in the northeast-southwest direction, with graves based to the north and south of it. Two graves were covered with stone lids, though earth and tile roofs were also recognized. The structural characteristics of the graves as well as items within them contribute to an estimated archaeological date of around the 7th century. (V. Onar, personal communication, April 14, 2024). In this study, remains of a plague-positive individual were retrieved from an uncovered area of the necropolis, where very few bone fragments and teeth were linked to an adult and child plausibly buried in close proximity.

2.4 References

- Aberth, J. 2018. 'If a German Migrates into Your Empire, Do Not Be Alarmed: The Decline and Fall of Rome'. In *Contesting the Middle Ages*. Routledge.
- Allen P. (1979). *The "Justinianic" plague*. Byzantion; revue internationale des etudes byzantines, 49, 5–20.
- Allen, P. (1981). *Evagrius Scholasticus, the Church Historian*. Leuven: Spicilegium sacrum Lovaniense.
- Archaeological remains from Byzantine era found during restoration of historic Istanbul station*. (2018, August 1). Hürriyet Daily News.
<https://www.hurriyetdailynews.com/archaeological-remains-from-byzantine-era-found-during-restoration-of-historic-istanbul-station-135155>
- Aslankaya, G., Ustundag, C. (2019). Structural Analysis and Evaluation of the Historic Haydarpasa Railway Station. In: Aguilar, R., Torrealva, D., Moreira, S., Pando, M.A., Ramos, L.F. (eds) *Structural Analysis of Historical*

Constructions. RILEM Bookseries, vol 18. Springer, Cham.
<https://doi.org/10.1007/978-3-319-99441-3>

- Aybek, S., Aygün E.M., Öz, A.K. (2009). *A mother goddess city in Ionia: Metropolis. An archaeological guide*. Istanbul: Homer Kitabevi.
- Aybek, S., Dreyer, B., & Sponsel, C. (2018). The sanctuary of Zeus Krezimos in Metropolis in Ionia. *Gephyra*, 15, 71–94.
<https://doi.org/10.37095/gephyra.420744>
- Bryce, T. (2009). *The Routledge Handbook of the Peoples and Places of Ancient Western Asia : The Near East from the Early Bronze Age to the fall of the Persian Empire*. Taylor & Francis Group.
- Caner Yüksel, Ç. (2019). A Tale of Two Port Cities: Ayasuluk (Ephesus) and Balat (Miletus) during the Beyliks Period. *Al-Masāq*, 31(3), 338–365.
<https://doi.org/10.1080/09503110.2019.1620998>
- Chronicler of Zuq̄nin. (1999). *The Chronicle of Zuq̄nīn, Parts III and IV: A.D. 488-775*. (A. Harrak, Trans.). Toronto: Pontifical Institute for Medieval Studies.
- Chronicler of Zuq̄nin (Pseudo-Dionysius of Tel-Mahre). (1996). *Chronicle: Part III*. (W. Witakowski, Trans.). Translated Texts for Historians. Liverpool: University Press.
- Chronicler of Zuq̄nin. (2017). *The Chronicle of Zuq̄nīn: Parts I and II. From the Creation to the Year 506/7 AD*. (A. Harrak, Trans.). *The Chronicle of Zuq̄nīn*. Gorgias Chronicles of Late Antiquity. Gorgias Press.
<https://doi.org/10.31826/9781463237370>.
- Cook, J., & Spawforth, A. (2012). Priene. In *The Oxford Classical Dictionary*. Oxford University Press. Retrieved 2 Jul. 2024, from <https://www-oxfordreference-com.libaccess.lib.mcmaster.ca/view/10.1093/acref/9780199545568.001.0001/acref-9780199545568-e-5326>.
- Cramer, J. A. (1832). *A Geographical and Historical Description of Asia Minor; with a Map: Vol. II*. Oxford: University Press Section X Caria.
- Cult of Zeus found in Metropolis*. (2015, December 16). Hürriyet Daily News.
<https://www.hurriyetaidailynews.com/cult-of-zeus-found-in-metropolis--92606>
- Demir, S. (2010). *Characterization of Pigments Used in the Execution of Wall Paintings in Kadıkalesi* [M.Sc., Izmir Institute of Technology (Turkey)].
<https://hdl.handle.net/11147/3815>

- Dyer, T.H. (1857). Perinthus. In *Dictionary of Greek and Roman geography. (Vol. 2)*, edited by William Smith, 577. London: Walton & Maberly.
<https://babel.hathitrust.org/cgi/pt?id=uc2.ark:/13960/t8df6z636&seq=593&q1=perinthus>
- Eraslan, S., & Altin, A. A., (2021). An Extraordinary Columnar Sarcophagus From Nikaia. *OLBA*, vol.29, 269-286.
- Ersoy, A. (2016). History of Excavations in Smyrna. In R. Bagnall, R. Casagrande-Kim, A. Ersoy & C. Tanriver (Ed.), *Graffiti from the Basilica in the Agora of Smyrna* (pp. 1-54). New York, USA: New York University Press.
<https://www.jstor.org/stable/j.ctt1w8h3mx>
- Ersoy, A., & Tekoğlu, Ş. R. (2021). New Inscriptions from Smyrna. *Gephyra*, 22, 167-180. <https://doi.org/10.37095/gephyra.987927>
- Evagrius Scholasticus. (2000). *The Ecclesiastical History of Evagrius Scholasticus*. (M. Whitby, Trans.). Translated Texts for Historians 33. Liverpool: University Press.
- Gibbons, A. (2018). Eruption made 536 ‘the worst year to be alive’. *Science*, 362(6416), 733–734. <https://doi.org/10.1126/science.362.6416.733>
- Greatrex, G. (2022). *Procopius of Caesarea: The Persian Wars: A Historical Commentary*. Cambridge: Cambridge University Press.
<https://doi.org/10.1017/9781107282025>.
- Gregory, T. (2005). Herakleia. In *The Oxford Dictionary of Byzantium*. Oxford University Press. <https://www-oxfordreference-com.libaccess.lib.mcmaster.ca/display/10.1093/acref/9780195046526.001.0001/acref-9780195046526-e-2257>
- Güngör Alper, E., Meriç, A. E., & Somuncu, F. (2022). Iznik Roman Theater Excavations Local Samples Of Esc Ceramics And Implications. *Dokuz Eylül Üniversitesi Sosyal Bilimler Enstitüsü Dergisi*, 24(2), 449-465.
<https://doi.org/10.16953/deusosbil.1102835>.
- Harper, K. (2017). *The fate of Rome climate, disease, and the end of an empire*. Princeton University Press. <https://doi.org/10.1515/9781400888917>
- Hays, J.N. (2006). ‘Historians and Epidemics: Simple Questions, Complex Answers’. In *Plague and the End of Antiquity: The Pandemic of 541–750*, edited by Lester K. Little, 33–56. Cambridge: Cambridge University Press. <https://doi.org/10.1017/CBO9780511812934.005>.
- Intact skeleton found in Haydarpaşa train station excavations*. (2018, October 26).

Hürriyet Daily News. <https://www.hurriyetdailynews.com/intact-skeleton-found-in-haydarpasa-train-station-excavations-138307>

Iznik Hisardere Necropolis | *DEU – Archaeology*. (n.d.). Dokuz Eylül University Faculty of Letters. Retrieved 2 July 2024, from https://arkeoloji.deu.edu.tr/?page_id=849&lang=en

Iznik Roman Theater Excavation and Restoration Works | *DEU – Archaeology*. (n.d.). Retrieved 2 July 2024, from https://arkeoloji.deu.edu.tr/?page_id=168&lang=en

Kanz, F., Pfeiffer-Taş, Ş., Forstenpointner, G., Galik, A., Weissengruber, G., Grossschmidt, K., & Risser, D. U. (2014). Investigations on human and animal remains from a medieval shaft well in Ayasuluk/Ephesos (Turkey). *Anthropologischer Anzeiger*, 71(4), 429–445. <http://www.jstor.org/stable/24252944>

Keller, M., Spyrou, M. A., Scheib, C. L., Neumann, G. U., Kröpelin, A., Haas-Gebhard, B., Pfüffgen, B., Haberstroh, J., Ribera i Lacomba, A., Raynaud, C., Cessford, C., Durand, R., Stadler, P., Nägele, K., Bates, J. S., Trautmann, B., Inskip, S. A., Peters, J., Robb, J. E., ... Krause, J. (2019b). Ancient *Yersinia pestis* genomes from across Western Europe reveal early diversification during the First Pandemic (541–750). *Proceedings of the National Academy of Sciences of the United States of America*, 116(25), 12363–12372. <https://doi.org/10.1073/pnas.1820447116>

Kırmızı, B., Göktürk, E. H., & Colombari, P. (2015). Colouring Agents in the Pottery Glazes of Western Anatolia: New Evidence for the Use of Naples Yellow Pigment Variations During The Late Byzantine Period. *Archaeometry*, 57(3), 476–496. <https://doi.org/10.1111/arcm.12101>

Kosebay Erkan, Y. (2013). Haydarpasa Train Station: present, past and future/Haydarpasa Tren Gari: Bugun, dun ve yarin kentin bedeninde bir yara. *METU Journal of the Faculty of Architecture*, 30(1), 99+. <https://doi.org/10.4305/metu.jfa.2013.1.6>

Long, G. (1856). Chalcedon. In *Dictionary of Greek and Roman geography. (Vol. 1)*, edited by William Smith, 596-597. London: Walton & Maberly.

Luterbacher, J., Newfield, T. P., Xoplaki, E., Nowatzki, E., Luther, N., Zhang, M., & Khelifi, N. (2020). Past pandemics and climate variability across the Mediterranean. *Euro-Mediterranean Journal for Environmental Integration*, 5(2), 46–46. <https://doi.org/10.1007/s41207-020-00197-5>

Meriç, A. E. (2018). Late Roman Pottery from the Theatre of Nicaea in Bithynia. *Anatolia Antiqua. Revue Internationale d'archéologie Anatolienne*, XXVI,

Article XXVI. <https://doi.org/10.4000/anatoliaantiqua.572>

- Meriç, A. E., & Dreyer, B. (2021). Inschriften auf Stein-Sarkophagen von der Hisardere-Nekropole von Nikaia. *Gephyra*, 21, 47-63.
<https://doi.org/10.37095/gephyra.864218>
- Mosaics restored in ancient Metropolis*. (2021, October 15). *Hürriyet Daily News*.
<https://www.hurriyetdailynews.com/mosaics-restored-in-ancient-metropolis-168639>
- Miszczak, I. (2016). *Around Ephesus and Kuşadası*. ASLAN Publishing House.
- Morony, M.G. (2006). “‘For Whom Does the Writer Write?’: The First Bubonic Plague Pandemic According to Syriac Sources”. In *Plague and the End of Antiquity: The Pandemic of 541–750*, edited by Lester K. Little, 59–86. Cambridge: Cambridge University Press.
<https://doi.org/10.1017/CBO9780511812934.006>.
- Mummified skeletons found in Turkey’s west*. (2021, October 9). *Hürriyet Daily News*.
<https://www.hurriyetdailynews.com/mummified-skeletons-found-in-turkeys-west-168485>
- Newfield, T.P. (2022). ‘One Plague for Another? Interdisciplinary Shortcomings in Plague Studies and the Place of the Black Death in Histories of the Justinianic Plague’. *Studies in Late Antiquity* 6 (4): 575–626.
<https://doi.org/10.1525/sla.2022.6.4.575>.
- Özgümüş, Ü. (2008). Byzantine glass finds in the Roman theater at İznik (Nicaea). *Byzantinische Zeitschrift*, 101(2), 727-735. <https://doi.org/10.1515/BYZS.2008.021>
- ‘Procopius of Caesarea’. (2004). In *Encyclopedia of World Biography*, 2nd ed., 12:457–58. Detroit, MI: Gale.
- Prokopios. (2014). *The Wars of Justinian*. (A. Kaldellis, Ed.; H.B. Dewing, Trans.). Hackett Publishing Company, Inc.
- Raeck, W. (2012). Priene. In *The Encyclopedia of Ancient History* (eds R.S. Bagnall, K. Brodersen, C.B. Champion, A. Erskine, and S.R. Huebner). <https://doi.org/10.1002/9781444338386>
- Şahin, M. & Taslialan, M., (2010). Sculptural Finds From the Agora of Smyrna. *OLBA*, vol.18, 175-240.
- Sayar, M.H. (2021). Perinthos (Herakleia). In *The Encyclopedia of Ancient History* (eds R.S. Bagnall, K. Brodersen, C.B. Champion, A. Erskine, and S.R.

Huebner). <https://doi.org/10.1002/9781444338386>

Schmitz, L. (1857a). Metro'polis. In *Dictionary of Greek and Roman geography. (Vol. 2)*, edited by William Smith, 351-352. London: Walton & Maberly.

<https://babel.hathitrust.org/cgi/pt?id=uc2.ark:/13960/t8df6z636&seq=593&q1=perinthus>

Schmitz, L. (1857b). Smyrna. In *Dictionary of Greek and Roman geography. (Vol. 2)*, edited by William Smith, 1016-1017. London: Walton & Maberly.

<https://babel.hathitrust.org/cgi/pt?id=uc2.ark:/13960/t8df6z636&seq=593&q1=perinthus>

Tepgec, F., & Gorgulu, M. (2022). The Mitochondrial Origins of the Hellenistic Individuals of Ayasuluk Hill. *Experimed*, 12(3),

139+. <https://doi.org/10.26650/experimed.1183293>

Thonemann, P. (2018). Priene. In *The Oxford Dictionary of Late Antiquity.*: Oxford University Press. Retrieved 2 Jul. 2024, from

<https://doi.org/10.1093/acref/9780198662778.001.0001>

Tsiamis, C., Poulakou-Rebelakou, E., Tsakris, A., & Petridou, E. (2011). Epidemic waves during Justinian's plague in the Byzantine Empire (6th-8th c. AD).

Vesalius: acta internationales historiae medicinae, 17(1), 36–41.

Chapter 3: Methods and Results

3.1 Introduction

This study seeks to retrieve evidence for the first *Y. pestis* genome from first pandemic Turkey. Plague is thought to have been immensely devastating in Turkey based on the written sources that address the presence of plague in the Northeast Mediterranean. Specifically, even a single genome from the Mediterranean would offer insight into the accuracy and merit of long-trusted historical sources. However, it is crucial to acknowledge that a single novel genome from this study cannot determine how many people died during the pandemic nor the direction it travelled. Nevertheless, its discovery may be used to shift the current understanding of the first pandemic, which has genomically been restricted to European sites.

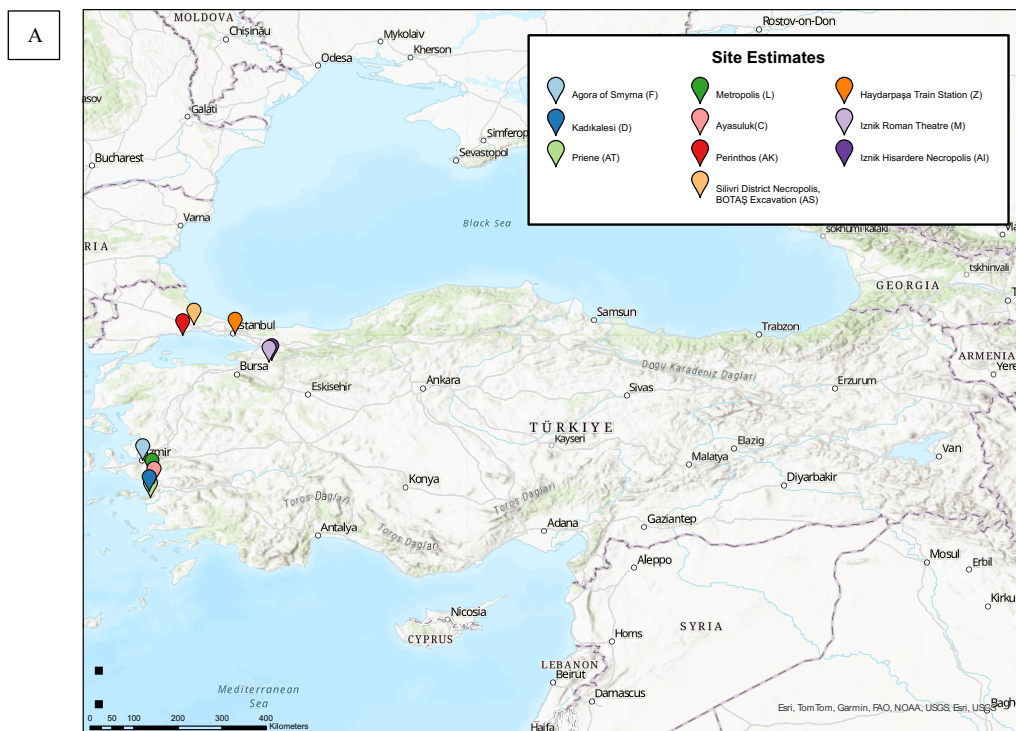
In summary, 134 human teeth archaeologically dated to around the 7th century in Turkey were processed. Screening and sequencing results support the presence of authentic ancient *Y. pestis* in a tooth belonging to individual BFP39. However, as this preliminary analysis only involved shotgun sequencing, very few relative *Y. pestis* reads were able to be mapped. Thus, enrichment will be required for future evolutionary analysis to selectively increase the pathogenic portion of a given extract.

3.2 Samples

3.2.1 Sample Size

Human and animal remains dating to the late Roman/early Byzantine period were retrieved from excavation archives by Dr. Vedat Onar from İstanbul University-Cerrahpaşa for genomic analysis at the McMaster University Ancient DNA Centre.

Remains from 9 known historical sites were analyzed: İznik Roman Theatre (M), Haydarpaşa Train Station (Z), İznik Hisardere Necropolis (AI), Ayasuluk (C), the Agora of Smyrna (F), Metropolis (L), Perinthos (AK), Priene (AT), and Kadikalesi (D). These sites are significant due to their spatial proximity to areas said to have harboured plague in ancient records and to areas long thought to have been devastated by first pandemic plague, particularly the great antique cities of Constantinople and Ephesus (Stathakopoulos, 2004; Mordechai and Eisenberg, 2019; Sarris 2022). An additional 76 teeth were retrieved from a necropolis revealed during a pipeline excavation in the Silivri district (AS). A total of 134 human teeth were analyzed (Table 3.1). Though multiple teeth were recovered for several individuals, only one tooth per individual was processed for shotgun sequencing in efforts to minimize destruction and consumption of ancient human remains.



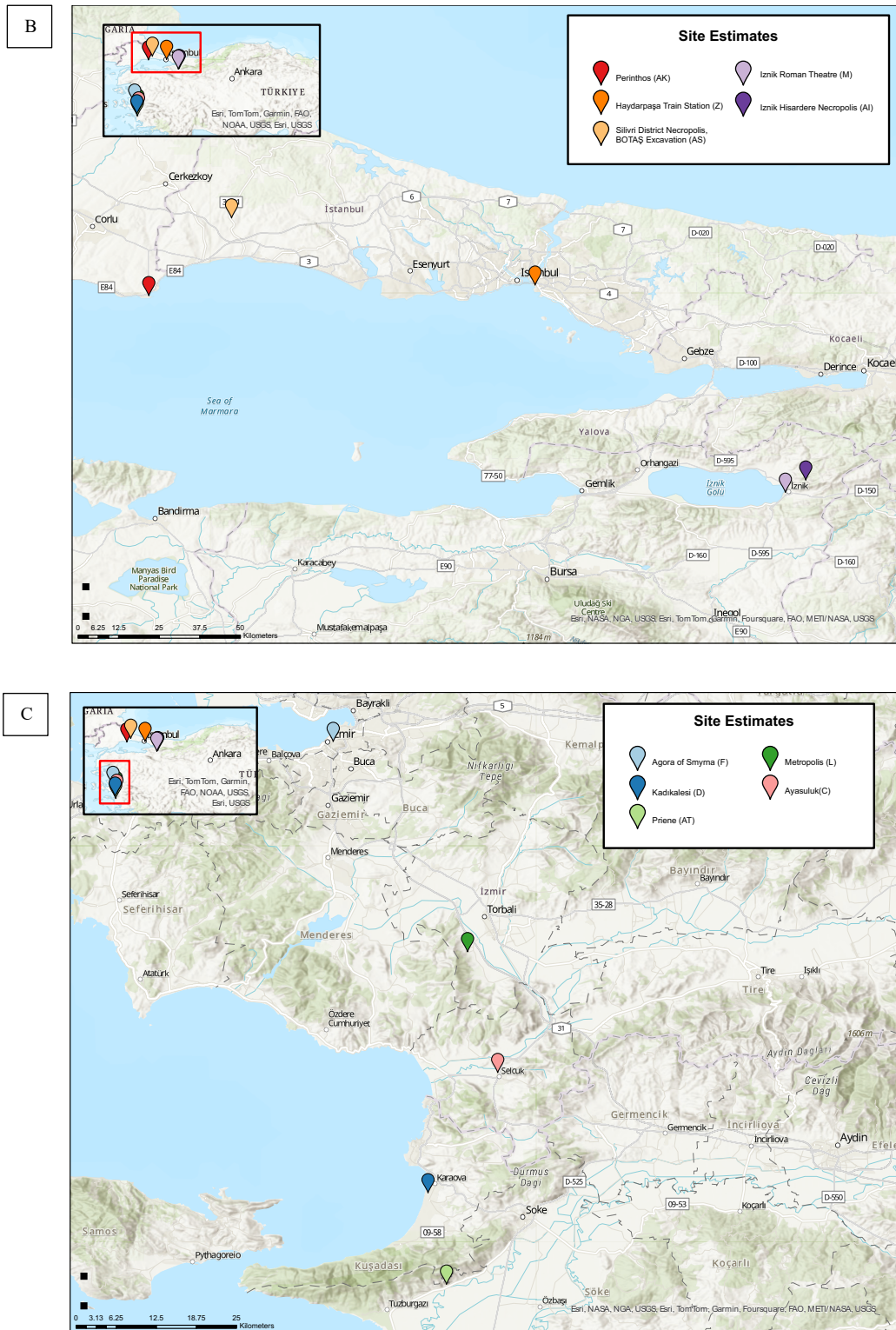


Figure 3.1 (a-c): Site Estimates. Remains have been sent by Dr. Vedat Onar from İstanbul University-Cerrahpaşa. a) An overview of all ten sites included in this study: İznik Roman Theatre (M), Haydarpaşa Train Station (Z), İznik Hisardere Necropolis (AI), Ayasuluk (C), Agora of Smyrna (F), Metropolis (L), Perinthos (AK), Priene (AT), Kadikalesi (D), and the necropolis in Silivri district (AS). b) Sites in northern Turkey (AK, AS, AI, M, Z). c) Sites in northwestern Turkey (AT, C, D, F, L). Created using ArcGIS Pro.

Number of Human Teeth Analyzed Per Site										
Site	Iznik Roman Theatre (M)	Haydarpaşa Train Station (Z)	Iznik Hisardere Necropolis (AI)	Silivri District Necropolis, BOTAŞ Excavation (AS)	Ayasuluk (C)	Agora of Smyrna (F)	Metropolis (L)	Perinthos (AK)	Priene (AT)	Kadıkalesi (D)
Count	8	1	5	76	13	1	7	10	12	1

Table 3.1: Number of Human Teeth Analyzed Per Site. A total of 134 teeth were processed and analyzed for the presence of ancient pathogens.

3.2.2 Ethics Approval

This study was approved by the Hamilton Integrated Research Ethics Board (HiREB) under Project #2023-15356-T. Notably, some aspects of the research were conducted before final approval was granted by the ethics board. Specifically, most of the teeth had already been subsampled and carried through library preparation as the application was being processed; this was in part due to how related plague studies conducted within the Ancient DNA Centre had been given prior approval, issues with timing, and largely because a standard protocol for ethical approval of ancient remains has yet to be established. Upon being granted HiREB approval, we were advised to detail why parts of the study were included despite the lack of REB oversight, with feedback mentioning that “rarity of the samples and the absence of risk to the participants” was sufficient. As mentioned, at the time of writing, there is no set protocol for ethical approval of ancient samples under HiREB. As will be expanded in Chapter 5 of this thesis, much more needs to be done in terms of how to ethically consider the integrity of ancient human remains; ethical consideration for ancient human remains is largely considered optional on many ethics boards if there is no risk to living participants. However, simply having an absence of risk to living participants should not be enough to warrant approval. Moreover, the pace of ancient DNA studies

played a role in why we chose to begin the project without being granted final approval. Though I acknowledge the obvious time constraints of a master's thesis, advocating for a more ancient DNA-oriented ethics process would have improved this project. Not only do we as aDNA researchers have to consider ethics approval as a priority, but so do the ethics boards themselves; as will be expressed in subsequent chapters, this notion must be of prime concern.

Current and future research projects rooted in ancient DNA, infectious disease, and beyond, should be committed to decentralizing the science (Fleskes *et al.*, 2022). There must be serious, active, and frequent attempts to contemplate any harm that may affect modern communities. Admittedly, distinguishing modern stakeholders and descendant populations may be more difficult to accomplish when interacting with ancient human remains. Nevertheless, it is the responsibility of pursuing researchers to align their goals with those of non-scientific perspectives. With current efforts expanding the global narrative for the first plague pandemic, there must be careful consideration when working with remains and communities outside of Europe, in efforts to integrate lasting, meaningful relationships cohesively and effectively.

3.3 Laboratory Procedures

3.3.1 Subsampling

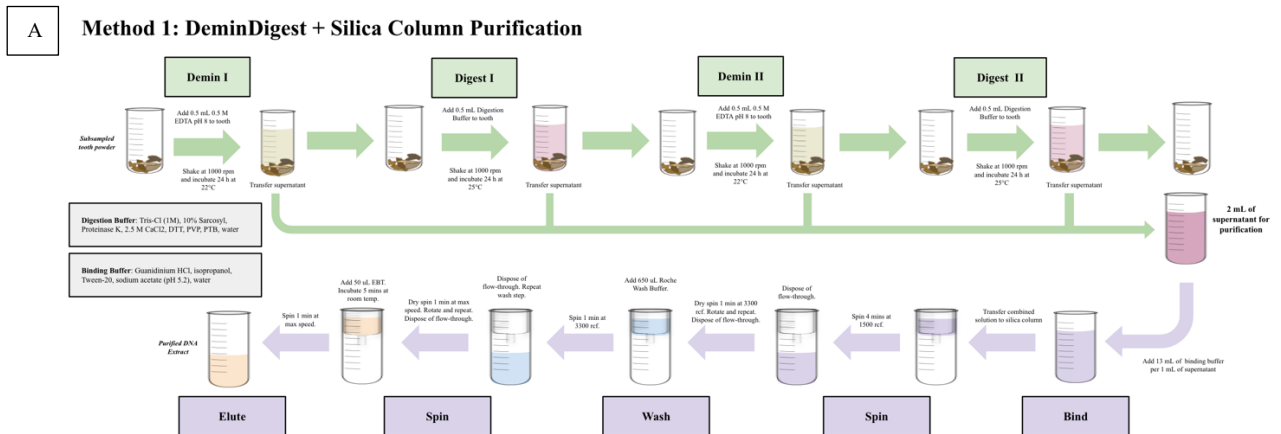
Currently, the only method of detecting *Y. pestis* in ancient remains is when it has entered the bloodstream of the deceased individual. The method of subsampling in most plague studies, of which has been utilized for several papers publishing first pandemic genomes, involves the use of a Dremel rotary tool on a tooth (Feldman *et al.*, 2018; Keller *et al.*, 2019). The tool cuts along the cemento-enamel junction of the

tooth, separating the crown, and then drilling with a pointed drill bit into the roots to collect pulp powder. About 10-50 mg of powder is then carried over to extraction (Klunk *et al.*, 2019). Notably, this method generates a significant amount of heat which can degrade DNA and increases the likelihood of fragmenting the tooth entirely.

3.3.2 *aDNA Extraction*

The subsampled powder underwent two different methods of extraction. The first method involves decalcification of the mineral matrix of the pulp powder using Ethylenediaminetetraacetic acid (EDTA) and then digestion of the exposed proteins using a digestion buffer (1 M Tris-Cl, Sarcosyl, calcium chloride, Polyvinylpyrrolidone, N-phenacyl thiazolium bromide, dithiothreitol, and Proteinase K); this process is repeated and is conducted over the course of five days or until the calcified tissues have demineralized (Schwarz, 2009). A high-volume binding buffer (guanidine hydrochloride, isopropanol, Tween-20, and sodium acetate) and silica column optimized for DNA extraction was employed (Dabney, Knapp, & Glocke *et al.*, 2013). The chaotropic salt Guanidinium chloride, the primary active ingredient in the buffer, binds DNA to the silica column so that non-positively charged molecules can be washed off, purifying the extract, and freeing it of inhibitors. An elution buffer using Tween-20 was then used to flush the purified DNA from the silica column into new tubes for screening and sequencing preparation. This method was used on subsamples from the known historical sites; this sample set was processed first as they were able to be linked to locations with known histories and were likely better preserved (Figure 2a).

The second method involved a cold-spin extraction after decalcification using EDTA and an in-house lysis solution consisting of 1 M Tris-Cl, SDS, calcium chloride, polyvinylpyrrolidone, N-phenacyl thiazolium bromide, dithiothreitol, and Proteinase K (Figure 2b). Then, a high-volume binding buffer (guanidine hydrochloride, isopropanol, Tween-20, and sodium acetate) was added to the supernatant before the combined solution was spun at 4°C for 24 hours. The cold-spun DNA was then purified through a silica-column-based extraction as previously mentioned (Murchie *et al.*, 2021; Dabney, Knapp, & Glocke *et al.*, 2013). This method was used for teeth retrieved from the Silivri Excavation (AS), which were predicted to have a greater amount of inhibition due to the poor condition of the remains; previous studies have seen a decrease in inhibitor co-elution with this technique (Murchie *et al.*, 2021).



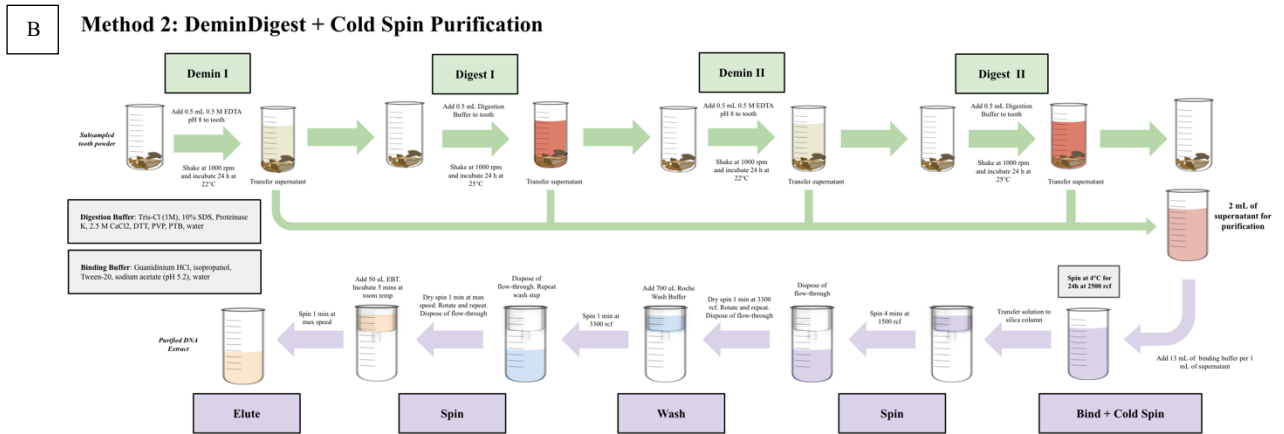


Figure 3.2 (a-b): Two methods of extraction. a) Extraction method 1: DeminDigest + Silica Column purification. Done for known historical sites. b) Extraction method 2: DeminDigest + Cold Spin purification. Done for the Silivri district necropolis and re-analysis of select extracts from historical sites. Created using Google Sheets.

3.3.3 Inhibition Testing

PCR inhibition tests were conducted to determine if the purified extracts contained inhibitors when undergoing downstream protocols of the sequencing workflow. Here, an HIV DNA standard was spiked into each extract. A quantitative PCR was conducted to estimate the working efficiency of the Taq polymerase within each DNA extract using its inhibition index (Murchie *et al.*, 2021). Inhibition indices utilize Cq values and RFU values of samples, formulaically comparing them to those of set standards. Murchie and colleagues (2021) also considered slopes of amplification in their calculations which this study did not include due to a lack of processing software. For more accurate analysis, more research must be dedicated to better understand the relationships between the three factors (slope, Cq values, and RFU values).

3.3.4 PCR Assay

A PCR assay was then used to screen for the presence of the *pla* gene. The *pla* gene is found on the pPCP1 plasmid in *Y. pestis* bacteria, which was chosen to act as an indicator for plague due to its high-copy number and thus increased likelihood of detection (Schuenemann *et al.*, 2011). Running alongside *pla* standards, plague-positive diagnosis using this screening method requires exponential amplification for 30-40 cycles across multiple runs and melting peaks within 0.5-1 degree of the standard; this is in accordance with existing McMaster Ancient DNA Centre protocol. A 1:10 dilution of each purified DNA extract was used in an initial qPCR; as the screening step is meant to be a preliminary test, dilutions were used in this first step to retain as much of the straight extract as possible. Samples meeting the mentioned requirements underwent a second confirmation using both a 1:10 dilution as well as its straight undiluted extract; straight extracts were used to introduce more DNA template, increasing the likelihood of target amplification, and achieving more accurate results.

3.3.5 Double-stranded Library Preparation, aDNA Quantification, and Indexing

Prior to sequencing, double-stranded library preparation and indexing was conducted based on existing protocols (Meyer and Kircher, 2010; Kircher *et al.*, 2012). The ends of the ancient DNA fragments were first blunt-ended as T4 DNA polymerase removed the overhanging 5' and 3' ends. Then, 5' phosphates were added using T4 polynucleotide kinase for adapters to ligate to the ends. In three consecutive ligation steps, P5 and P7 adapters were ligated to the ends of the DNA fragments using T4 DNA ligase before Bst polymerase was used to remove discontinuities within the

strand in a fill-in reaction (Meyer and Kircher, 2010). Then, a quantitative PCR was conducted to quantify the amount of adapted (non-indexed) molecules in each library; this was performed in conjunction with previous studies to estimate the amount of indexing cycles required for each extract (Gansauge *et al.*, 2020). Illumina sequencers assign unique barcodes to each DNA fragment in a given sample, allowing for multiple libraries to be pooled and then sequenced on the same run. Forward and reverse indexing primers were ligated to the ends of each DNA library using KAPA SYBR® FAST for subsequent detection by the Illumina sequencer.

3.3.6 Pooling and Shotgun Sequencing

A quantitative PCR was conducted to estimate the number of indexed molecules in each library. The indexed DNA libraries were then pooled into equimolar concentrations. The pooled DNA extracts were then sequenced to 2 million reads using the Illumina HiSeq 2000 system at the Farncombe Metagenomics Facility within McMaster University. Extracts of BFP39 were shotgun sequenced to 10 million reads for more in-depth bioinformatic analysis. Shotgun sequencing investigates a sample's metagenome, overviewing all molecules within a sample and its environment.

3.3.7 Radiocarbon Dating

Ancient remains from each site were sent to the Keck Carbon Cycle Accelerator Mass Spectrometry (KCCAMS) facility for carbon-14 dating. About 0.5g - 3g of bone from an individual of each site were sent for external analysis; this amount was either collected via subsampling with a Dremel or by using remnants of subsampled teeth if

bone was not available. Individuals were chosen based on the condition of the remains, if a pathogen was detected, or if existing subsampled remains were available; this study attempted to limit the amount of sampling done on the individuals. The radiocarbon dates were calibrated using the CALIB 8.2 calibration program with the IntCal20 calibration curve for locations in the Northern Hemisphere.

3.4 Bioinformatic Analysis

3.4.1 Quality Control

Raw sequencing data files for each sample were retrieved from the Farncombe Metagenomics Facility and underwent FastQC quality control checks. Specifically, the tool analyzed the following: sequence counts, sequence quality, per base sequence content, per sequence GC content, sequence length distribution, sequence duplication levels, overrepresented sequences, and adapter content. For FastQC analysis, Phred quality scores are used to display sequence quality by describing the probability of an incorrect base call. For instance, a Phred Quality Score (Q) of 10 indicates a 90% base call accuracy while a Phred Quality Score of 30 indicates a 99.9% base call accuracy; a Q Score of 30 is considered the standard for next-generation sequencing (Illumina, 2011). The data was visualized using MultiQC which reports data in HTML format (Ewels *et al.*, 2016).

3.4.2 Mapping to Reference Genomes

Reads from each sequencing data file were then mapped to reference genomes of interest using Burrows-Wheeler Aligner (bwa). First, the forward and reverse reads for each paired-end library were merged upon being trimmed of their technical sequences (adapters and primers). Using the Legacy pipeline created by Ana Duggan

at McMaster University, the reads were then mapped to the pathogen reference genomes as well as the human genome to check for endogenous preservation. The Legacy pipeline is coded to primarily filter the alignments to a length of 24 base pairs and remove unmapped molecules and PCR duplicates. Upon deduplication, the reads were manually filtered to a minimum of 35 base pairs for more accurate read-calling and a mapping quality of either 30 or 35 depending on the pathogen and the stage of the protocol. Mapping quality scores are logarithmic and function similarly as Phred Quality Scores. As such, the higher the mapping quality, the less likely a read is misplaced along the genome. For instance, a mapping quality of 30 means a 99.9% chance the read is correctly aligned; a higher mapping quality (ex. 35, 40) would be even more accurate. Pathogenic analysis as mentioned in this study utilizes mapped reads with a minimum length of 35 bp (with less stringent analysis of BFP39 using a minimum length of 30 bp) and a mapping quality of 30.

3.4.3 Pathogenic Confirmation and Visualization

Ancient DNA molecules are shorter, damaged fragments of an organism's original DNA; damage profiles and fragment length distributions were used to authenticate aDNA and each extract was visualized using the bioinformatic analysis program mapDamage (Jónsson *et al.*, 2013). Ancient DNA is associated with the deamination of cytosines into uracil, which results in the incorporation of adenine and then thymine during DNA replication (Dabney, Meyer, & Pääbo *et al.*, 2013). Thus, a typical profile indicative of what is expected in ancient DNA involves frequent damage on the 5' and 3' ends of a molecule; in a damage map, this is seen in smooth lines with more frequent C → T transitions on the 5' end and more frequent G → A transitions on the 3' end, with frequencies decreasing as you move inwards from the ends.

Kraken 2 and BLAST are bioinformatic tools that classify and assign a sample’s molecules to organisms within a curated database (Morgulis *et al.*, 2008; Camacho *et al.*, 2009; Sayers *et al.*, 2022). Kraken 2 uses stringent k-mer matches for its taxonomic classification and its output was visualized via Krona in HTML format (Wood *et al.*, 2019; Ondov *et al.*, 2011). Reads mapped to the *Y. pestis* reference genome were also put through the blastn (nucleotide) database using Megablast for taxonomic classification (Altschul *et al.*, 1990). While Megablast and blastn function similarly in that they are both used for nucleotide sequence identification, Megablast focusses on longer alignments with higher similarity. In addition, reads mapping to the chromosome were mapped using version 0.4 of the bioinformatic visualization software Geneious (2024).

Summary of Extracts with Evidence of Pathogens									
Archaeological ID	Project ID	Site	Extraction Method	Pathogen	Total Reads (IcHom output)	# of reads mapping to pathogen (min35MQ30)	Mapped % (Pathogen)	# of reads mapping to hg38HM (min35, MQ30)	Mapped % (Endogenous)
AS40	CS-BFP39	Silivri District Necropolis	2	<i>Yersinia pestis</i>	16,597,968	57	0.00034%	13,668	0.0823%
AS40	ME-BFP39	Silivri District Necropolis	1*	<i>Yersinia pestis</i>	15,815,438	68	0.00043%	45,345	0.2867%
AK62	TFP39	Perinthos	1	Hepatitis B virus	8,943,130	10	0.0001%	3,428	0.0383%
M37	TFP13	Iznik Roman Theatre	1	<i>Mycobacterium tuberculosis</i> **	5,100,280	486	0.010%	403,855	7.9183%
AT6	TFP50	Priene	1	<i>Mycobacterium tuberculosis</i>	7,018,139	438	0.006%	29	0.0004%
AS19	BFP18	Silivri District Necropolis	2	<i>Mycobacterium tuberculosis</i>	3,851,194	374	0.0097%	25	0.0006%
AS56	BFP55	Silivri District Necropolis	2	<i>Mycobacterium tuberculosis</i> **	3,414,310	181	0.0053%	295,425	8.6526%
AS62	BFP61	Silivri District Necropolis	2	<i>Mycobacterium tuberculosis</i>	7,795,613	506	0.0065%	144,952	1.8594%

Table 3.2: Summary of Extracts with Evidence of Pathogens. See section 3.3.2 for details on two different extraction methods.

* Extract was purified with an additional MinElute column to remove inhibitors.

** Extract chosen because of its relatively high endogenous content. *M. tuberculosis* content is present, though not a likely candidate for enrichment.

3.5 Results: Historic Sites Sample Set

*3.5.1 Preliminary *pla* Screening*

A total of 58 teeth were analyzed from 9 known historic sites in Turkey. Each tooth was given a project number beginning with TFP (Turkey First Pandemic). Upon subsampling, extraction, and inhibition testing, the extracts underwent qPCR screening to test for the presence of the *pla* gene. Out of the 58 samples, only 1 replicate amplified (TFP39), with a Cq value of 39.48 and a melt peak of 76; these values indicate either a weak positive or false positive for *Y. pestis*. For confirmation, a second qPCR was run with both 1:10 dilutions and straight extracts. As mentioned, 1:10 dilutions were used initially to retain as much of the original extract as possible. An argument can be made that a 1:10 dilution is too diluted to accurately test for the presence of the *pla* gene in each sample. Though this is a valid argument, the *pla* screen is only intended to serve as a crude overview of the possible pathogenic content of the extracts and a definitive plague diagnosis can only be confirmed through sequencing data; all samples were shotgun sequenced. No replicates from this sample set were amplified in the amplification qPCR, indicating that TFP39 was indeed a false positive for *Y. pestis*.

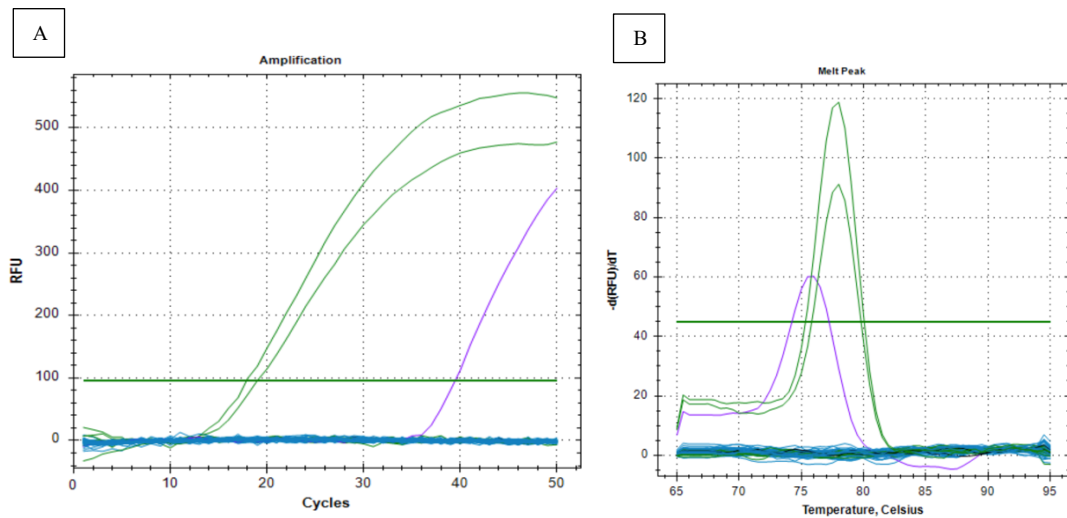


Figure 3.3 (a-b): Initial qPCR Screen of TFP39. a) A 1:10 dilution was used for the initial screen. One out of two replicates (purple) amplified with a Cq value of 39.48 and melt peak of 76°C. b) A confirmation screen using both diluted and straight extracts revealed that TFP39 was a false-positive for *Y. pestis*.

3.5.2 Shotgun Data Analysis

Shotgun sequencing provides a glimpse of the metagenome of an extract, that is, an overview of all DNA molecules within a sample, including its environmental DNA. This is particularly useful for researchers who have a general inquiry into all possible pathogenic infections within an individual. All 58 samples in the sample set showed evidence of extremely poor preservation. When mapped to the hard masked hg38 human reference genome, about 93% (54/58) of samples yielded <1% endogenous human DNA. Masked reference genomes conceal regions of low complexity and thus prevent reads from aligning to regions of high similarity; as the human reference genome consists of over 3 billion base pairs, mapping to a masked reference genome more accurately estimates on-target percentage. The highest percentage of human content was around 7.91% from TFP13 (Figure 3.4). The next highest percentages were 4.84%, 2.03%, and 1.5% for individuals TFP38, and TFP02 and TFP19, respectively (Table S.1). Thus, total human DNA from human teeth is an evidently

minor constituent, suggesting poor overall preservation within these extracts. The fragment misincorporation plot for TFP13 uncovered smooth C → T and G → A transitions, with over 5% more frequent C → T transitions on the 5' ends of molecules.

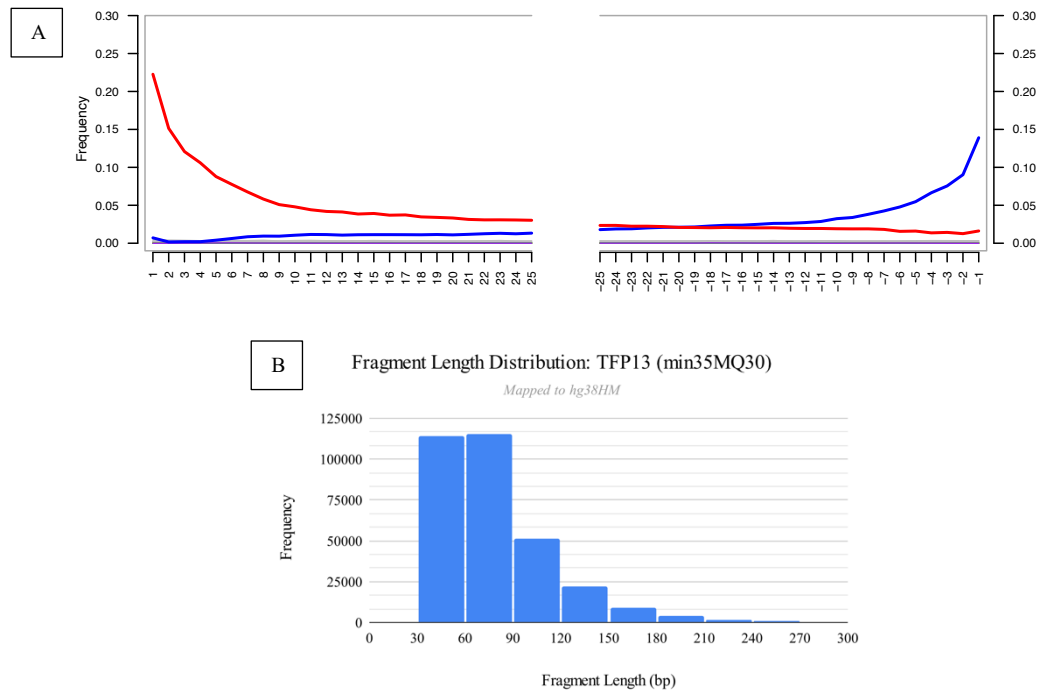


Figure 3.4 (a-b): TFP13 mapped to the masked human reference genome hg38 (min35, MQ30). a) ancient DNA authentication using mapDamage. The red line represents C → T substitutions, and the blue line represents G → A substitutions. Purple lines represents insertions relative to the reference. b) Fragment length distribution.

The samples were then mapped to various pathogen reference genomes. All 58 extracts were mapped to the modern *Y. pestis* CO92 reference genome (minimum length 35, minimum quality 30), and all revealed <0.001% reads exclusively attributed to the pathogen amongst all sequenced reads. TFP24 was the only sample that had reads mapping to both the pPCP1 plasmid as well as the chromosome of *Y. pestis*. The single read mapping to the pPCP1 plasmid returned Megablast results of *Y. pestis* and *E. coli*. 10 reads mapping to the *Y. pestis* chromosome returned Megablast results comprising mostly of *Y. pestis* and bacteria of the genera *Pseudomonas* and

Vibrio. Interestingly, the bioinformatic program Kraken 2 (visualization through Krona) did not match any reads from TFP24 to *Y. pestis*. Contrastingly, the highest number of classified *Y. pestis* reads by Kraken 2 is seven from TFP14 though also recovered 23 reads classifying within the genus *Serratia* (Figure S5.5). Megablast analysis of TFP14's mapped reveal results of *Y. pestis*, *Proteus mirabilis*, and *E. coli*.

Additionally, each sample was analyzed for the presence of members of the *Orthopoxvirus* genus, namely variola major virus. When mapped to the variola major reference (minimum length 35, mapping quality 30), TFP58 had 2 variola major virus reads. When analyzed through Megablast, variola major and cowpox virus hits returned. Preliminary taxonomic classification via Kraken 2 of TFP58 also classified 3 reads as belonging to *Orthopoxvirus*, with 1 read specifically classifying as variola major virus and another as vaccinia virus (Figure S5.6). Furthermore, Kraken 2 classified 15 *Orthopoxvirus* reads in TFP06, with 3 reads attributed specifically to variola virus (Figure S5.7). Interestingly, Megablast did not yield any hits for variola major, but instead for cowpox virus, monkeypox virus, and vaccinia virus.

Additionally, Kraken 2 taxonomically classified 200 reads as specific to *M. tuberculosis* in TFP13 (Figure S5.8). When mapped to the reference genome (minimum length 35, mapping quality 30), 486 reads returned (Table 3.2). However, when visualized using Geneious, coverage across the genome was sparse at 0.006X mean coverage (Figure S5.8b). The fragment misincorporation plot for TFP13 is atypical for truly authentic aDNA molecules, revealing unclear C → T and G → A transitions. A slight increase to a 5' C → T misincorporation frequency of 10% is apparent, which just meets the frequency indicative of authentic aDNA (Sawyer *et al.*, 2012; Hodgins *et al.*, 2023). Visualizing TFP50 using Geneious, however, displayed

greater coverage across the genome at 0.005X mean coverage; Kraken 2 revealed 7 reads specific to *M. tuberculosis* (Figure S5.9). When mapped using the Legacy pipeline, 438 reads returned with a minimum length of 35 and mapping quality of 30 (Table 2.2). Additionally, the fragment misincorporation plot for TFP50 is also atypical for truly authentic aDNA molecules, revealing unclear C → T and G → A transitions. A slight increase in damage level to 5% on the 3' end can be argued, though is well below the value of 10% suggesting the presence of authentic aDNA (Sawyer *et al.*, 2012; Hodgins *et al.*, 2023).

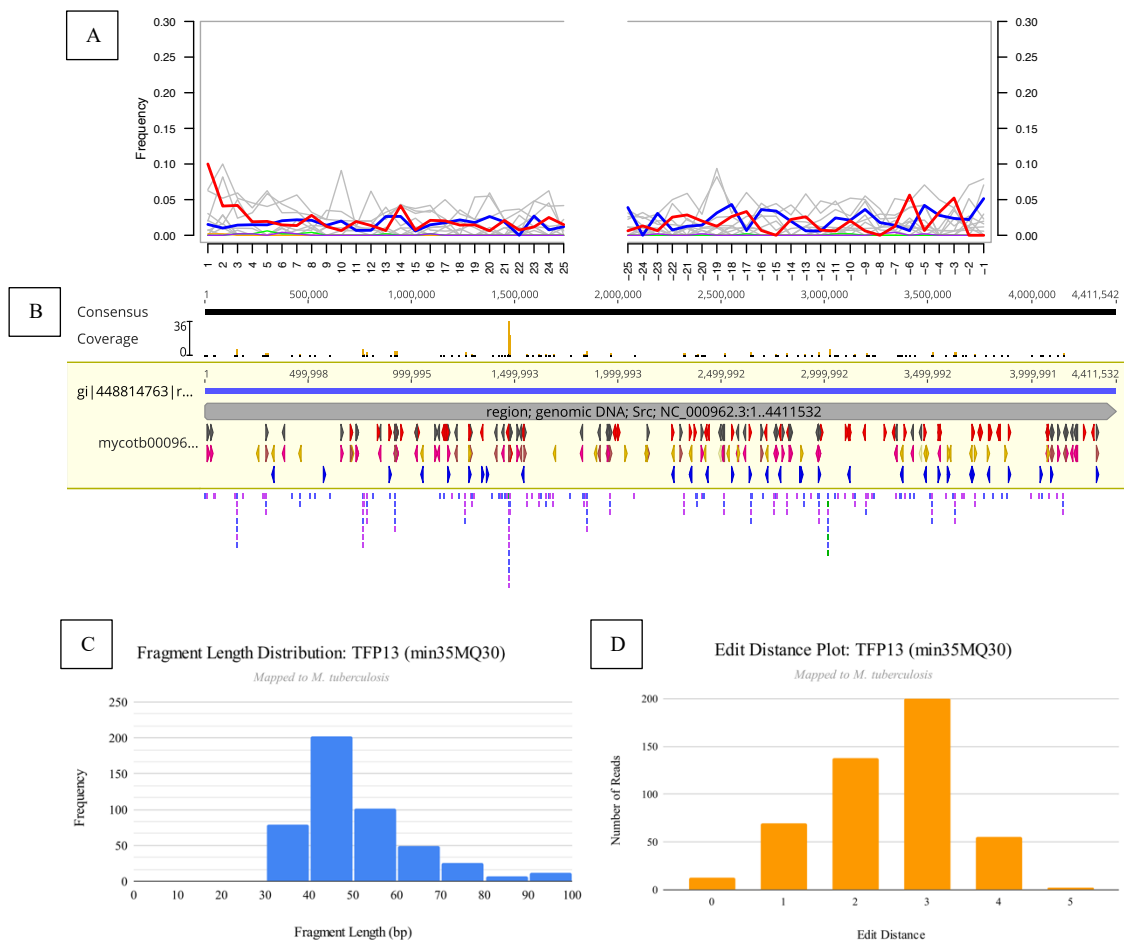


Figure 3.5 (a-d): TFP13 mapped to the *M. tuberculosis* reference genome (min35, MQ30). a) ancient DNA authentication using mapDamage. The red line represents C → T substitutions, and the blue line represents G → A substitutions. Purple lines represents insertions relative to the reference, green represents deletions relative to the reference, and grey represents all other substitutions. b) Coverage plot using Geneious with 0.006X mean coverage. c) Fragment length distribution. d) Plot of edit distances.

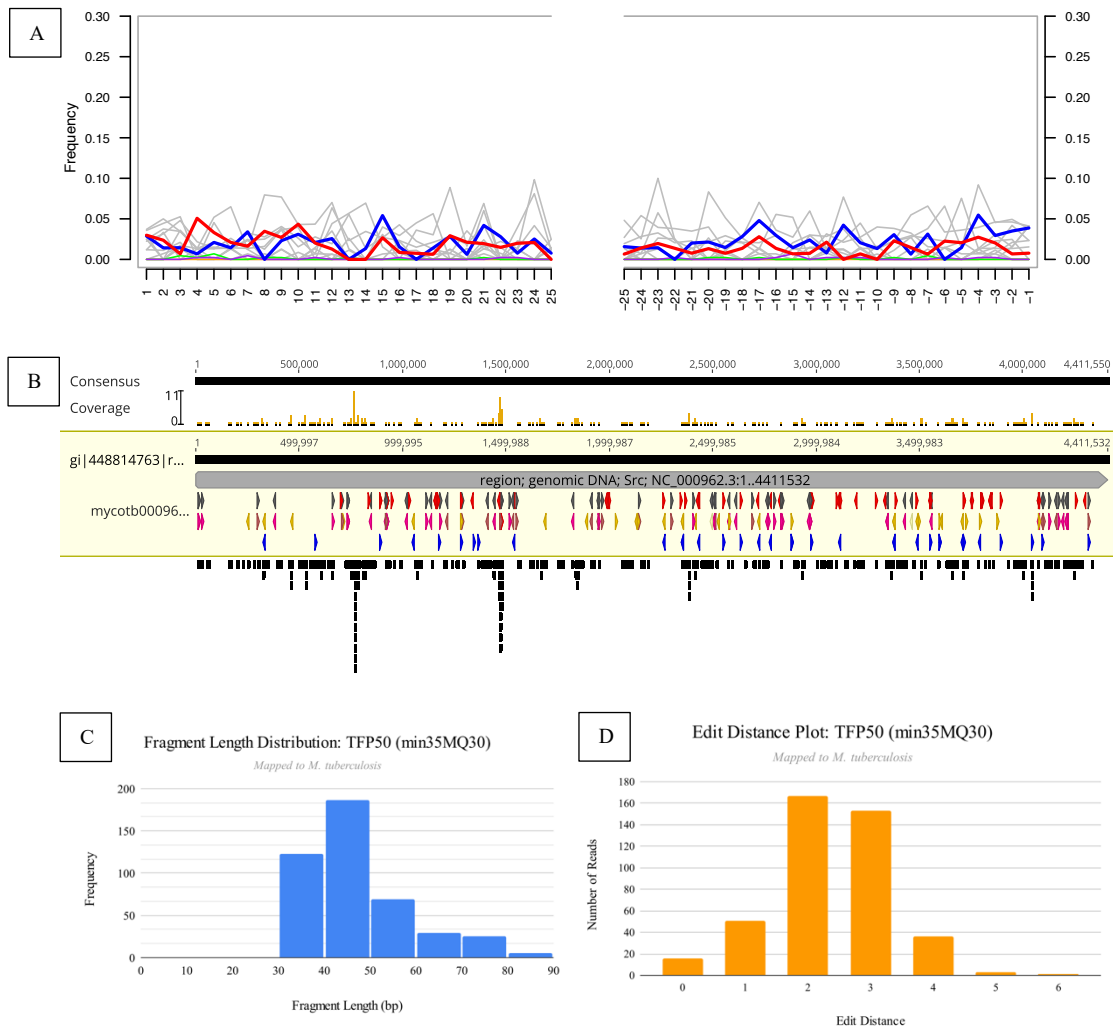


Figure 3.6 (a-d): TFP50 mapped to the *M. tuberculosis* reference genome (min35, MQ30). a) ancient DNA authentication using mapDamage. The red line represents C → T substitutions, and the blue line represents G → A substitutions. Purple lines represents insertions relative to the reference, green represents deletions relative to the reference, and grey represents all other substitutions. b) Coverage plot using Geneious with 0.005X mean coverage. c) Fragment length distribution. d) Plot of edit distances.

Notably, TFP39 was the only sample in this set to show evidence for hepatitis B virus.

A total of 15 reads were classified by Kraken 2 and visualized using Krona (Figure S5.10). When mapped using the Legacy pipeline with a minimum length of 35 and mapping quality of 30, 10 reads returned using the RefSeq reference genome for hepatitis B virus, and 23 reads returned when mapped to a different hepatitis B genome (GenBank: X65257.1) (Table 3.2). When analyzed using Megablast, only

results for hepatitis B virus returned. Furthermore, when visualized using Geneious, the reads returned were annotated as glycoproteins on the outer surface of the hepatitis B virus. As depicted, the lack of overall reads for both generated an indecipherable mapDamage plot, highlighting the need for further enrichment.

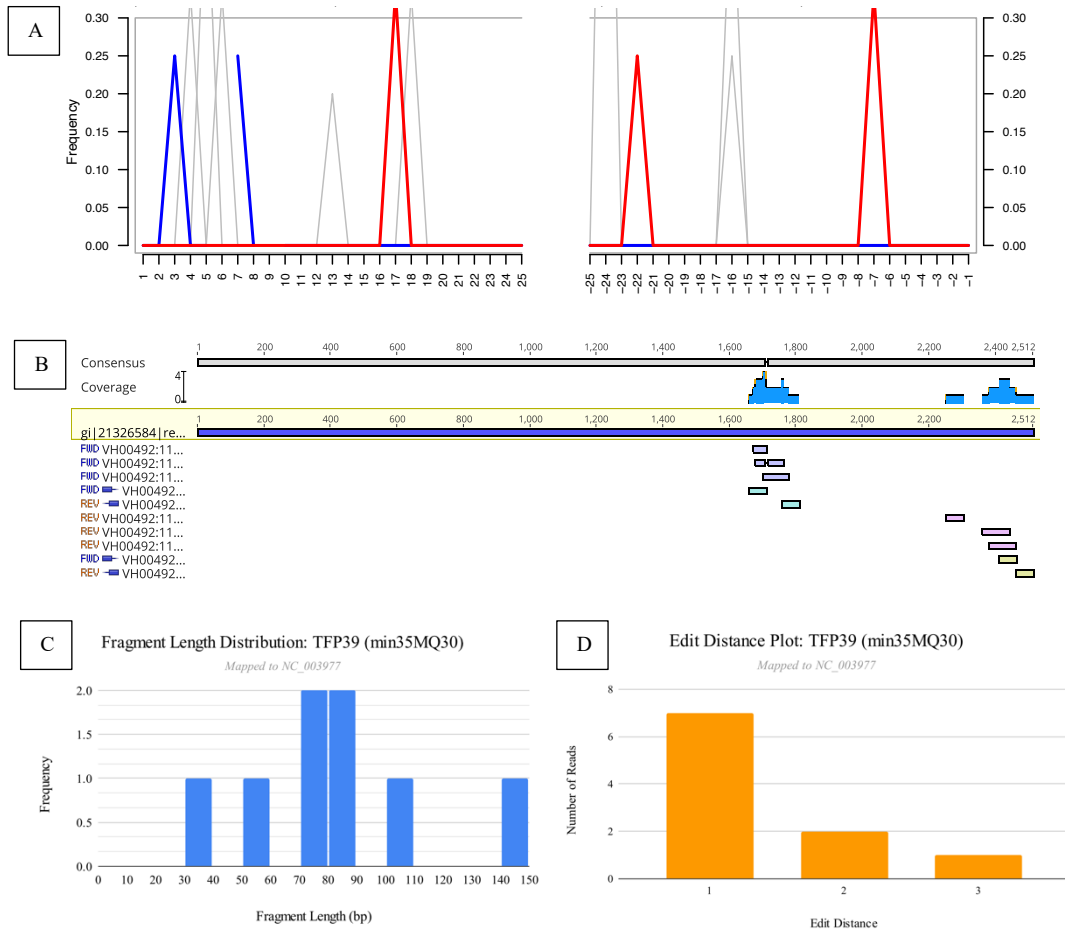
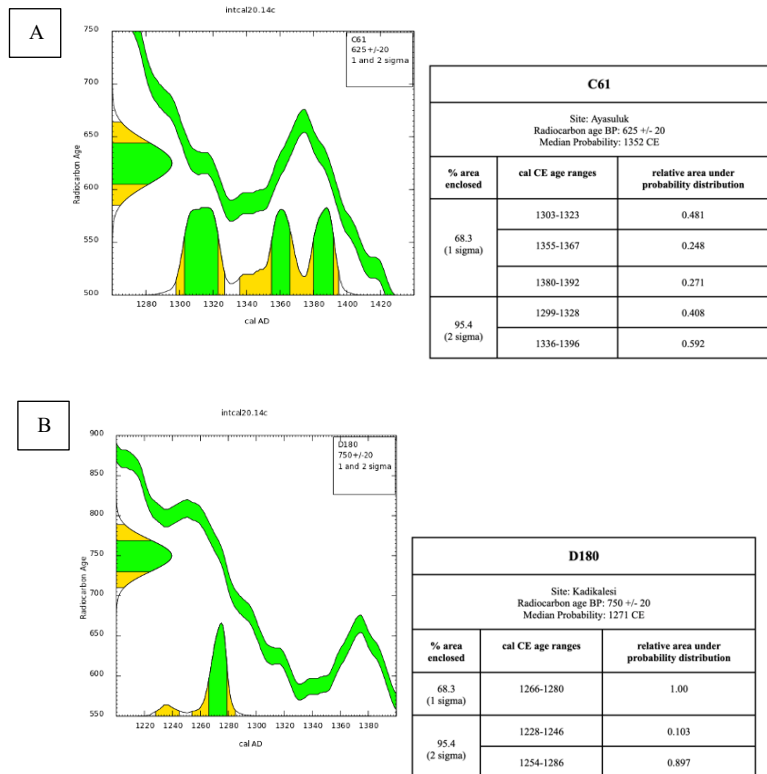
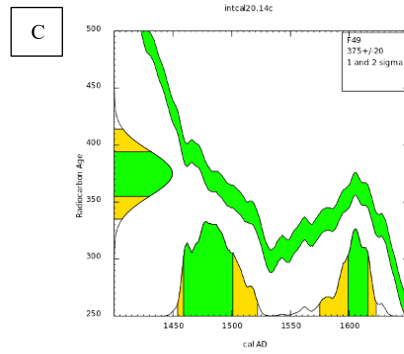


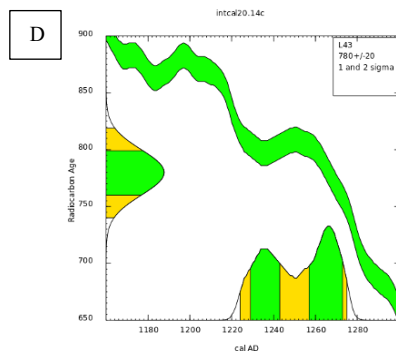
Figure 3.7 (a-d): TFP39 mapped to the hepatitis B virus reference genome. Too few reads were mapped to the reference genome, resulting in indecipherable authentication graphs. a) ancient DNA authentication using mapDamage. b) Coverage plot using Geneious with 0.244X mean coverage. c) Fragment length distribution. d) Plot of edit distances.

of dating to 1208 CE and another from Ayasuluk (C61) dated to 1352 CE. Furthermore, a Metropolis individual (L43) was dated to 1252 CE and an individual from Kadikalesi (D180) was dated to 1271 CE. The youngest individuals in this sample set are from the Agora of Smyrna (F49) with a median probability of dating to 1498 CE, and from Perinthos (AK62) dating to 1434 CE. The individual from Priene (AT16) and Haydarpaşa Train Station (Z30) were among the oldest of the set, with calibrated dates of 302 BCE and 112 CE respectively. Remains from İznik Hisardere Necropolis were unable to be dated in three attempts as the carbon-dating facility was unable to yield any collagen for analysis.

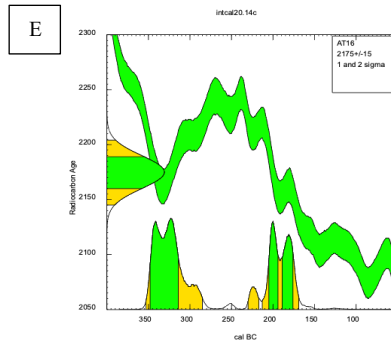




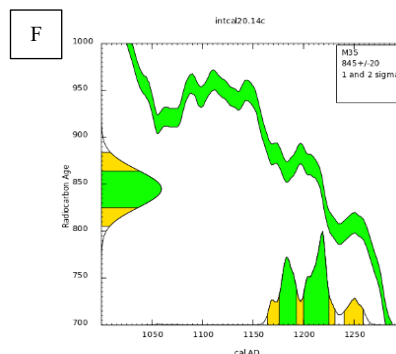
F49		
Site: Smyrna Agora Radiocarbon age BP: 375 +/- 20 Median Probability: 1498 CE		
% area enclosed	cal CE age ranges	relative area under probability distribution
68.3 (1 sigma)	1459-1502	0.724
	1599-1616	0.276
95.4 (2 sigma)	1454-1522	0.658
	1575-1624	0.342



L43		
Site: Metropolis Radiocarbon age BP: 780 +/- 20 Median Probability: 1252 CE		
% area enclosed	cal CE age ranges	relative area under probability distribution
68.3 (1 sigma)	1229-1244	0.424
	1257-1274	0.576
95.4 (2 sigma)	1454-1522	1.000



AT16		
Site: Priene Radiocarbon age BP: 2175 +/- 15 Median Probability: 302 BCE		
% area enclosed	cal BCE age ranges	relative area under probability distribution
68.3 (1 sigma)	347-314	0.612
	205-193	0.187
	189-175	0.201
95.4 (2 sigma)	352-284	0.580
	230-216	0.039
	212-168	0.381



M35		
Site: Izmik Roman Theatre Radiocarbon age BP: 845 +/- 20 Median Probability: 1208 CE		
% area enclosed	cal CE age ranges	relative area under probability distribution
68.3 (1 sigma)	1176- 1194	0.377
	1200-1225	0.623
95.4 (2 sigma)	1165-1232	0.884
	1240-1260	0.116

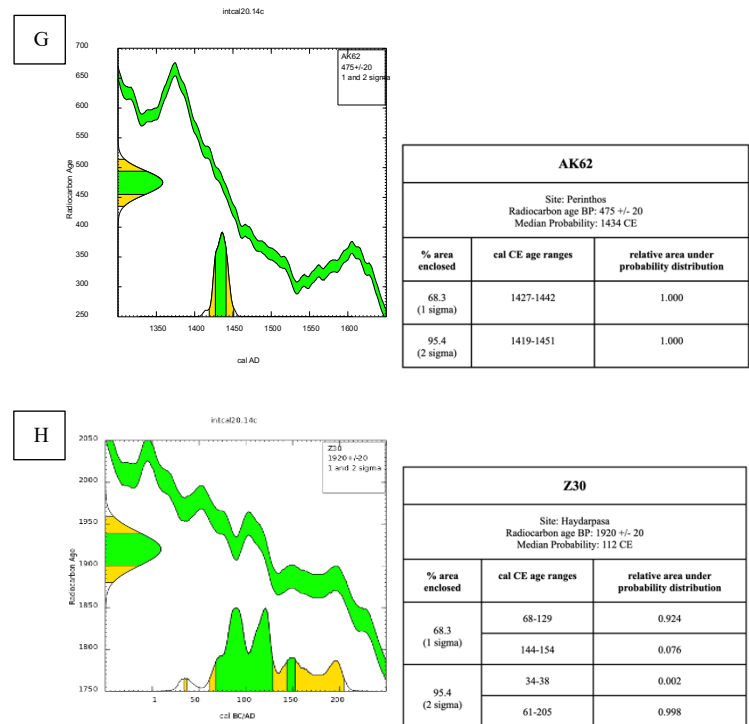


Figure 3.9 (a-h): Calibrated radiocarbon dates for the Historical Sites sample set. Samples were sent for radiocarbon dating at the University of California, Irvine and calibrated using CALIB 8.2. a) Calibrated dates for Ayasuluk (C). The median probability is 1352 CE, with a 95% likelihood the sample is from between 1299-1396 AD. b) Calibrated dates for Kadikalesi (D). The median probability is 1271 CE with a 95% likelihood the sample is from between 1228-1286 CE. c) Calibrated dates for the Agora of Smyrna (F). The median probability is 1498 AD with a 95% likelihood the sample is from between 1454-1624 CE. d) Calibrated dates for Metropolis (L). The median probability is 1252 CE with a 95% likelihood the sample is from between 1454 – 1522 CE. e) Calibrated dates for Priene (AT). The median probability is 302 BCE with a 95% likelihood the sample is from between 352 – 168 BCE. f) Calibrated dates for Iznik Roman Theatre (M). The median probability is 1208 CE with a 95% likelihood the sample is from between 1165 – 1260 CE. g) Calibrated dates for Perinthos (AK). The median probability is 1434 CE with a 95% likelihood the sample is from between 1419 – 1451 CE h) Calibrated dates for Haydarpasa (Z). The median probability is 112 CE with a 95% likelihood the sample is from between 34-205 CE.

3.6 Results: Silivri Excavation Sample Set

3.6.1 Preliminary *pla* Screening

A total of 76 teeth were analyzed from the Silivri district necropolis. Each tooth was given a project number beginning with BFP (BOTAŞ First Pandemic). Upon subsampling and purification, the extracts underwent qPCR screening to test for the presence of the *pla* gene. For the first set of 42 samples, a total of 8 replicates of the

1:10 dilutions amplified, indicating either weak positive or false positive *Y. pestis*. For confirmation, a second qPCR was run with both 1:10 dilutions and straight extracts. In the confirmation qPCR, both replicates of the straight extracts of BFP39 amplified. For even further confirmation, a different extract of BFP39 (not cold-spun) was re-purified and underwent the confirmation qPCR. For both the cold-spun and non-cold-spun extracts, both straight replicates amplified, indicating a high likelihood of *Y. pestis* in BFP39 (Table 3.3). For the second set of 34 samples, 2 sample replicates amplified. A confirmation qPCR was done, and only a 1:10 dilution replicate of BFP71 amplified, indicating false positives for *Y. pestis*.

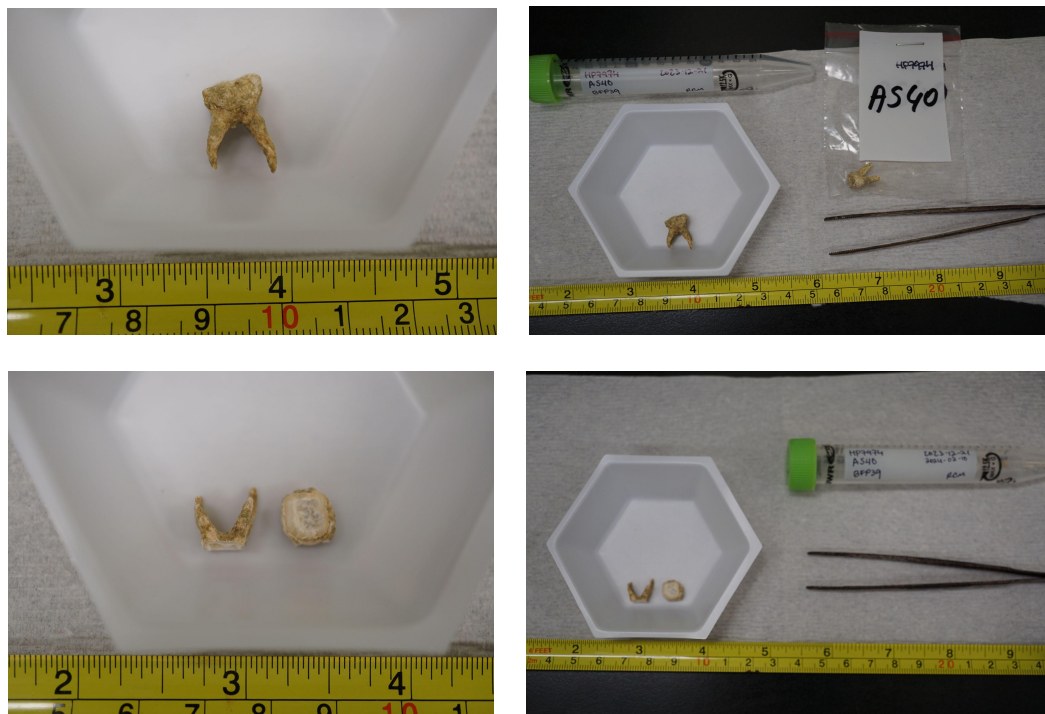


Figure 3.10: Subsampling photos of tooth belonging to individual BFP39.

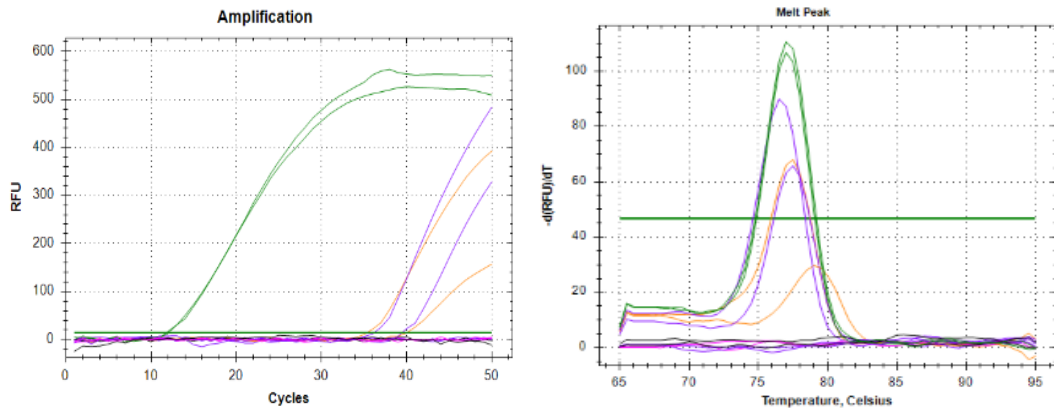


Figure 3.11: *pla* Screening Amplification and Melt Curves for BFP39 extracts. Green lines indicate 1.00E+08 standards. Orange lines indicate cold-spun BFP39 extract (CS-BFP39). Purple lines indicate twice-MinEluted BFP39 extract (ME-BFP39).

<i>pla</i> Screen: BFP39 Extracts									
Sample	Straight Cq (Rep 1)	Straight Cq (Rep 2)	1:10 Dilution Cq (Rep 1)	1:10 Dilution Cq (Rep 2)	Straight Melt Peak (Rep 1)	Straight Melt Peak (Rep 2)	1:10 Dilution Melt Peak (Rep 1)	1:10 Dilution Melt Peak (Rep 2)	Plague Positive?
Std 1.00E+08	12.42	12.40			77	77.5			Plague Positive
NTC	N/A	N/A			N/A	N/A			Plague Negative
ME-BFP39	36.18	39.45	N/A	N/A	76.5	77.5	N/A	N/A	Plague Positive
CS-BFP39	35.33	40.02	N/A	N/A	77.5	N/A	N/A	N/A	Plague Positive

Table 3.3: Cycle Amplification and Melt Peak values for BFP39 extracts. Both replicates of the straight extracts met the criteria for a preliminary plague-positive diagnosis. The 1:10 dilutions did not amplify. One replicate of the CS-BFP39 straight extract was not detectable with the PCR threshold.

Summary of BFP39 Extracts										
Bioinformatic Specifics	Archaeological ID	Project ID	Site	Extraction Method	Pathogen	Total Reads (IcHOM output)	# of reads mapping	Mapped % (Pathogen)	# of reads mapping to hg38HM	Mapped % (Endogenous)
min30MQ30	AS40	CS-BFP39	Silvri District Necropolis	2	<i>Yersinia pestis</i>	16,597,968	100	0.00060%	17,327	0.10439%
	AS40	ME-BFP39	Silvri District Necropolis	1*	<i>Yersinia pestis</i>	15,815,438	120	0.00076%	52,980	0.33499%
min35MQ30	AS40	CS-BFP39	Silvri District Necropolis	2	<i>Yersinia pestis</i>	16,597,968	57	0.00034%	13,668	0.08235%
	AS40	ME-BFP39	Silvri District Necropolis	1*	<i>Yersinia pestis</i>	15,815,438	68	0.00043%	45,345	0.28671%

Table 3.4: Summary of BFP39 Extracts. See section 3.3.2 for details on two different extraction methods.

* Extract was purified with an additional MinElute column to remove inhibitors.

3.6.2 Shotgun Data Analysis

As with the 58 samples from the known historical sites, all 76 samples in this sample set revealed <10% of human DNA, indicating poor preservation. Specifically, when mapped to the hard masked hg38 human reference genome (minimum length 35, minimum quality 30), about 88% (67/76) of samples yielded <1% endogenous human DNA. The highest percentage of human content was 8.65% for BFP55, with the next highest percentage being 1.86% for BFP61. Notably, despite successful qPCR screens, the plague positive extracts for individual BFP39 had low endogenous human content at 0.08% for CS-BFP39 and 0.29% for ME-BFP39.

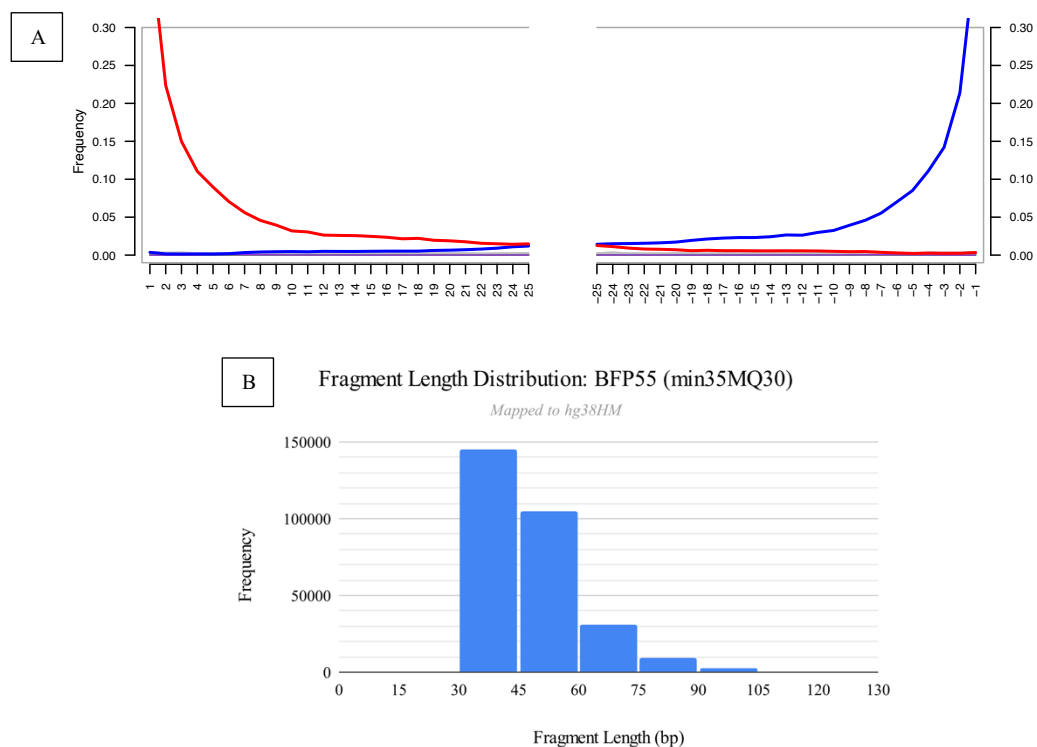


Figure 3.12 (a-b): BFP55 mapped to the masked human reference genome hg38 (min35, MQ30). a) ancient DNA authentication using mapDamage. b) Fragment length distribution.

The samples were mapped to the *Y. pestis* CO92 reference genome (minimum length 35, minimum quality 30) using the Legacy pipeline. As with the previous set, all

samples (including both BFP39 extracts) revealed <0.001% reads exclusively attributed to *Y. pestis*. Bioinformatic analysis of the plague positive sample BFP39 is covered in Section 4.3.

Additionally, preliminary taxonomic classification via Kraken 2 and visualization with Krona revealed reads mapping to the genome of *M. tuberculosis*. Specifically, Kraken 2 classified 6 reads of BFP18 as *M. tuberculosis* (Figure S5.13). When mapped to the *M. tuberculosis* reference genome using the Legacy pipeline (minimum length 35, mapping quality 30), BFP18 returned 374 mapped reads. Visualization using Geneious noted mean coverage across the genome as 0.004X (Figure 13b). The damage profile for BFP18 highlights a slight trend of increased damage along the 5' and 3' ends of molecules, though the levels either meet or fall short of the 10% frequency indicative of authentic aDNA. Additionally, BFP55 had 121 classified reads using Kraken 2 (Figure S5.14). Mapping to the *M. tuberculosis* reference genome returned 181 reads. Geneious listed mean coverage across the genome at 0.002X (Figure 14b). Additionally, the fragment misincorporation plot for BFP55 contains C → T and G → A transitions with no clear trends, though a slight increase in damage level to 10% on the 5' end is apparent before a sudden drop. Furthermore, BFP61 had 165 exact k-mer matches to *M. tuberculosis* (Figure S5.15). Mapping to the reference genome revealed a total of 506 reads (Table 3.2). Mean coverage as depicted using Geneious was only moderately improved at 0.005X (Figure 15b). The misincorporation plot for BFP61 covers a slight increasing trend of 5' C → T and 3' G → A misincorporation rates, though the levels just meet the 10% frequency indicative of authentic aDNA.

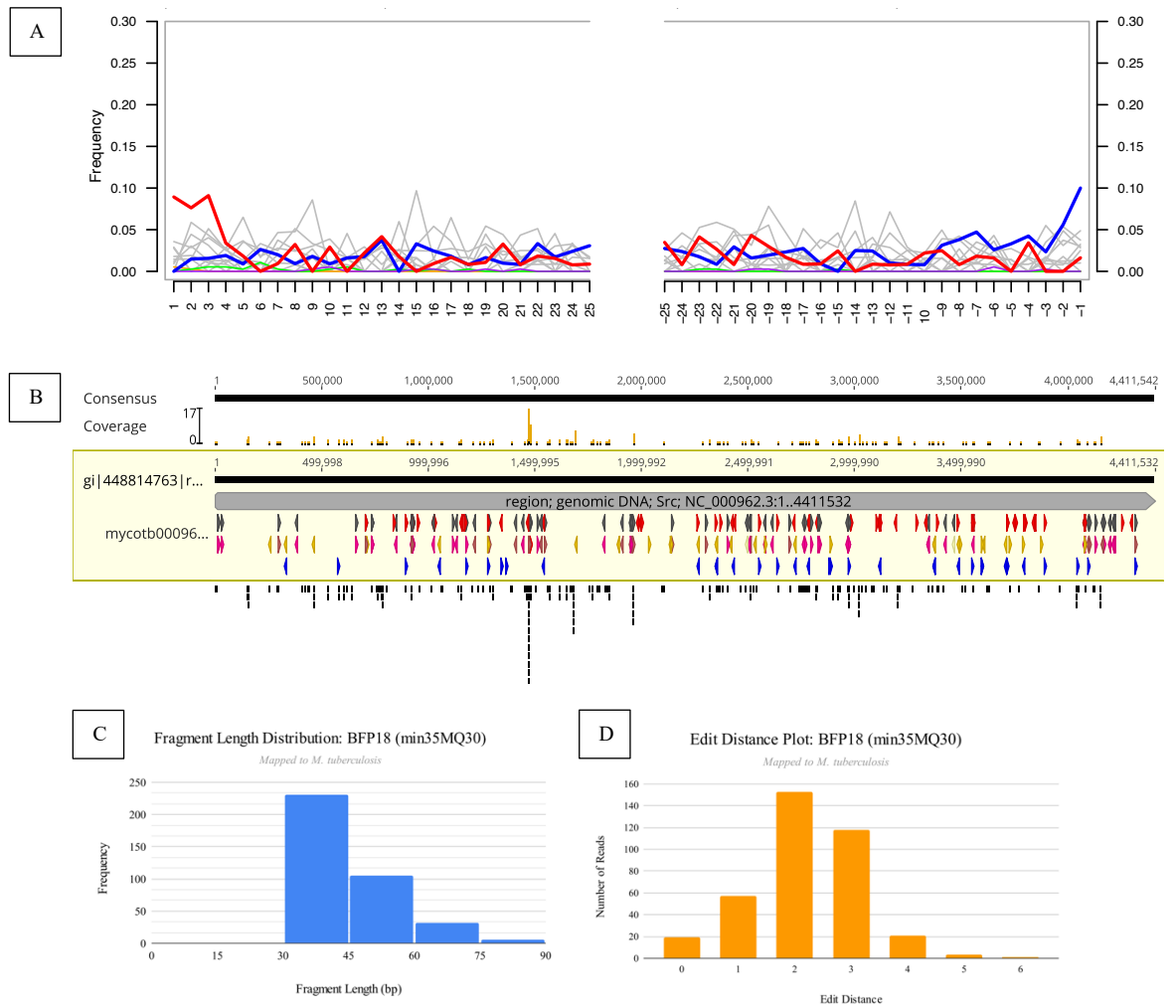


Figure 3.13 (a-d): BFP18 mapped to the *M. tuberculosis* reference genome (min35, MQ30). a) ancient DNA authentication using mapDamage. b) Coverage plot using Geneious with 0.004X mean coverage. c) Fragment length distribution. d) Plot of edit distances.

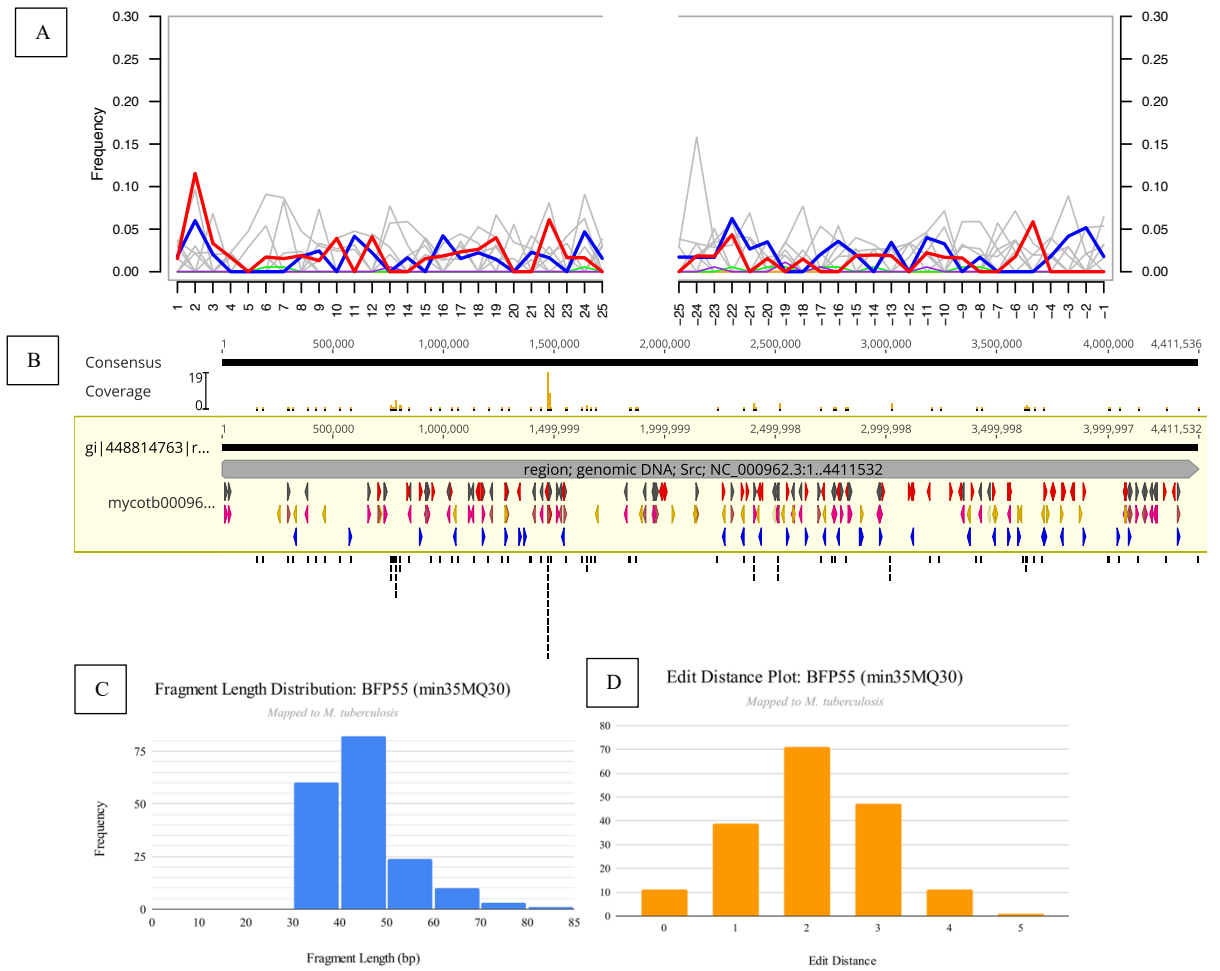


Figure 3.14 (a-d): BFP55 mapped to the *M. tuberculosis* reference genome (min35, MQ30). a) ancient DNA authentication using mapDamage. b) Coverage plot using Geneious with 0.002X mean coverage. c) Fragment length distribution. d) Plot of edit distances.

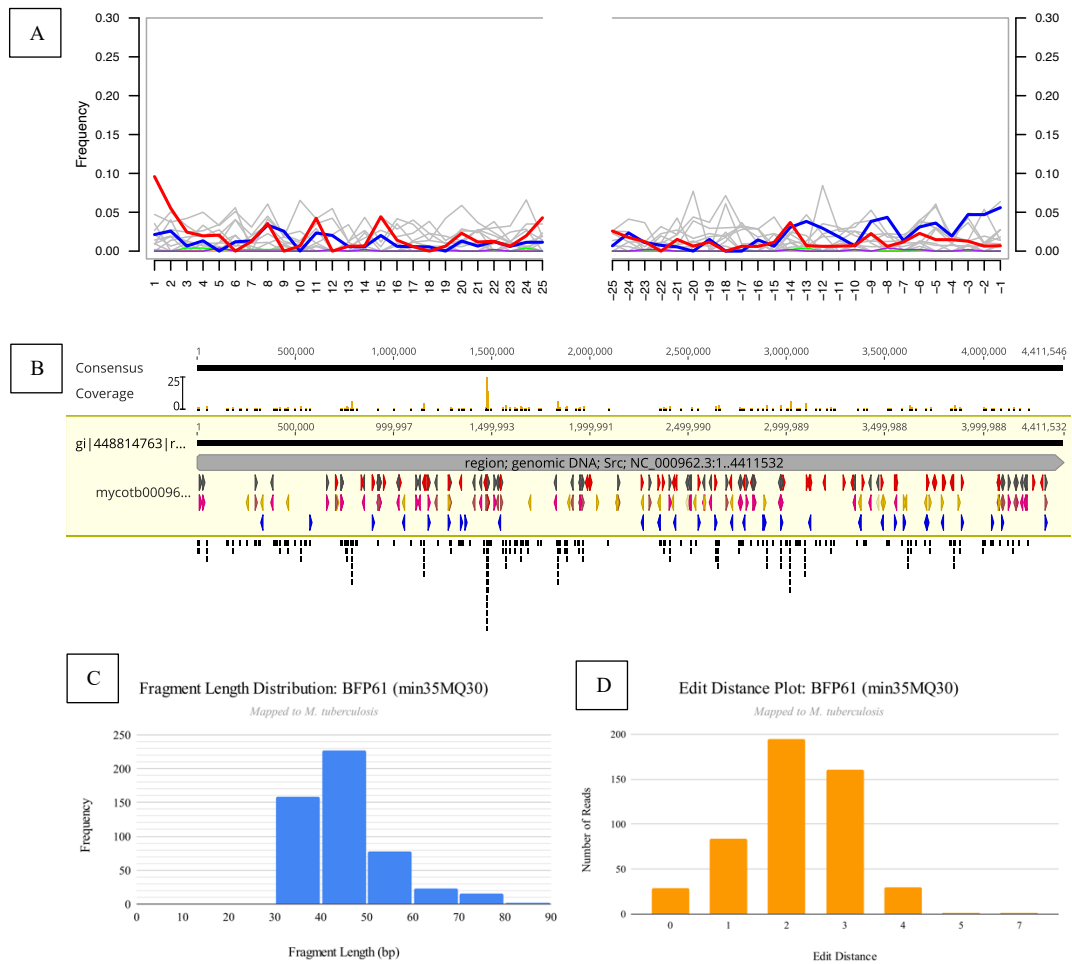


Figure 3.15 (a-d): BFP61 mapped to the *M. tuberculosis* reference genome (min35, MQ30). a) ancient DNA authentication using mapDamage. b) Coverage plot using Geneious with mean coverage 0.005X. c) Fragment length distribution. e) Plot of edit distances.

3.6.3 Estimated Dates

Remains from three individuals in the Silvri Excavation sample set were sent to the KCCAMS facility for carbon-dating; these individuals were chosen based on the overall condition of the remains and/or showing evidence of pathogenicity. As with the Historical Sites sample set, the radiocarbon dates were calibrated using CALIB 8.2 using the IntCal20 calibration curve and are depicted in Figure 3.16 (Stuiver and Reimer, 1993).

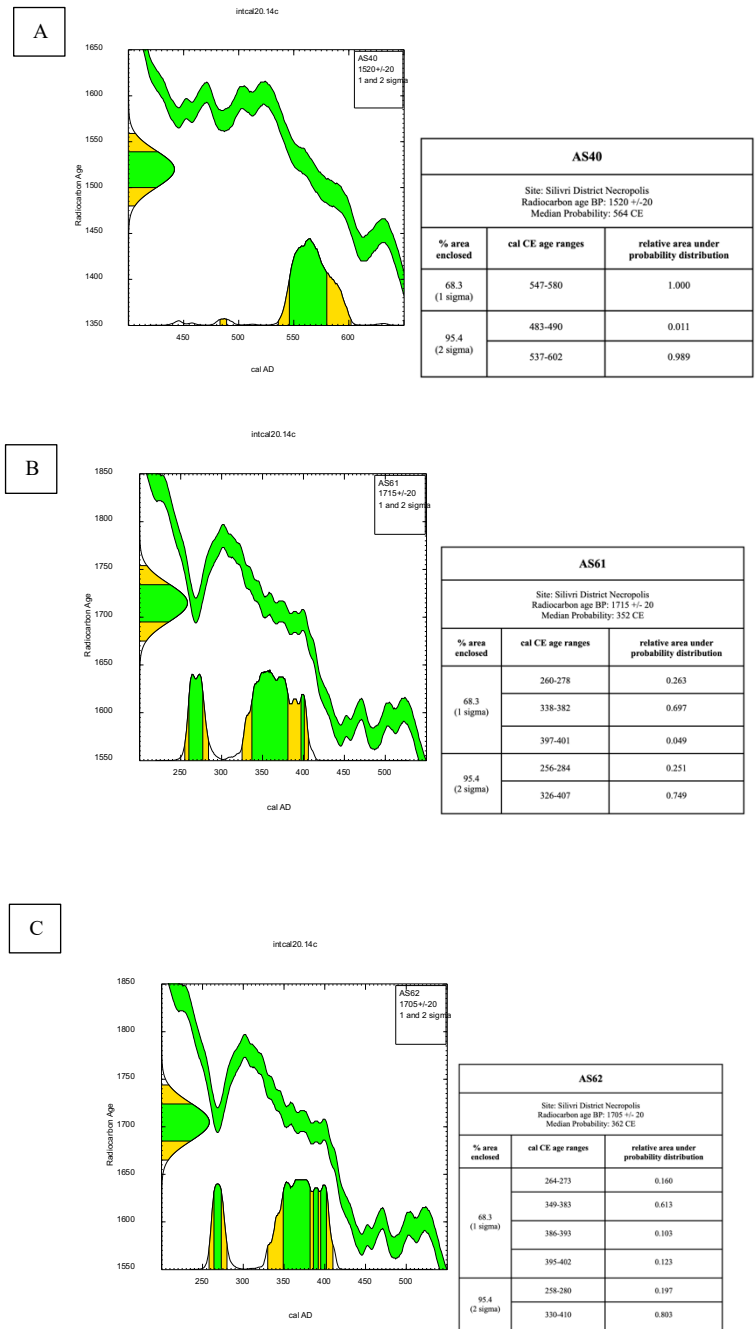


Figure 3.16 (a-c): Calibrated radiocarbon dates for the Silivri Excavation sample set. Samples were sent for radiocarbon dating at the University of California, Irvine and calibrated using CALIB 8.2. a) Calibrated dates for individual BFP39. The median probability is 1352 CE, with a 95% likelihood the sample is from between 483-602 CE. b) Calibrated dates for individual BFP61. The median probability is 352 CE with a 95% likelihood the sample is from between 256-407 CE. c) Calibrated dates for individual BFP62. The median probability is 362 AD with a 95% likelihood the sample is from between 258-410 CE.

3.7 References

- Altschul, S. F., Gish, W., Miller, W., Myers, E. W., & Lipman, D. J. (1990). Basic local alignment search tool. *Journal of molecular biology*, 215(3), 403–410. [https://doi.org/10.1016/S0022-2836\(05\)80360-2](https://doi.org/10.1016/S0022-2836(05)80360-2)
- Camacho, C., Coulouris, G., Avagyan, V., Ma, N., Papadopoulos, J., Bealer, K., & Madden, T. L. (2009). BLAST+: architecture and applications. *BMC bioinformatics*, 10, 421. <https://doi.org/10.1186/1471-2105-10-421>
- Dabney, J., Knapp, M., Glocke, I., Gansauge, M. T., Weihmann, A., Nickel, B., Valdiosera, C., García, N., Pääbo, S., Arsuaga, J. L., & Meyer, M. (2013). Complete mitochondrial genome sequence of a Middle Pleistocene cave bear reconstructed from ultrashort DNA fragments. *Proceedings of the National Academy of Sciences of the United States of America*, 110(39), 15758–15763. <https://doi.org/10.1073/pnas.1314445110>
- Dabney, J., Meyer, M., & Pääbo, S. (2013). Ancient DNA damage. *Cold Spring Harbor perspectives in biology*, 5(7), a012567. <https://doi.org/10.1101/cshperspect.a012567>
- Ewels, P., Magnusson, M., Lundin, S., & Käller, M. (2016). MultiQC: summarize analysis results for multiple tools and samples in a single report. *Bioinformatics (Oxford, England)*, 32(19), 3047–3048. <https://doi.org/10.1093/bioinformatics/btw354>
- Feldman, M., Harbeck, M., Keller, M., Spyrou, M. A., Rott, A., Trautmann, B., Scholz, H. C., Pääffgen, B., Peters, J., McCormick, M., Bos, K., Herbig, A., & Krause, J. (2016). A High-Coverage *Yersinia pestis* Genome from a Sixth-Century Justinianic Plague Victim. *Molecular Biology and Evolution*, 33(11), 2911–2923. <https://doi.org/10.1093/molbev/msw170>
- Fleskes R.E., Bader A.C., Tsosie K.S., Wagner J.K., Claw K.G., Garrison N.A. 2022. Ethical Guidance in Human Paleogenomics: New and Ongoing Perspectives. *Annual Review of Genomics and Human Genetics*; 23: 627–52.
- Gansauge, M. T., Aximu-Petri, A., Nagel, S., & Meyer, M. (2020). Manual and automated preparation of single-stranded DNA libraries for the sequencing of DNA from ancient biological remains and other sources of highly degraded DNA. *Nature protocols*, 15(8), 2279–2300. <https://doi.org/10.1038/s41596-020-0338-0>
- Geneious Prime 2024.0.4. Retrieved from <https://www.geneious.com>
- Hodgins, H. P., Chen, P., Lobb, B., Wei, X., Tremblay, B. J. M., Mansfield, M. J., Lee, V. C. Y., Lee, P. G., Coffin, J., Duggan, A. T., Dolphin, A. E., Renaud,

- G., Dong, M., & Doxey, A. C. (2023). Ancient Clostridium DNA and variants of tetanus neurotoxins associated with human archaeological remains. *Nature communications*, 14(1), 5475. <https://doi.org/10.1038/s41467-023-41174-0>
- Jónsson, H., Ginolhac, A., Schubert, M., Johnson, P. L., & Orlando, L. (2013). mapDamage2.0: fast approximate Bayesian estimates of ancient DNA damage parameters. *Bioinformatics*, 29(13), 1682–1684. <https://doi.org/10.1093/bioinformatics/btt193>
- Keller, M., Spyrou, M. A., Scheib, C. L., Neumann, G. U., Kröpelin, A., Haas-Gebhard, B., Pääffgen, B., Haberstroh, J., Ribera i Lacomba, A., Raynaud, C., Cessford, C., Durand, R., Stadler, P., Nägele, K., Bates, J. S., Trautmann, B., Inskip, S. A., Peters, J., Robb, J. E., ... Krause, J. (2019). Ancient *Yersinia pestis* genomes from across Western Europe reveal early diversification during the First Pandemic (541–750). *Proceedings of the National Academy of Sciences of the United States of America*, 116(25), 12363–12372. <https://doi.org/10.1073/pnas.1820447116>
- Klunk, J., Duggan, A. T., Redfern, R., Gamble, J., Boldsen, J. L., Golding, G. B., Walter, B. S., Eaton, K., Stangroom, J., Rouillard, J.-M., Devault, A., DeWitte, S. N., & Poinar, H. N. (2019). Genetic resiliency and the Black Death: No apparent loss of mitogenomic diversity due to the Black Death in medieval London and Denmark. *American Journal of Physical Anthropology*, 169(2), 240–252. <https://doi.org/10.1002/ajpa.23820>
- Kircher, M., Sawyer, S., & Meyer, M. (2012). Double indexing overcomes inaccuracies in multiplex sequencing on the Illumina platform. *Nucleic Acids Research*, 40(1), e3. <https://doi.org/10.1093/nar/gkr771>
- Meyer, M., & Kircher, M. (2010). Illumina Sequencing Library Preparation for Highly Multiplexed Target Capture and Sequencing. *Cold Spring Harbor Protocols*. <https://doi.org/10.1101/pdb.prot5448>
- Morgulis, A., Coulouris, G., Raytselis, Y., Madden, T. L., Agarwala, R., & Schäffer, A. (2008). Database indexing for production MegaBLAST searches. *Bioinformatics*, 24(16), 1757–1764. <https://doi.org/10.1093/bioinformatics/btn322>
- Murchie, T. J., Kuch, M., Duggan, A. T., Ledger, M. L., Roche, K., Klunk, J., ... Poinar, H. (2021). Optimizing extraction and targeted capture of ancient environmental DNA for reconstructing past environments using the PalaeoChip Arctic-1.0 bait-set. *Quaternary Research*, 99, 305–328. doi:10.1017/qua.2020.59
- Ondov, B. D., Bergman, N. H., & Phillippy, A. M. (2011). Interactive metagenomic visualization in a Web browser. *BMC bioinformatics*, 12, 385. <https://doi.org/10.1186/1471-2105-12-385>

- Quality Scores for Next-Generation Sequencing*. (2011). Illumina.
https://www.illumina.com/documents/products/technotes/technote_Q-Scores.pdf
- Sawyer, S., Krause, J., Guschanski, K., Savolainen, V., & Pääbo, S. (2012). Temporal patterns of nucleotide misincorporations and DNA fragmentation in ancient DNA. *PLoS one*, 7(3), e34131. <https://doi.org/10.1371/journal.pone.0034131>
- Sayers, E. W., Bolton, E. E., Brister, J. R., Canese, K., Chan, J., Comeau, D. C., Connor, R., Funk, K., Kelly, C., Kim, S., Madej, T., Marchler-Bauer, A., Lanczycki, C., Lathrop, S., Lu, Z., Thibaud-Nissen, F., Murphy, T., Phan, L., Skripchenko, Y., Tse, T., ... Sherry, S. T. (2022). Database resources of the national center for biotechnology information. *Nucleic acids research*, 50(D1), D20–D26. <https://doi.org/10.1093/nar/gkab1112>
- Schuenemann, V. J., Bos, K., DeWitte, S., Schmedes, S., Jamieson, J., Mittnik, A., Forrest, S., Coombes, B. K., Wood, J. W., Earn, D. J. D., White, W., Krause, J., & Poinar, H. N. (2011). Targeted enrichment of ancient pathogens yielding the pPCP1 plasmid of *Yersinia pestis* from victims of the Black Death. *Proceedings of the National Academy of Sciences*, 108(38), E746–E752. <https://doi.org/10.1073/pnas.1105107108>
- Schwarz, C., Debruyne, R., Kuch, M., McNally, E., Schwarcz, H., Aubrey, A. D., Bada, J., & Poinar, H. (2009). New insights from old bones: DNA preservation and degradation in permafrost preserved mammoth remains. *Nucleic Acids Research*, 37(10), 3215–3229. <https://doi.org/10.1093/nar/gkp159>
- Stuiver, M., & Reimer, P. J. (1993). Extended 14C Data Base and Revised CALIB 3.0 14C Age Calibration Program. *Radiocarbon*, 35(1), 215–230. <https://doi.org/10.1017/S0033822200013904>
- Wagner, D. M., Klunk, J., Harbeck, M., Devault, A., Waglechner, N., Sahl, J. W., Enk, J., Birdsell, D. N., Kuch, M., Lumibao, C., Poinar, D., Pearson, T., Fourment, M., Golding, B., Riehm, J. M., Earn, D. J. D., DeWitte, S., Rouillard, J.-M., Grupe, G., ... Poinar, H. (2014b). *Yersinia pestis* and the Plague of Justinian 541–543 AD: A genomic analysis. *The Lancet Infectious Diseases*, 14(4), 319–326. [https://doi.org/10.1016/S1473-3099\(13\)70323-2](https://doi.org/10.1016/S1473-3099(13)70323-2)
- Wood, D. E., Lu, J., & Langmead, B. (2019). Improved metagenomic analysis with Kraken 2. *Genome biology*, 20(1), 257. <https://doi.org/10.1186/s13059-019-1891-0>

Chapter 4: Discussion and Analysis

4.1 Historical Sites and Silivri Excavation Sample Sets

Notably, the Historical Sites sample set demonstrated evidence of extremely poor preservation, evident in the low amount of endogenous human preservation. Only 3/58 had endogenous human content >1%, with none exceeding levels >10%. Similarly, the Silivri Excavation sample set yielded an extremely low amount of endogenous human preservation. Once again, only about 2/76 samples yielded endogenous human content > 1%, with no sample exceeding 10%. BFP55 yielded the greatest amount of endogenous human content of both sets at 8.65%. As all 76 samples were recovered from the same excavated necropolis, the large variation in preservation reflects the scarcity of finding the presence of detectable *Y. pestis* in a similarly sized sample set. Interestingly, despite its higher amount of human content compared to the plague-positive sample and being from the same archaeological site, no plague was detected in it. Comparatively, BFP39, yielding human preservation <0.3%, still contained detectable reads of *Y. pestis*, revealing the fastidious nature of retrieving pathogenic DNA in the field of plague studies.

Typically, as the sample is taken directly from the interior of a human tooth, we would expect there to be a large proportion of human DNA recovered in the ancient sample. We can first consider the amount of sample used and extracted. In efforts to be as minimally destructive as possible, the McMaster Ancient DNA lab retrieves between 30-70 mg of powder from the pulp chamber of each tooth. In comparison to DNA retrieval from other parts of the skeleton (which may yield more starting material but decrease pathogenic specificity), a low amount of starting material being decreased even further as it goes through the subsequent steps of the

protocol may be a factor in the low amount of retained endogenous human content. The most likely factor would be the influences of climate and environment on the structural and chemical integrity of human remains in the Mediterranean region.

The endogenous content of individuals from this study were compared to second pandemic samples from Denmark and the UK. Human content was retrieved from plague-positive individuals in Denmark as examined in Eaton *et al.*, 2023. Also included is unpublished data from previous studies in the McMaster Ancient DNA Centre which attempted to identify candidates for whole genome sequencing (see Table S5.5). As presented, there is a stark difference in endogenous human preservation (Figure 4.1). Specifically, only individuals from Denmark and the UK yielded endogenous human preservation >10% whereas only 4/141 samples from Turkey had human content exceeding 5%. One caveat of this comparison is the difference of sample size; this comparison viewed 141 extracts from first pandemic Turkey and 87 extracts from studies of the second pandemic (12 from Denmark as presented in Eaton *et al.*, 2023, 37 from Denmark, and 38 from the UK in an unpublished study). Though limited in scope, it is apparent that the individuals from Turkey demonstrated less endogenous preservation than extracts from sites in Europe. Future research should further investigate the comparison of endogenous content from sites different geographically but similar temporally.

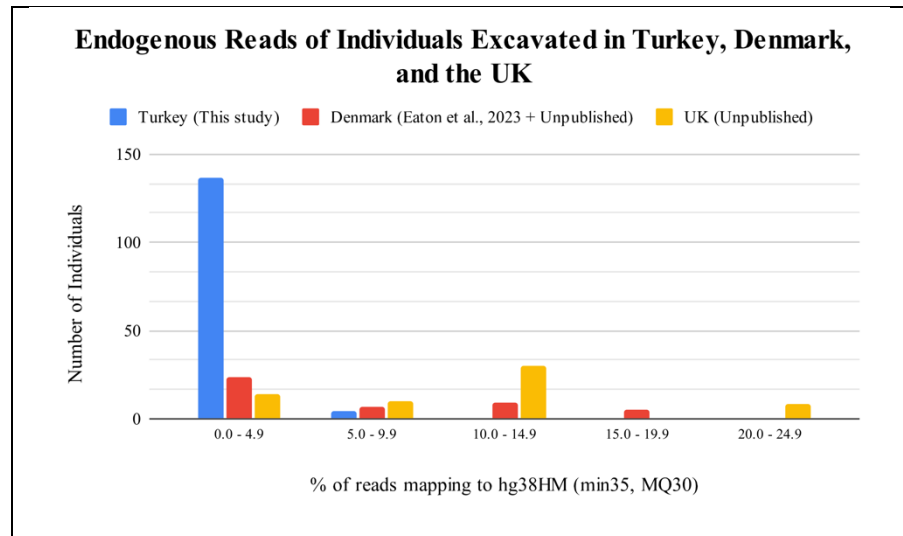


Figure 4.1: Percentage of Endogenous Reads of Individuals Excavated in Turkey, Denmark, and the UK. Endogenous human content of samples from this study compared to samples from Denmark as analyzed in Eaton *et al.*, 2023 and unpublished data of individuals from Denmark and the UK. Evidently, more individuals in Denmark and the UK have individuals showing >10% endogenous human content, whereas more individuals in Turkey have <5% of endogenous human content.

Evidently, locations with cooler or more temperate climates are more successful in retaining endogenous human content. A study conducted by Bollongino and colleagues (2008) concluded that climatic and geographic factors primarily affect the preservation of cattle remains from locations in Europe, the Near East, and Northern Africa. Notably, the study concluded that the high temperatures and ceaseless humidity of the Near East rendered the poorest preservation of its samples in the study. The bones of cattle from the Near East were described to be of “a porous and soft structure,” a description similar to both sample sets outlined in this thesis (Bollongino *et al.*, 2008, p. 92). Thus, not only is ease of access attributed to sampling bias for Western locations but also the *quality* of the samples retrieved in their climates; this may be connected to the dispersal and proliferation of Eurocentric narratives as evident in the current standing of academic publications that appear to value positive results above all else.

Of the Historical Sites sample set, TFP13 had the highest endogenous human

content at about 6.9%. This may be attributed to its retrieval from a relatively well-preserved archaeological site in the Iznik Roman Theatre. Iznik has a rich cultural history and its preservation of human remains adds to its interest. The distribution of sites in this study are all within the Köppen climate classification of temperate, hot, dry summer, with Iznik close to the temperate, hot, warm summer region of Turkey (Beck *et al.*, 2018). Köppen classifications are based on seasonal precipitation and temperature. It can be argued that, although all the sites are of similar climate classification, the quality of the burial and its decreased exposure to climatological elements may have resulted in remains from Iznik being better preserved than other sites.

TFP50 presented the strongest case for the presence of *M. tuberculosis* for the Historical Sites sample set. Specifically, mean coverage of the genome at 0.005X as visualized using Geneious was among the highest in its sample set, and its taxonomic classification using Kraken 2 and the Legacy pipeline classify many of its reads as belonging to the pathogen (Table 3.2). As the sample is from Priene, a site inhabited continuously from around the 4th century BCE to the 14th century CE, the presence of *M. tuberculosis* within any of the centuries of occupation would be a promising analysis. Remains from individual TFP50 were unable to be carbon-dated due to a lack of collagen yield. However, an individual (AT16) from the same site was radio-carbon dated with a 95% likelihood to 352 BCE – 168 BCE (Figure 3.9). Under the assumption that individual TFP50 lived around the same time as individual AT16, this finding may be linked to the presence of *M. tuberculosis* in the Hellenistic period; occupation of Priene during this period has been corroborated by the unearthing of Hellenistic carvings on the Temple of Athena Polias as well as a bouleuterion. Human

disease caused by *Mycobacterium tuberculosis* has been hypothesized to have occurred over several millennia, with documented histories from Ancient Egyptian papyri and comments from Ancient Greek and Byzantine physicians. (Barberis *et al.*, 2017). Archaeological and genomic evidence has been recovered from Peruvian mummies, with three 1000-year-old genomes presenting the hypothesis that the disease-causing agent was present in South American populations before European contact (Bos *et al.*, 2014).

All extracts from the Silivri Excavation sample set were also screened for *M. tuberculosis*; considering total mapped reads using the Legacy pipeline as well as taxonomic classification using Kraken 2, BFP18 and BFP61 presented the most convincing cases. For individual BFP18, 374 reads were mapped using the Legacy pipeline (Figure 3.13). Individual BFP61 mapped 506 reads and, despite the rigorous k-mer matching methods of Kraken 2, manages to retrieve 165 taxonomically classified reads (Figure S5.15). Notably, this extract had the second highest amount of human content in this set at 1.86%. The two individuals from the Silivri Excavation sample set (BFP61 and BFP62) had median probabilities of dating to 352 CE and 362 CE respectively, predating the Justinianic plague (Figure 3.16). Evidently, the necropolis found within the Silivri District may bountifully add to histories of disease in the early Byzantine Empire. Also, as it contained the highest amount of endogenous content for this sample set, an extract from individual BFP55 was also mapped to *M. tuberculosis*. Interestingly, 121 reads were taxonomically classified as *M. tuberculosis* for this extract, though coverage along the genome visualized through Geneious was sparse at 0.002X (Figure 3.14). As with the pathogenic content for all other samples,

further confirmation using targeted enrichment is required for more conclusive analysis.

Additionally, when mapped to *M. tuberculosis*, all extracts of interest in the Historical Sites and Silivri Excavation sample sets revealed a series of stacked reads in near identical regions of the chromosome. Visualization in Geneious linked the regions to the 16S and 23S rRNA genes, of which are ubiquitous in species of bacteria. As such, upon extraction of the stacked reads, they were run through Megablast displaying several bacterial species as results.

Furthermore, there is a strong case for the presence of hepatitis B virus in an extract of TFP39, an individual recovered from Perinthos. As mentioned in Chapter 3, TFP39 has been radiocarbon dated to around 1434 AD during the late Middle Ages. Though much of the numismatic research within Perinthos is rooted in both classical and late antiquity, further investigation into this individual may shed light into the presence of hepatitis B virus in the medieval period. As listed in Chapter 3, the extract was mapped to two hepatitis B virus genomes. Though <1% of its mapped reads can be attributed to the pathogen, their BLAST results exclusively list hepatitis B virus hits. Despite this evidence, targeted enrichment is needed to conclusively determine the presence of hepatitis B virus in the extract. Notably, thanks to advancements in next-generation sequencing, there has been a recent surge in studies dedicated to hepatitis B virus in ancient civilizations. Particularly, 12 genomes were recovered from Bronze-Age individuals though their geographic locations differ from modern distribution of hepatitis B virus, thus presenting questions on how human migration may have played a role in its distribution (Mühlemann *et al.*, 2018). A robust study of 137 ancient hepatitis B genomes revealed its 10,000-year-long relationship with

humans, particularly in its presence in early post-Neolithic farming civilizations and migration into the Americas around 900 years ago (Kocher *et al.*, 2021). As most individuals sampled were from Western Eurasia and thus introduced sampling bias in the study, Sun and colleagues (2024) presented 34 genomes retrieved from individuals recovered in eastern Eurasia that were dated to be 5000 to 400 years old. Despite these advancements, research dedicated to ancient hepatitis B virus is diminutive in comparison to research on *Y. pestis*. Thus, further investigation into this individual would not only add to knowledge of disease in the late Middle Ages, but also to the complexity of the relationship between humans and hepatitis B virus through migration, trade, and settlement patterns. Despite the convincing Megablast results, low quality damage profiles driven by a lack of mapped reads and genomic coverage display how TFP39 is a candidate for targeted enrichment in future studies.

4.2 Positive Plague Sample

4.2.1 Preliminary Pathogenic Confirmation

One tooth from the Silivri District Necropolis (BOTAŞ Excavation) tested positive for the presence of *Y. pestis*. BFP39 was subsampled twice (Figure 3.10). Despite being very small and likely belonging to a juvenile individual, the tooth was tough and remained intact during drilling. As stated in subsection 3.32, two extraction methodologies yielded two extracts of the same tooth (ME-BFP39 and CS-BFP39).

We used the *pla* PCR screening assay to look for the presence of *pla* and plague. Running alongside *pla* standards, plague-positive diagnosis using this screening method requires cycle amplification (Cq) values for 30-40 cycles across multiple runs and melting peaks within 0.5-1 degree of the standard melt curve, which

is typically 77°C. For both ME-BFP39 and CS-BFP39, diluted and undiluted runs of each extract were tested to indicate the presence of the *pla* gene (Figure 3.11).

Although the 1:10 dilutions of each extract did not amplify, both straight extracts followed the criteria for plague-positive identification; it is plausible that the 1:10 dilutions were simply so diluted that plague signal was not detectable (Table 3.3).

Nevertheless, the amplification of the straight extracts suggests that BFP39 is indeed plague-positive.

Sequenced molecules were mapped to the *Y. pestis* genome to further verify the presence of the pathogen. With a minimum length of 35 base pairs and a mapping quality of 30, 57 reads from CS-BFP39 and 68 reads from ME-BFP39 were mapped to the CO92 reference genome. If analyzed using a minimum length of 30 base pairs and a mapping quality of 30 (min30MQ30), a less stringent approach, 100 reads from CS-BFP39 and 120 reads from ME-BFP39 were mapped. Although the overall proportion of total mapped *Y. pestis* molecules appears low, it is still relatively high for recovery of the pathogen in an ancient sample and supports the results of the initial *pla* screen. There is also some semblance of the typical ancient C → T and G → A transitions in the fragment misincorporation plots of both extracts, though the low number of total mapped reads prevents a normal smooth curve; the low number of reads included in the analysis only highlights the noise seen in other substitutions, as well as deletions and insertions relative to the reference. Furthermore, stacked reads are present in the Geneious figures displayed by both extracts. Several genera of bacteria (*Pseudomonas*, *Vibrio*, *Yersinia*, etc.) were classified when the reads were extracted and run through Megablast, which are likely attributed to conserved regions in bacteria. In any case, further analysis and more reads are required to determine the

significance of the series of the stacking. Overall, although some reads have been mapped to the reference sequence, low quality damage profiles and a lack of genomic coverage reveal BFP39’s need for targeted enrichment.

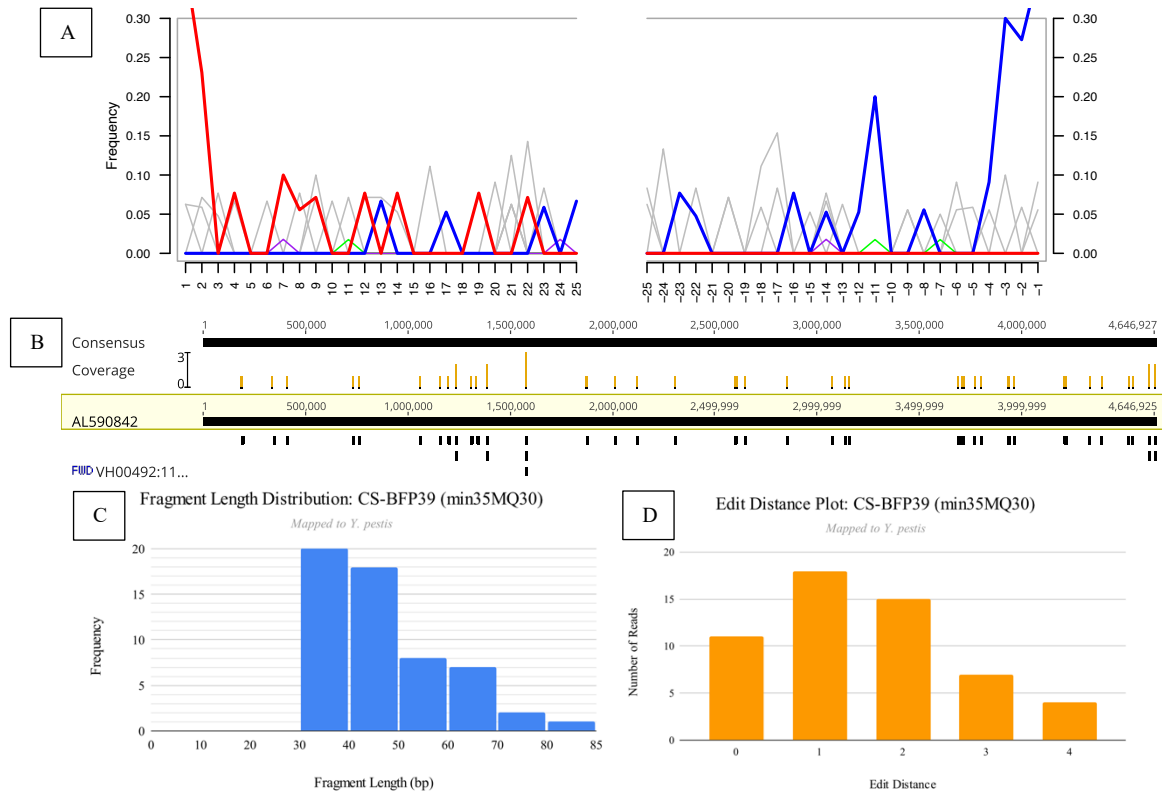
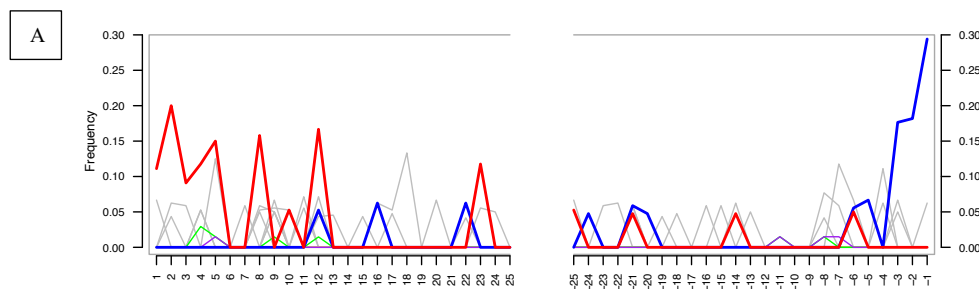


Figure 4.2: CS-BFP39 mapped to the *Y. pestis* reference genome (min35, MQ30). a) Ancient DNA authentication using mapDamage. The red line represents C to T substitutions, and the blue line represents G to A substitutions. Purple represents insertions relative to the reference, green represents deletions relative to the reference, and grey represents all other substitutions. b) Geneious visualization of reads mapping to the *Y. pestis* chromosome. c) Fragment length distribution. d) Plot of edit distances.



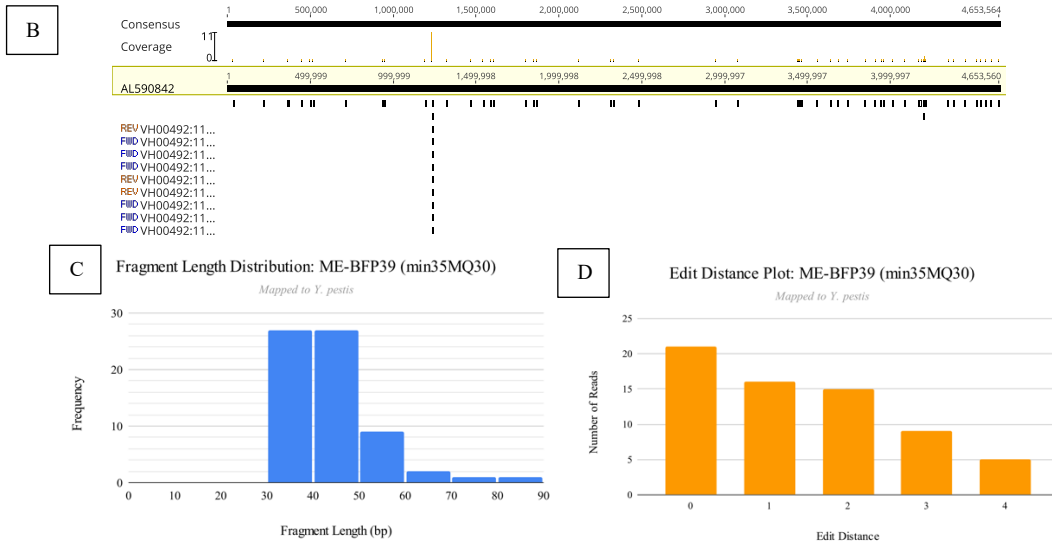


Figure 4.3 (a-d): ME-BFP39 mapped to the *Y. pestis* reference genome (min35, MQ30). a) Ancient DNA authentication using mapDamage. The red line represents C to T substitutions, and the blue line represents G to A substitutions. Purple represents insertions relative to the reference, green represents deletions relative to the reference, and grey represents all other substitutions. b) Geneious visualization of reads mapping to the *Y. pestis* chromosome at 0.001X mean coverage. c) Fragment length distribution. d) Plot of edit distances.

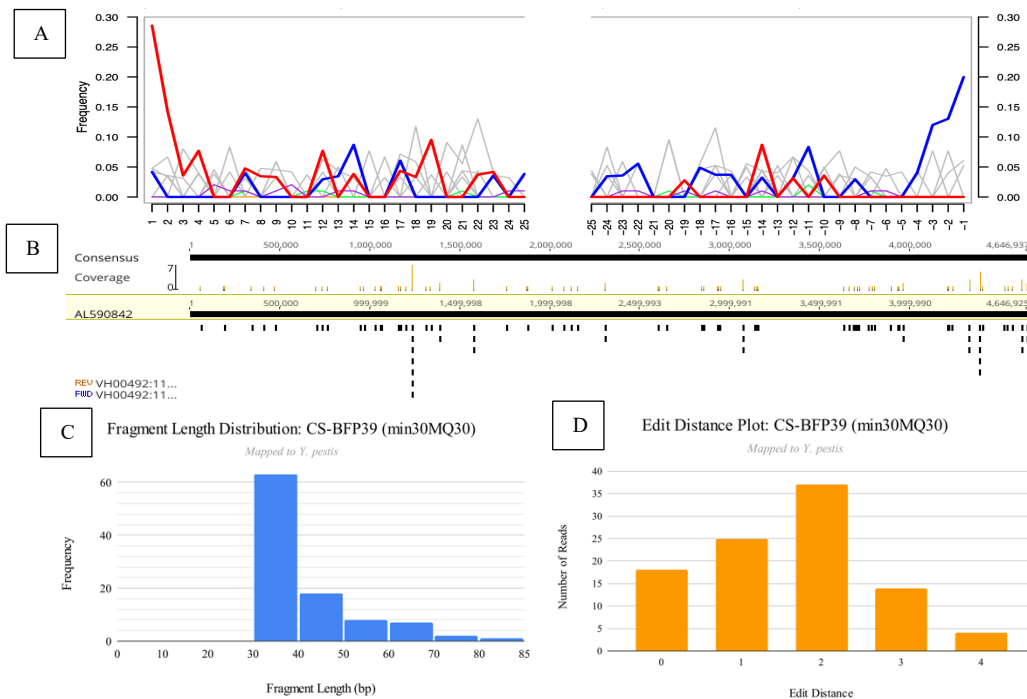


Figure 4.4 (a-d): CS-BFP39 mapped to the *Y. pestis* reference genome (min30, MQ30). a) Ancient DNA authentication using mapDamage. The red line represents C to T substitutions, and the blue line represents G to A substitutions. Purple represents insertions relative to the reference, green represents deletions relative to the reference, and grey represents all other substitutions. b) Geneious visualization of reads mapping to the *Y. pestis* chromosome at 0.001X mean coverage. c) Fragment length distribution. d) Plot of edit distances.

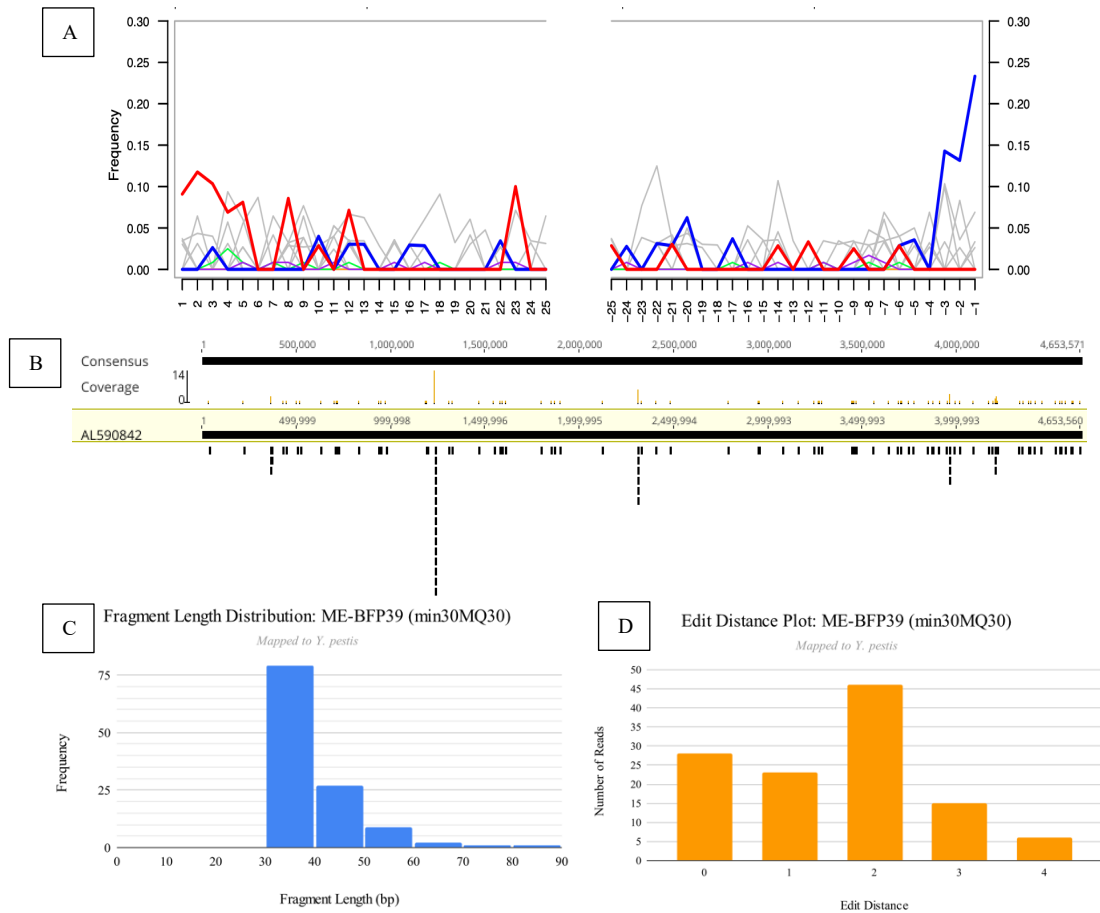


Figure 4.5 (a-d): ME-BFP39 mapped to the *Y. pestis* reference genome (min30, MQ30). a) Ancient DNA authentication using mapDamage. The red line represents C to T substitutions, and the blue line represents G to A substitutions. Purple represents insertions relative to the reference, green represents deletions relative to the reference, and grey represents all other substitutions. b) Genomic visualization of reads mapping to the *Y. pestis* chromosome at 0.001X mean coverage. c) Fragment length distribution. d) Plot of edit distances.

Furthermore, both BFP39 extracts were mapped to the hard-masked human reference genome 38 (hg38). About 0.0823% or 13,668 sequenced molecules were mapped for the CS-BFP39 extract whereas about 0.2867% or 43,345 molecules were mapped for the ME-BFP39 extract (Table 3.4). Under less stringent analysis using a minimum length of 30, only about 0.104% or 17,327 sequenced molecules were mapped for CS-BFP39, and only about 0.335% or 52,980 sequenced molecules were mapped for ME-BFP39. In both cases, these extracts present very low endogenous human aDNA which is indicative of poor overall preservation of the human tooth. Additionally,

despite a low number of reads mapped to the human reference genome, both extracts reveal a high level of damage on the terminal ends of their DNA molecules. In contrast to the damage profiles of reads mapped to the *Y. pestis* sequence, the hg38 damage profiles of both extracts presents what is expected in ancient samples, most likely due to the greater number of mapped reads (Figure 4.6a). Specifically, both BFP39 extracts have smooth misincorporation frequency signals reaching above 30% at their terminal ends which, as detailed in Chapter 1, is consistent with authentic ancient DNA molecules.

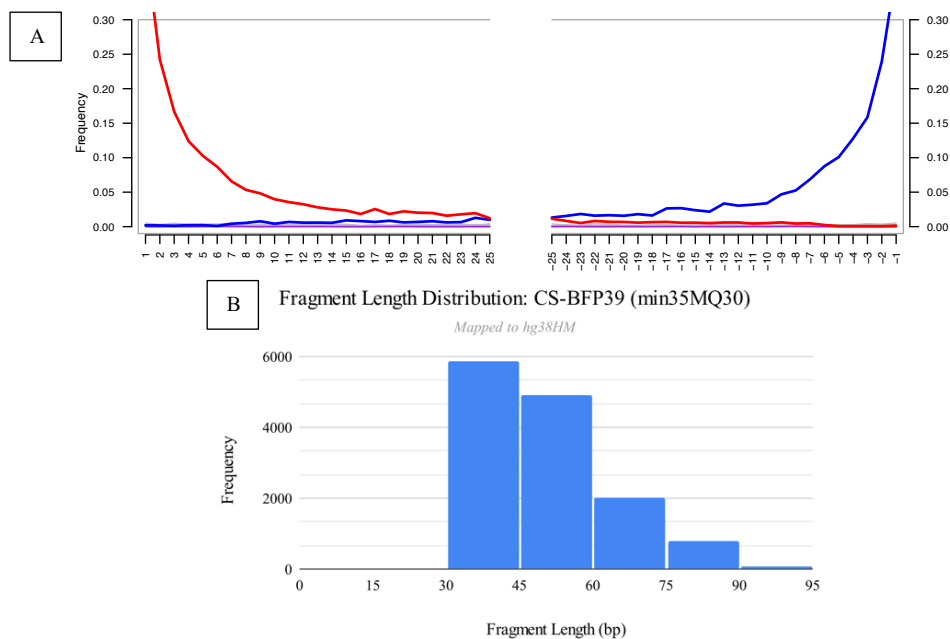


Figure 4.6 (a-b): CS-BFP39 mapped to the masked human reference genome hg38 (min35, MQ30). a) Ancient DNA authentication using mapDamage. The red line represents C to T substitutions, and the blue line represents G to A substitutions. The purple line represents insertions relative to the reference. b) Fragment length distribution.

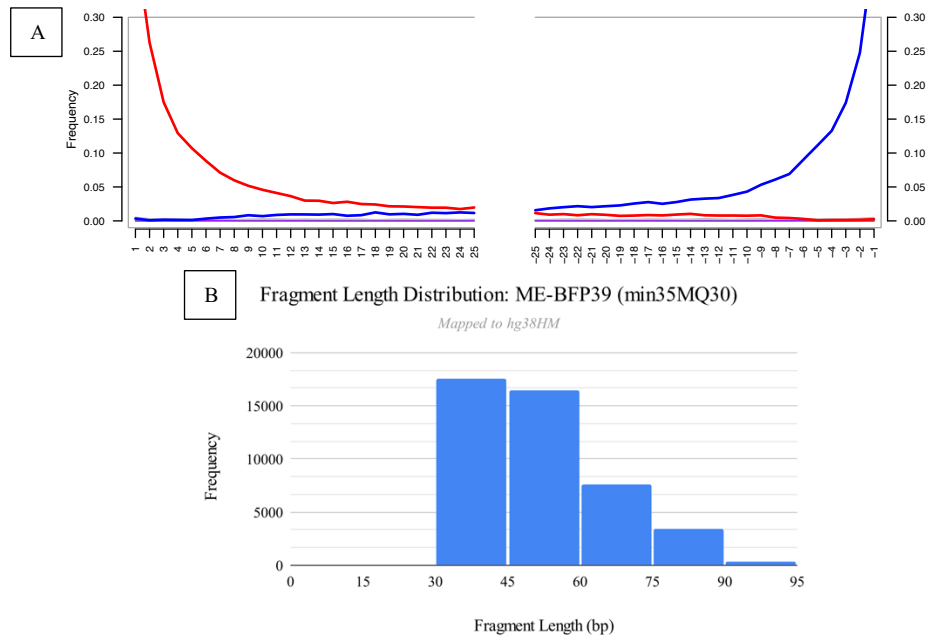


Figure 4.7 (a-b): ME-BFP39 mapped to the masked human reference genome hg38 (min35, MQ30). a) Ancient DNA authentication using mapDamage. The red line represents C to T substitutions, and the blue line represents G to A substitutions. The purple line represents insertions relative to the reference. b) Fragment length distribution.

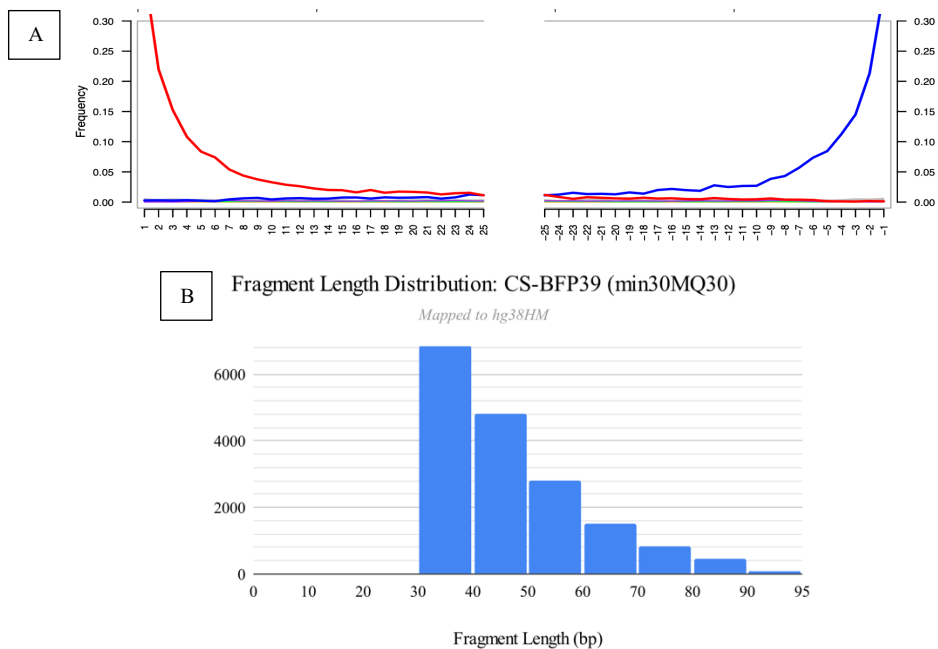


Figure 4.8 (a-b): CS-BFP39 mapped to the masked human reference genome hg38 (min30, MQ30). a) Ancient DNA authentication using mapDamage. The red line represents C to T substitutions, and the blue line represents G to A substitutions. The purple line represents insertions relative to the reference. b) Fragment length distribution.

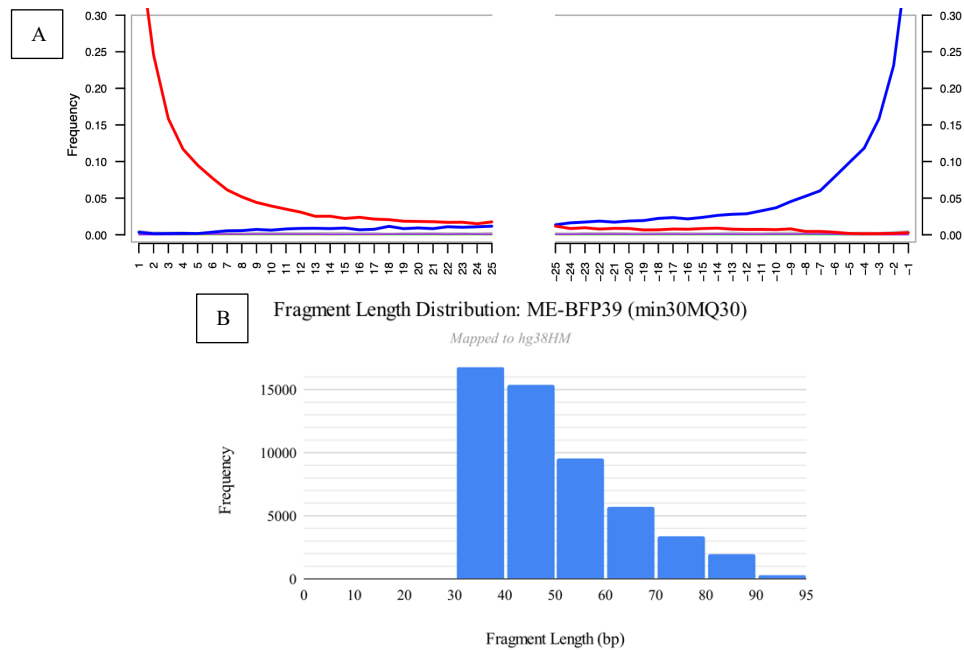


Figure 4.9 (a-b): ME-BFP39 mapped to the masked human reference genome hg38 (min30, MQ30). a) Ancient DNA authentication using mapDamage. The red line represents C to T substitutions, and the blue line represents G to A substitutions. The purple line represents insertions relative to the reference. b) Fragment length distribution.

As mentioned, Kraken 2 and BLAST are bioinformatic tools that classify and assign a sample's molecules to organisms within a curated database. A total of 38 molecules for CS-BFP39 and 48 molecules for ME-BFP39 were identified by Kraken2 as belonging to the *Yersinia* genus. Only one read from each extract was specifically attributed to *Y. pestis*. As mentioned in Chapter 3, Kraken2 relies on exact k-mer matches and is especially specific; some of the unassigned *Yersinia* reads (19 for CS-BFP39 and 30 for ME-BFP39) may indeed be *Y. pestis* but are not specific enough to be definitively categorized. Furthermore, reads mapping to the chromosome were mapped using the bioinformatic visualization software Geneious. Unsurprisingly, as only shotgun sequencing data has been conducted thus far, few overall reads have been able to cover the genome; multiple rounds of targeted enrichment will be

4.2.2 Significance in First Pandemic Studies

Remains of the subsampled tooth from individual BFP39 were sent for radiocarbon dating. Results revealed a 95% likelihood that the remains are dated to 483-602 CE, with a greater probability that the individual is from 537-602 CE. Incredibly, this date places individual BFP39 right near the cusp of the Justinianic Plague and the initial outbreaks of the first plague pandemic. Thus, if successfully enriched, a genome from BFP39 would be the first *Y. pestis* genome from the ancient Mediterranean attributed to the first pandemic. Additionally, the tooth from which this extract was sampled was likely from a juvenile individual. Though, unlike many of the remains from the same sample set that fragmented easily, the tooth attributed to BFP39 was surprisingly durable. As such, the significance of the individual's age at death and burial context should be further investigated. Notably, an ancient genome from this region in Turkey would improve the validity of trusted historical sources. Once again, though a single novel genome from this study cannot determine how many people died during the pandemic nor the direction it travelled as a whole or within Turkey, its discovery may be used to shift the current perception of first pandemic in a broader, more global direction.

4.3 Limitations of aDNA

As methods and technologies advance, there must be a careful and shared understanding that science is and never has been completely objective. A common misconception in both past and present studies on ancient infectious disease is that science has the answer to every question. In studies of the first pandemic, researchers must be held accountable and outwardly address any dubious claims. As such, those

seeking to use scientific technologies to address questions of the histories of the past must be acutely aware of its limitations; this is evidently applicable to the field of paleogenomics and ancient DNA. In the case of plague specifically, it is crucial to note that genomes are simply strings of nucleotides and that conclusive results can only be generated by placing them into context. This section will cover underlying biases in the field of ancient DNA to compliment the section on the importance of publishing negative results in Chapter 5.

For instance, despite the advancements in genetic technologies creating *Y. pestis* phylogenies of strains from first pandemic individuals, it is important to remember that the genomes, as scarce as they are, are nearly genetically identical, only differing by less than five non-synonymous SNPs in most cases along a phylogeny (Damgaard *et al.*, 2018). In addition, many of these SNPs affect genes that code for hypothetical proteins, greatly diminishing the ability to deduce and analyze functional ramifications. This lack of variance in genetic makeup and virulence renders it impossible to generate convincing arguments regarding origins and transmission of *Y. pestis*; at best, they can introduce theories but require a wider set of evidence of different subfields to support them.

One key issue with the integration of genomic data into histories of the first plague pandemic is a lack of effective interaction, thus limiting holistic interpretation and meaningful understanding. Integrating plague narratives, as one example, may be able to deduce regions that are most likely to confirm the presence of the pathogen. However, as we have seen, the genome discovered at Edix Hill in London had had no record of plague until at least 100 years after the date attributed to existing genomes (Keller *et al.*, 2019; Sarris, 2022). Whether this lack of available records is because

there were so few written, so few that survived, or a combination of both, may never be definitively known; the first genomes from Aschheim and Altenerding in Germany were remarkable as there is no existing written evidence within these regions. Thus, records of plague may only account for a small subset of what was truly present, demonstrating the limitation that we are only left with the stories that survived over the centuries. In addition, research biases may be present in analysis, whether intentional or not. Crucially, as often stated in anthropological and historical research, absence of evidence is not evidence of absence. Specifically, deductions and analyses are often limited by the methods and criteria for measuring success. For instance, metagenomics may convey a bias towards less damaged or contaminated DNA (Poinar, 2022). This results in a particular bias against many of the samples available for the first pandemic in the Mediterranean region as they are known for their poor archaeological preservation. Expansion on these various biases is presented in the fifth chapter of this study.

Furthermore, though it has been hailed as one of the reasons for a boom in genomic sequencing, polymerase chain reaction (PCR) has been historically known to be sensitive to contamination, opening the door for misinterpretation; again, science can never be considered objective. In this study, the preliminary *pla* qPCR screen proved to have its own set of challenges. First and foremost, the screen is not technically a qPCR as no amount of DNA is being quantified; instead, the Cq values are being compared to one set of *pla* standards. Also, the use of dilutions (specifically in the presence of primer dimers due to decreased template) increased the number of false positives and required a confirmation step. Additionally, as the coverage of some plague-positive individuals are so low, they are often excluded from further analysis.

For instance, although 3X is often considered to be the minimum coverage for a publishable genome, studies should consider decreasing the threshold especially in areas where remains show a decreased level of preservation. As such, future advancements should seek to increase the amount of genomic diversity by incorporating data that is not considered to be “of value” by Western standards, or at the very least publishing negative results.

As stated by numerous archaeologists, historians, anthropologists, and biologists alike, it is imperative that a wide selection of sampling, testing, contextualization, and re-visitation is required for genomes to make sense of past histories of plague. For instance, with the improvement of genetic technology, it is evidently clear that the traditional (and heavily proliferated) notion of the three historical plagues needs revisitation; as modern strains are derived from those of the Second Plague Pandemic, it can be argued that we are still genetically living in the Second Plague Pandemic (Keller *et al.*, 2019; Eaton *et al.*, 2023). It is also important to note that the century-long gap between reports of more modern outbreaks from the 18th to 19th centuries stem from a Eurocentric perspective; plague in fact persisted in the Mediterranean during this period (Poinar, 2022; Varlık 2020). These findings have demonstrated the need for a more inclusive, global view of past and present plague outbreaks, as well as the necessity to question popular narratives.

Importantly, a single genome (or even a handful of genomes) would not be able to resolve any current debates. What would be of interest, however, are multiple genomes from regions of the world that have yet to express genomic evidence for the first plague pandemic, namely those within the Mediterranean and northern Africa. Doing so would allow for new interpretations of the transmission of plague through

the centuries of the first pandemic, corroborating contemporary plague narrators, while stressing that these conclusions are in no way immutable and definitive. Furthermore, deducing the rate of mortality from a single genome, even with an extensive phylogeny, is impossible. Doing so would require extensive context on what might have contributed to changes in the frequency of death during a certain period and affecting a certain group of people. Novel discovery or interpretation of historical records would be useful, though they are only as convincing as the modern arguments derived from them. Only in contextualization with numerous other streams of information and multiple lines of evidence would we be able to map a disease's spread across a geographic region; even then, these deductions can only be regarded as hypotheses and should be continually revisited. Additionally, although one genome would certainly be insufficient in proposing a definitive number of plague victims attributed to the Justinianic Plague or first plague pandemic in general, mere confirmation of classically trusted historical sources may inspire more historians to actively implement the results of genomic studies into their histories of the first plague pandemic.

4.4 References

- Barberis, I., Bragazzi, N. L., Galluzzo, L., & Martini, M. (2017). The history of tuberculosis: from the first historical records to the isolation of Koch's bacillus. *Journal of preventive medicine and hygiene*, 58(1), E9–E12.
- Beck, H. E., Zimmermann, N. E., McVicar, T. R., Vergopolan, N., Berg, A., & Wood, E. F. (2018). Present and future Köppen-Geiger climate classification maps at 1-km resolution. *Scientific data*, 5, 180214.
<https://doi.org/10.1038/sdata.2018.214>
- Bollongino, R., Tresset, A., & Vigne, J.-D. (2008). Environment and excavation: Pre-lab impacts on ancient DNA analyses. *Comptes Rendus Palevol*, 7(2), 91–98.
<https://doi.org/10.1016/j.crpv.2008.02.002>

- Bos, K. I., Harkins, K. M., Herbig, A., Coscolla, M., Weber, N., Comas, I., Forrest, S. A., Bryant, J. M., Harris, S. R., Schuenemann, V. J., Campbell, T. J., Majander, K., Wilbur, A. K., Guichon, R. A., Wolfe Steadman, D. L., Cook, D. C., Niemann, S., Behr, M. A., Zumarraga, M., Bastida, R., ... Krause, J. (2014). Pre-Columbian mycobacterial genomes reveal seals as a source of New World human tuberculosis. *Nature*, *514*(7523), 494–497. <https://doi.org/10.1038/nature13591>
- Damgaard, P. de B., Marchi, N., Rasmussen, S., Peyrot, M., Renaud, G., Korneliussen, T., Moreno-Mayar, J. V., Pedersen, M. W., Goldberg, A., Usmanova, E., Baimukhanov, N., Loman, V., Hedeager, L., Pedersen, A. G., Nielsen, K., Afanasiev, G., Akmatov, K., Aldashev, A., Alpaslan, A., ... Willerslev, E. (2018). 137 ancient human genomes from across the Eurasian steppes. *Nature*, *557*(7705). <https://doi.org/10.1038/s41586-018-0094-2>
- Eaton, K., Featherstone, L., Duchene, S., Carmichael, A. G., Varlık, N., Golding, G. B., Holmes, E. C., & Poinar, H. N. (2023). Plagued by a cryptic clock: Insight and issues from the global phylogeny of *Yersinia pestis*. *Communications Biology*, *6*(1), 23. <https://doi.org/10.1038/s42003-022-04394-6>
- Harkins, K. M., Buikstra, J. E., Campbell, T., Bos, K. I., Johnson, E. D., Krause, J., & Stone, A. C. (2015). Screening ancient tuberculosis with qPCR: challenges and opportunities. *Philosophical transactions of the Royal Society of London. Series B, Biological sciences*, *370*(1660), 20130622. <https://doi.org/10.1098/rstb.2013.0622>
- Keller, M., Spyrou, M. A., Scheib, C. L., Neumann, G. U., Kröpelin, A., Haas-Gebhard, B., Pfüffgen, B., Haberstroh, J., Ribera i Lacomba, A., Raynaud, C., Cessford, C., Durand, R., Stadler, P., Nägele, K., Bates, J. S., Trautmann, B., Inskip, S. A., Peters, J., Robb, J. E., ... Krause, J. (2019). Ancient *Yersinia pestis* genomes from across Western Europe reveal early diversification during the First Pandemic (541–750). *Proceedings of the National Academy of Sciences of the United States of America*, *116*(25), 12363–12372. <https://doi.org/10.1073/pnas.1820447116>
- Kocher, A., Papac, L., Barquera, R., Key, F. M., Spyrou, M. A., Hübler, R., Rohrlach, A. B., Aron, F., Stahl, R., Wissgott, A., van Bömmel, F., Pfefferkorn, M., Mitnik, A., Villalba-Mouco, V., Neumann, G. U., Rivollat, M., van de Loosdrecht, M. S., Majander, K., Tikhbatova, R. I., Musralina, L., ... Kühnert, D. (2021). Ten millennia of hepatitis B virus evolution. *Science (New York, N.Y.)*, *374*(6564), 182–188. <https://doi.org/10.1126/science.abi5658>
- Mühlemann, B., Jones, T. C., Damgaard, P. B., Allentoft, M. E., Shevnina, I., Logvin, A., Usmanova, E., Panyushkina, I. P., Boldgiv, B., Bazartseren, T., Tashbaeva, K., Merz, V., Lau, N., Smrčka, V., Voyakin, D., Kitov, E., Epimakhov, A., Pokutta, D., Vicze, M., Price, T. D., ... Willerslev, E. (2018). Ancient hepatitis

B viruses from the Bronze Age to the Medieval period. *Nature*, 557(7705), 418–423. <https://doi.org/10.1038/s41586-018-0097-z>

Poinar, H. (2022). Past Plagues: On the Synergies of Genetic and Historical Interpretations of Infectious Disease. In L. Jones & N. Varlık (Eds.), *Death and Disease in the Medieval and Early Modern World: Perspectives from across the Mediterranean and Beyond* (pp. 319–340). Boydell & Brewer. <https://doi.org/10.1017/9781800107861.013>

Sarris, P. (2022). Viewpoint New Approaches to the ‘Plague of Justinian’. *Past & Present*, 254(1), 315–346. <https://doi.org/10.1093/pastj/gtab024>

Sun, B., Andrades Valtueña, A., Kocher, A., Gao, S., Li, C., Fu, S., Zhang, F., Ma, P., Yang, X., Qiu, Y., Zhang, Q., Ma, J., Chen, S., Xiao, X., Damchaabadgar, S., Li, F., Kovalev, A., Hu, C., Chen, X., Wang, L., ... Cui, Y. (2024). Origin and dispersal history of Hepatitis B virus in Eastern Eurasia. *Nature communications*, 15(1), 2951. <https://doi.org/10.1038/s41467-024-47358-6>

Varlık, N. (2020). The plague that never left: Restoring the Second Pandemic to Ottoman and Turkish history in the time of COVID-19. *New Perspectives on Turkey*, 63, 176–189. <https://doi.org/10.1017/npt.2020.27>

Chapter 5: Conclusions and Future Directions

5.1 Summary

5.1.1 Ancient DNA: Realistic Expectations

The discovery of *Y. pestis* genomes has considerably widened and nuanced contemporary interpretations of the first plague pandemic. Nevertheless, given the limitations of ancient DNA and paleogenomics, plague researchers of all disciplines share equal responsibility to integrate interdisciplinary analyses, shortcomings, and ethical consideration into their work. First, one great misconception about ancient DNA is the false notion of its objectivity. It is important to remember that only “quality” genomes are utilized in published phylogenies. Though an individual may be found to have been plague positive (a rare case in itself), the genome will not be carried into downstream analyses if it does not meet selection criteria; with their scarcity, re-visiting existing genomes is warranted as scientific methods advance. Additionally, a lack of unpublished work feeds the belief that only positive results can advance the field. Examples of such findings could be a poorly designed study with inadequate resources failing to produce defensible results, a well-planned study with sufficient resources that nevertheless yields inconclusive evidence, and a study that produces the opposite of the desired outcome of its researchers (Sandercock, 2012). Withholding negative results is thus able to skew conclusions in given fields with the introduction of biases, affects decisions created by policymakers, and proliferates misinformation among the public (Mlinarić *et al.*, 2017). As studies of ancient infectious disease are becoming quickly intertwined with conclusions derived from the analysis of ancient DNA, it is crucial to highlight the evident publication biases that

feed into the notion of the latter's invulnerability. Publication of negative results would undoubtedly shed light into exactly how much work is involved in processing and analyzing data for historic contextualization, ensure that, in matters of ethics, parties in underrepresented regions of the world are able to have their work seen on a global scale, and offer a sobering view of the realistic expectations of ancient DNA. In-depth studies and re-analysis of the SNPs even within current genomes may also propose novel hypotheses associated with *Y. pestis* pathogenicity; biological approaches in consultation with modern clinical studies may be undertaken at an individual level to consider these hypotheses. Although some journals are now shifting towards the purposeful inclusion of negative results, it is up to others (namely those most influential) and their editors alike to follow suit (Bik, 2024).

There is a chance that the long-standing debate over the origins of the first plague pandemic will never be solved as the definition of "origin" varies among researchers and various cross-field factors are involved in addressing them. Although expanding the current definition of what is considered worthy of research and investigating alternative interpretations would be an asset, researchers should be acutely wary of their own underlying biases. As mentioned in the introductory chapter, the impact of the work done for the Black Death has skewed public and academic perception of the destructive capabilities of plague in general, which are then superimposed onto the already limited findings associated with the first plague pandemic. Similarly, ancient plague studies cannot be separated from the large amount of ascertainment bias involved with the retrieval of human and animal remains for sampling. Ascertainment bias prevents a complete and true interpretation of a set of data due to improper and unequal representation of all members or groups in a

target population. Preliminary factors such as the presence of detailed historical accounts, preserved written records, noteworthy burials, and ease of access to sets of human remains can affect distribution of funds, resources, and attention. (Poinar, 2022). Notably, Eaton and colleagues (2023) attributed sampling bias to irreproducible temporal signals in populations across studies in the *Pestoides* (0.PE) and *Antiqua* (0.ANT) biovars of the *Y. pestis* phylogeny. In the same study, they mention that informative temporal estimates can only be retrieved if *Y. pestis* is sufficiently sampled over multiple decades—a feat severely hindered by ascertainment bias in studies of the first plague pandemic. As mentioned, published articles of the first pandemic have come from outside the Mediterranean region; these biases counter the existence of known historical evidence but can be explained by preservation bias (or how the preservation of a sample negatively affected by weather and temperature may have a decreased likelihood of DNA retrieval) and accessibility to sites within the region due to political, temporal, and geographical factors. As such, concrete conclusions about the demographic impact of the first plague pandemic are unlikely to be derived from genomic evidence. For instance, changes in SNP profiles are difficult to interpret on levels of bacterial pathogenicity, much less a regulated effect on the economy or directional travel. If future research was to attempt to do so, it must not rely on genomic findings alone to minimize the risk of over-interpretation.

Given these limitations, what then does science bring to the study of past plague pandemics? Can the field of ancient DNA exist without the influence of genomes? Primarily, the field of genetics is able to bring in new perspectives. As previously stated, traditional and persistent depictions of the First Plague Pandemic were formed through analysis, translation, and interpretation of historical accounts;

new perspectives are required to recontextualize these sources and prevent their mere reiteration. Future genomic analysis may also provide further insight into the current list of genomes as well. For instance, the presence of genomes in England over a hundred years before the first-recorded presence of plague in the area around the seventh century has yet to be addressed. Furthermore, genomes from non-European sites would direct studies on the significance of the DA101 genome found in Kyrgyzstan. In theory, a newly discovered genome that falls between DA101 and genomes discovered at Edix Hill would be particularly interesting as it may contribute to (though not solve) the debate on plague's possible journey from Central Asia to western Europe crossing Anatolia. However, for better or for worse, the influence of its proliferated inviolability has the capacity to direct the current landscape.

When working with human remains and destructive sampling in the field of ancient DNA, very few publications comment on the toll these actions have on the researchers; if one does not have the proper constitution to do such work, it is perceived that they should not be doing it at all. For this thesis, as I was subsampling a set of very fragile ancient teeth likely belonging to children, I found myself needing to take frequent breaks. On a particularly small tooth, likely deciduous and difficult to keep intact, I wrote down my thoughts as I was experiencing these emotions: "*Does it ever get any easier destroying children's teeth? We have skeletons in our closets and pray they won't haunt us. If I push too hard against the wheel, I'll break underneath it.*" I do not believe, on a mechanical and practical level, it will get any easier destroying children's teeth with the current state or priority of protocols; more action must be taken to implement methods that prioritize keeping the structural integrity of a tooth or remains in general. On an emotional level, I do not believe it *should* get any

easier to sample the remains of those who lived long before us; I disagree with the presumption that working on ancient remains involves a conscious separation between the researcher and the remains of the deceased individual. By this I do not mean that a researcher should always emotionally attach themselves to a set of human remains as doing so may cause issues in the interpolation of data and subsequent defence of it. Rather, researchers should refrain from dissociating when sampling human remains. When irreversibly destroying human material, no matter the quantity, a researcher should be acutely aware of what they are doing, why they are doing it, and consider its implications. At the time of writing, the field of ancient DNA is a wheel that churns out high-profile publications with rigid protocols and seemingly no time or space for change. The road between the past and the present may now be a one-way street, though the road between the present and the future is yet to be paved. The bricks we lay in the next few years will become the foundation for future ancient DNA research—where will they lead us?

5.1.2 Rejecting Eurocentrism in First Pandemic Studies

This study sought to retrieve the first *Y. pestis* genome from Turkey, which would serve as an extremely significant discovery for first plague pandemic studies, considering that the written accounts of the pandemic that have long informed our estimations of it both primarily concern the spread and devastation of plague in Turkey. As stated, current literature lacks a plague genome from Turkey let alone the wider the northeastern Mediterranean region, even though plague is thought by some to have spread through it to reach Europe and even though, again, it is the experience of plague at Constantinople in the sixth century that has most influenced the histories

of the first plague pandemic in literature (Stathakopoulos 2004; Harper 2017; Mordechai and Eisenberg 2019; Sessa 2019; Newfield 2022). Genomic analyses provide one way to greatly improve our understanding of the plague by investigating how, when, and from where it reached the Mediterranean region, questioning epidemiologically orientalist narratives. Admittedly, although a single novel genome from this study cannot determine how many people died during the pandemic nor the direction it travelled, it measurably advances our understanding of the pandemic by shifting its current perception of being genomically restricted to European sites. Accordingly, plague studies have overwhelmingly been conducted by Western institutions and a system that has been created to generate and answer primarily Eurocentric questions (Poinar, 2022). Contextualization of genomes using substantive methods utilizing textual and archaeological analyses will allow for a more nuanced grasp of the pandemic's demographic, cultural, and economic effects on populations in Turkey during the first plague pandemic.

5.1.3 Less Harm: The Necessity of Ethics in Ancient DNA Analysis

The study of infectious disease is currently undergoing a momentous shift in bridging new historic and molecular discoveries together. As such, with the dynamic environment of ancient DNA and infectious disease moving at a breakneck pace, research groups must avoid prioritizing research productivity over active community and interdisciplinary engagement (Kowal *et al.*, 2023). Additionally, it is critical to acknowledge that most of the opportunities to analyze plague have been claimed by Western institutions (Blakey *et al.*, 1999; Sidhu and Parry, 2022). One way of viewing the evolution of these systems is by considering how relationships between Western

institutions and Indigenous Peoples have started, ended, endured, and have attempted to be repaired. In spaces deeply rooted in the notion that the objects of research are simply incapable of adequately contributing to research, it is imperative to acknowledge that “objectification is a process of dehumanization” (Tuhiwai Smith, 2021, p. 44). Tuhiwai Smith’s chapter on colonizing knowledges details how Indigenous knowledge was extracted and distributed while simultaneously dubbed as novel discoveries; she comments on how modern Indigenous researchers must now sift through the remnants of what was taken in the past to study what has been left in the present. Importantly, it is warranted to take a step back and consider exactly who has historically been able to perform this research, who has been permitted to respond, and consider which and why certain voices have been louder than others. As such, scholars must be aware of the limited access to burial sites and human remains, and further acknowledge that much of this access can be attributed to the remnants and influence of colonial powers (Poinar, 2022). Furthermore, as it has been increasingly evident that retrieval of samples in key locations within northern Africa and the Mediterranean, it is critical that researchers are sensitive and made aware of the different socio-political factors that may have affected access to critical sites and burials.

Furthermore, as plague technologies and methodologies continue to advance, efforts to minimize destructive sampling is necessary. When plague genomics first began to surface, whole tooth roots were crushed to screen for the presence of *Y. pestis*, proving to be an efficient method yet effectively destroying the entire sample. The current methodology, as was used to retrieve many of the first pandemic genomes, involves cutting off the crown of the tooth to drill into the roots. Here, only

tooth powder is retrieved for testing. This method, however, introduces the possibility of fragmenting the tooth, generates a relatively large amount of heat into the pulp cavity which may degrade DNA, and is more time-consuming. Future ancient DNA retrieval methods should prioritize reducing DNA degradation, as well as generating the least amount of destruction on the tooth. Furthermore, in projects where DNA retrieval is performed on the remains of those linked to living populations, it is crucial that researchers meet with, explain, and remain transparent with community researchers with regards to how those remains will be treated prior to any destructive sampling.

Initially, a large part of this thesis attempted to pioneer a less destructive subsampling technique. Specifically, it was created to target DNA more accurately within the pulp cavity, simultaneously decreasing chances of tooth fragmentation and DNA degradation. The novel method would have involved embedding each tooth in resin to be longitudinally cut in half, effectively exposing the pulp chamber entirely for subsequent DNA extraction. The teeth would first undergo a series of visual analyses to determine positioning as any holes penetrating a tooth's outer layer may allow epoxy resin to seep into the pulp cavity and contaminate any DNA present; each tooth would be treated as its own respective case and have its own individual protocol.

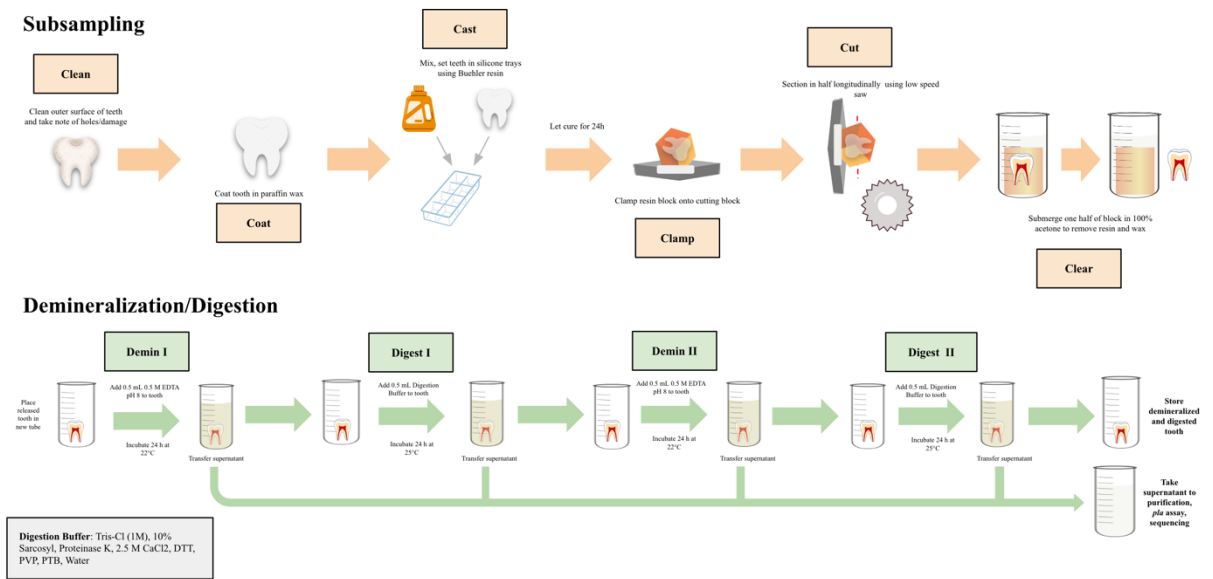


Figure 5.1: Workflow of the proposed resin-casting subsampling method.

The teeth would then be embedded in an epoxy resin optimized for reduced heat production and left for 24 hours to ensure proper setting before being mounted onto cutting blocks. The blocks would then be placed into a low-speed saw and each resin block will be cut longitudinally, ensuring proper cleaning between runs to prevent contamination. The DNA of each subsampled tooth would then be extracted. Recent studies have combined the use of EDTA and Proteinase K in a single step and have posited that a 60-minute digestion time is sufficient for extracting the majority of pathogen DNA from ancient teeth (Clavel *et al.*, 2023). In accordance, this method would utilize a novel extraction method by pipetting digestion buffer into the exposed pulp chamber of the bisected tooth, serving as the most direct method of extracting DNA from the pulp chamber. The teeth would then be incubated at a temperature of 37°C to allow for proper activation of Proteinase K (Figure 5.1). The liquid would then be extracted and placed in separate tubes before the subsequent purification and sequencing steps as listed in previous chapters.

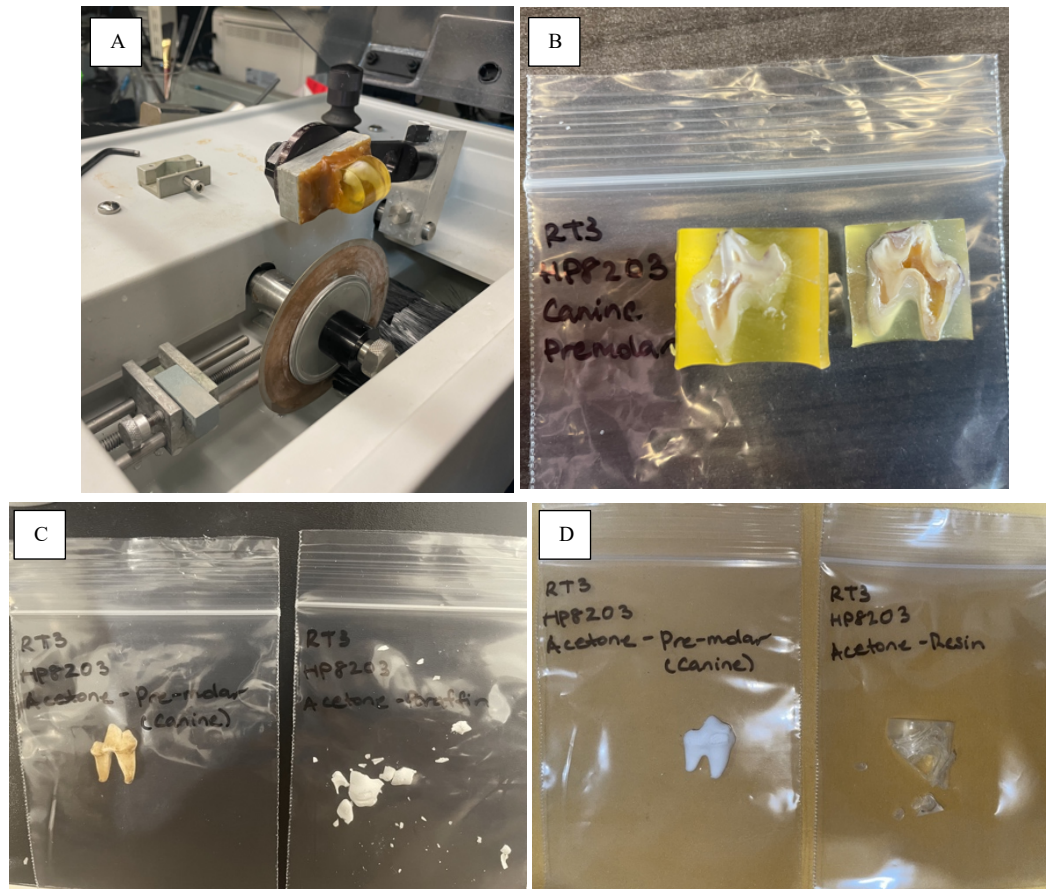


Figure 5.2 (a-d): Experimentation with the resin-casting method. a) Tooth after being set in epoxy resin for 24 hours, mounted using dental wax onto low-speed saw. b) Halves of tooth post-cut, revealing pulp chamber while still embedded in epoxy. c) One half of tooth after overnight acetone submersion, distributed into coated half of tooth and epoxy remnants. d) One half of tooth upon manual peeling of paraffin coating.

This methodology did not come to fruition. As highlighted, all the ancient remains were processed using the common drill method. Reflecting on this experience, it was not realistic to attempt to implement a new methodology within the given span of a two-year thesis; the endeavor would likely be a separate degree all on its own. In other words, the steps required for such a change in methodology to be tested, rendered sufficiently convincing, and put into practice would have been too lengthy of a process. In recent years, it has been observed that the accelerated strides in ancient DNA progress have simultaneously resulted in limited space for underheard voices and deviation from protocol (Yáñez *et al.*, 2023). The sheer difference in the

competitive, quick nature of ancient DNA publications and the slower, detail-oriented work in biological anthropology accentuates the lack of adequate community-based framework in the former and how the interlacing of disciplines into each other demands comprise. Therefore, intentional action must be taken to ensure that the field moves in a more ethically sound direction. The effort should not be to move in a direction that causes *no* harm, but to move forward in a direction that causes *less* harm in all that we do (R.A. McKay, personal communication, March 15, 2023); the concept of “no harm” simply does not exist in the field of ancient DNA. As researchers, we must be acutely aware of the implications of the work we are doing and accept that we may never truly be able to fathom all the groups that may be affected by our studies. I had to learn how the wheel of ancient DNA churns out ground-breaking publications and how the road we must take to unlearn it, though difficult, has come into view. As years pass, we can hope to see less focus on the cyclical nature of the field and instead prioritize ethical consideration in all our projects.

In the cases outlined above as well as with many others, current and future research projects rooted in ancient DNA, infectious disease, and beyond, should be committed to decentralizing the science (Fleskes *et al.*, 2022). There must be serious, active, and frequent attempts to consider any harm that may affect modern communities. Admittedly, distinguishing modern stakeholders and descendant populations may be more difficult to accomplish when considering ancient human remains. Nevertheless, it is the responsibility of pursuing researchers to align their goals with those of non-scientific perspectives. With the current efforts to expand the global narrative for the first plague pandemic, there must be careful consideration

when working with remains and communities outside of Europe, in efforts to cohesively and effectively integrate lasting, meaningful relationships.

5.2 Future Research

Notably, the field of plague studies is currently undergoing a momentous shift in bridging new historical, archaeological, and molecular discoveries. By going beyond analysing how a population was affected, we must deduce the factors that contributed to *why* a specific population was affected. Then, we will be able to better investigate the origins and subsequent evolution of plague and other infectious diseases. The goal of this project, rooted in the anthropology of plague, was to consider a broader, global depiction of the first plague pandemic and the human-environment and human-human interactions that may have proliferated its spread. Inadequate exchange between history and science has proven detrimental to the interpretation of available evidence, though active and serious engagement with multiple fields of study is what will bridge gaps in knowledge of past plague pandemics.

Plague studies must refuse to remain stagnant and unyielding, and researchers must be open to new ideas to counter extremes that have halted successful academic progression. For instance, although the novel subsampling methodology outlined previously was not actualized, further action must be implemented. Furthermore, a deeper understanding of the significance of historical texts will help scientists interpret genomic and computational methods. Similarly, reliance on and biasing the use of historical texts severely limits the scope of a study; a healthy balance must be sought after. Newfield (2022) suggests pursuing “smaller-scale analyses” as frameworks into building effective interdisciplinary collaboration are created. The

pursuit of quality interdisciplinary work is at times quite difficult as each discipline's research goals are different; finding overlapping hypotheses are key to ensuring effective collaboration (Cunningham, 2002; Gould, 2003; Herring and Swedlund, 2003 as cited in Mitchell, 2017.) Perhaps future studies may seek to take a step back and critique what can be deduced with the evidence presented thus far. Upon contextualization of the primary written sources, the evolution of their translations, as well as reviewing *all* past and present narratives attributed to the Justinianic Plague, the pros and cons of quantitative and qualitative analyses, as well as any limitations that may arise, should be addressed. The questions historians and scientists ask themselves when advancing retrospective diagnoses to make sense of past epidemics should also be investigated (Hays, 2006; Stein 2014; Mitchell 2017). Doing so may serve as a baseline for a more holistic approach to unravelling the mysteries of the Justinianic Plague and other ancient epidemics.

As stated, one genome is insufficient to solve debates involving the mortality rate of late antique plague – indeed we must be weary when addressing a great deal of Black Death ‘baggage’ in the contextualization of individual genomes. At the same time, it may be used to investigate relationships with and between the currently published genomes. In addition, future methods must consider more effective yet simultaneously ethical approaches in efforts to avoid reproducing Eurocentric narratives; collaboration with community researchers may offer novel perspectives and generate lasting professional global relationships. Overall, these findings have demonstrated the need for a more global view of the plague pandemics and contributed to the broadening of the overly European-scope of first-pandemic plague

studies. It is, after all, within this need to constantly revisit and question results of the past that we can truly and purposefully move forward.

5.3 References

- Bik E. M. (2024). Publishing negative results is good for science. *Access microbiology*, 6(4), 000792. <https://doi.org/10.1099/acmi.0.000792>
- Blakey M.L. (1999). Beyond European Enlightenment: Toward a Critical and Humanistic Human Biology. In: *Building a New Biocultural Synthesis: Political-Economic Perspectives on Human Biology*. Ann Arbor, United States: University of Michigan Press.
- Clavel, P., Louis, L., Sarkissian, C., Thèves, C., Gillet, C., Chauvey, L., Tressières, G., Schiavinato, S., Calvière-Tonasso, L., Telmon, N., Clavel, B., Jonvel, R., Tzortzis, S., Bouniol, L., Fémolant, J. M., Klunk, J., Poinar, H., Signoli, M., Costedoat, C., Spyrou, M. A., ... Orlando, L. (2023). Improving the extraction of ancient *Yersinia pestis* genomes from the dental pulp. *iScience*, 26(5), 106787. <https://doi.org/10.1016/j.isci.2023.106787>
- Cunningham, A. (2002). Identifying disease in the past: cutting the gordian knot. *Asclepio*, 54(1), 13–34. <https://doi.org/10.3989/asclepio.2002.v54.i1.133>
- Fleskes R.E., Bader A.C., Tsosie K.S., Wagner J.K., Claw K.G., Garrison N.A. (2022). Ethical Guidance in Human Paleogenomics: New and Ongoing Perspectives. *Annual Review of Genomics and Human Genetics*, 23: 627–52.
- Gould, S. (2003). *The Hedgehog, the Fox, and the Magister's Pox: Mending the Gap between Science and the Humanities*. Cambridge, MA and London, England: Harvard University Press. <https://doi.org/10.4159/harvard.9780674063402>
- Hays, J.N. (2006). Historians and Epidemics: Simple Questions, Complex Answers. In *Plague and the End of Antiquity: The Pandemic of 541–750*, edited by Lester K. Little, 33–56. Cambridge: Cambridge University Press. <https://doi.org/10.1017/CBO9780511812934.005>.
- Kowal E, Weyrich LS, Argüelles JM, et al. (2023). Community partnerships are fundamental to ethical ancient DNA research. *Human Genetics and Genomics Advances*, 4: 100161.
- Mitchell, P.D. (2017). Improving the Use of Historical Written Sources in Paleopathology. *International Journal of Paleopathology*, 19: 88–95. <https://doi.org/10.1016/j.ijpp.2016.02.005>.

- Mlinarić, A., Horvat, M., & Šupak Smolčić, V. (2017). Dealing with the positive publication bias: Why you should really publish your negative results. *Biochemia medica*, 27(3), 030201. <https://doi.org/10.11613/BM.2017.030201>
- Newfield, T. P. (2022). One Plague for Another? Interdisciplinary Shortcomings in Plague Studies and the Place of the Black Death in Histories of the Justinianic Plague. *Studies in Late Antiquity*, 6(4), 575–626. <https://doi.org/10.1525/sla.2022.6.4.575>
- Poinar, H. (2022). Past Plagues: On the Synergies of Genetic and Historical Interpretations of Infectious Disease. In L. Jones & N. Varlik (Eds.), *Death and Disease in the Medieval and Early Modern World: Perspectives from across the Mediterranean and Beyond* (pp. 319–340). Boydell & Brewer. <https://doi.org/10.1017/9781800107861.013>
- Sandercock, P. (2012). Negative results: why do they need to be published? *International Journal of Stroke*, 7(1), 32–33. <https://doi.org/10.1111/j.1747-4949.2011.00723.x>
- Sidhu R. & Parry A. (2022). [Unpublished manuscript]. McMaster University.
- Stein C. (2014). 'Getting' the Pox: Reflections by an Historian on How to Write the History of Early Modern Disease. *Nordic journal of science and technology studies*, 2(1), 53–60. <https://doi.org/10.5324/njsts.v2i1.2137>
- Tuhiwai Smith, L. (2021). *Decolonizing Methodologies: Research and Indigenous Peoples* (Third edition.). Bloomsbury Publishing Plc. <https://doi.org/10.5040/9781350225282>
- Yáñez, B., Fuentes, A., Silva, C. P., Figueiro, G., Menéndez, L. P., García-Deister, V., de la Fuente-Castro, C., González-Duarte, C., Tamburrini, C., & Argüelles, J. M. (2023). Pace and space in the practice of aDNA research: Concerns from the periphery. *American Journal of Biological Anthropology*, 180(3), 417–422. <https://doi.org/10.1002/ajpa.24683>

Supplemental Tables and Figures

Table S5.1: Overview of samples processed from historical sites in Turkey.

Project ID	HP Number	Original ID	Site	Notes
TFP01	HP7927	Z30	Haydarpaşa Train Station	Had to pry tooth out of mandible. Chose single root tooth as it loosened the easiest. Molars fragment if prying too hard. Got 50mg of pulp powder out of tooth, but perhaps future subsampling of molars is needed.
TFP02	HP8092	D179	Kadıkalesi	Possible pulp stones within roots. Went in with thinner drill bit to subsample roots.
TFP03	HP8040	F49	Agora of Smyrna	Roots very thin. Couldn't drill into without high chance of fragmenting. May want to re-subsample with smaller drill head, but already had over 50mg to work with.
TFP04	HP8042	L40	Metropolis	Comparatively soft dentin.
TFP05	HP8043	L41	Metropolis	Broke in two upon removal from mandible. One tooth remains. Did not cut off crown and drilled along pulp chamber of both halves.
TFP06	HP8044	L42	Metropolis	Unique shape of roots. Crown fragmented.
TFP07	HP8046	L44	Metropolis	Roots damaged upon arrival. Large holes. Crown very easy to drill. One root fragmented upon subsampling.
TFP08	HP8047	L45	Metropolis	Root damaged on arrival. Roots fragmented during subsampling.
TFP09	HP8048	L46	Metropolis	One root split in half during subsampling.
TFP10	HP8049	L47	Metropolis	Model subsampling tooth. Great preservation and strong roots.
TFP11	HP7916	M31	Iznik Roman Theatre	Tough tooth. Big head drill bit did not gather much powder. Thin needle drill bit generated significantly more powder.
TFP12	HP7917	M32	Iznik Roman Theatre	Cavity-like hole on crown on arrival. Tough tooth. Big head drill bit did not gather much powder. Thin needle drill bit generated more powder.
TFP13	HP7922	M37	Iznik Roman Theatre	Difficult to bisect. Crown fragmented.
TFP14	HP7923	M38	Iznik Roman Theatre	Crown fragmented. Large holes at apex. Thinner drill bit worked the best. Relatively easier to bisect than others in site.
TFP15	HP7924	M39	Iznik Roman Theatre	No fragmenting and clean bisection. Large tooth. Only used thin needle drill bit to generate subsample.
TFP16	HP7925	M40	Iznik Roman Theatre	No fragmenting and clean bisection. Large tooth. Only used thin needle drill bit to generate subsample.
TFP17	HP7926	M41	Iznik Roman Theatre	No fragmenting and clean bisection. Large tooth. Only used thin needle drill bit to generate subsample.
TFP18	HP8052	M44	Iznik Roman Theatre	Different shipment. Chose single root tooth as it had the least likelihood to fragment. Very hard tooth. Went in with different drill bits and barely any powder was generated. Crown fragmented, root intact after subsampling.
TFP19	HP8018	C49	Ayasuluk	Extremely small tooth. Roots fragmented upon bisecting and again upon drilling with thin drill bit. Crown stayed intact.
TFP20	HP8020	C51	Ayasuluk	Complete fragmentation. Tooth exploded upon first touch of circular saw bit. Going in even lightly with thin drill bit crumbled roots and crown. Second subsample is small pieces of root (not powder).
TFP21	HP8021	C52	Ayasuluk	Strong tooth. Ball-headed drill bit did not generate much powder, unlike the thin drill bit. MinEluted extract was lost due to broken tube. Re-subsampled and cold-spun.
TFP21-subB	HP8021	C52	Ayasuluk	Strong tooth. Did not drill too deep back into roots as they were rather thin. Majority of pulp powder retrieved from crown (~18 mg from roots).
TFP22	HP8022	C53	Ayasuluk	Roots fragmented in bag. Did not bisect as holes were already apparent and tooth was very soft. Thin drill bit fragmented roots. Possible pulp stone in crown added to sub-A
TFP23	HP8025	C56	Ayasuluk	Fused root. Difficult to drill into roots even with thin drill bit. Some fragmentation on root upon subsampling.
TFP24	HP8026	C57	Ayasuluk	Fused root. Difficult to drill into roots even with thin drill bit. Some fragmentation on root upon subsampling.
TFP25	HP8027	C58	Ayasuluk	Relatively softer than other teeth in site. Slight fragmenting along roots.
TFP26	HP8033	C64	Ayasuluk	Strong tooth. More difficult to generate powder than other in site.
TFP27	HP8034	C65	Ayasuluk	Strong tooth. More difficult to generate powder than other in site. Piece of mandible wedged in tooth on arrival.

TFP28	HP8035	C66	Ayasuluk	Piece of mandible wedged in tooth on arrival. Roots fragmented upon subsampling.
TFP29	HP8036	C67	Ayasuluk	Large amounts of excess tooth matter on molar on arrival. Chose molar as it appeared to have less chance of fragmentation. Relatively strong tooth compared to others in site.
TFP30	HP8037	C68	Ayasuluk	Relatively harder than other teeth in site. Fragmented down along the middle of roots.
TFP31	HP8038	C69	Ayasuluk	Single root tooth. Crown split upon bisecting. Relatively hard and strong.
TFP32	HP8061	AK53	Perinthos	Hard tooth. Very slight fragmenting of roots upon subsampling.
TFP33	HP8062	AK54	Perinthos	String-like threads/fibres on roots upon arrival. Hard tooth. No fragmentation.
TFP34	HP8064	AK56	Perinthos	Thin roots. Fragmented upon bisecting. Tried to manually scrape, some fragmentation occurred.
TFP35	HP8066	AK58	Perinthos	Roots missing on arrival. Did not bisect. Only used thin drill bit. Minimal fragmenting.
TFP36	HP8067	AK59	Perinthos	Tooth still in mandible on arrival. Fragmentation of roots upon drilling.
TFP37	HP8068	AK60	Perinthos	Extremely small but surprisingly strong roots. No fragmentation. Could possibly re-subsample for more powder at risk of further damaging tooth.
TFP38	HP8069	AK61	Perinthos	Single root tooth. Still one single root tooth left in bag. Chosen because slightly bigger than other and could be less prone to fragmenting. Root split upon subsampling.
TFP39	HP8070	AK62	Perinthos	Very large tooth. No fragmentation. Could further re-subsample at risk of breakage.
TFP40	HP8071	AK63	Perinthos	Strong tooth. Roots thin but surprisingly strong. Could further subsample at risk of breakage.
TFP41	HP8072	AK64	Perinthos	Tooth still in mandible on arrival. Prying out of mandible cracked and split tooth. Subsampling fragmented roots.
TFP42	HP7929	A14	İznik Hisardere Necropolis	Incredibly soft tooth. Still in mandible on arrival. Even only light pressure was enough to take of crown from roots still in mandible. Chalk-like. Subsampled crown (A), then subsampled roots (B) separately due to high amount of powder generated. Kept both in same 50 mL Falcon tube. Other tooth with no crown on arrival left un-subsampled in same piece of mandible.
TFP43	HP7930	A15	İznik Hisardere Necropolis	Incredibly soft tooth. Still in mandible on arrival. One tooth still had crown upon arrival. Even only light pressure was enough to take of crown from roots still in mandible. Chalk-like.
TFP44	HP7931	A16	İznik Hisardere Necropolis	One root fragmented upon subsampling. Piece of mandible still attached prior to subsampling.
TFP45	HP7932	A17	İznik Hisardere Necropolis	Soft tooth. Roots completely fragmented. Went in with thin drill bit to sand down fragments.
TFP46	HP7933	A18	İznik Hisardere Necropolis	Subsampled directly in mandible. Crown already off, drilled with thin drill bit in holes. A crown was loose in the bag but could not definitively state which tooth it came from, so did not subsample.
TFP47	HP8075	AT1	Priene	Only crown on arrival. Very soft. Slight fragmenting along outer edges of crown.
TFP48	HP8076	AT2	Priene	Large holes at apex on arrival. Roots fragmented upon bisecting.
TFP49	HP8077	AT3	Priene	Soft tooth. Lucky bisecting. Roots fragmented upon subsampling.
TFP50	HP8080	AT6	Priene	Soft tooth. Lucky bisecting. Could subsample more but did not this time as roots may have given out and fragmented.
TFP51	HP8081	AT7	Priene	Relatively harder tooth than others in site, Appears to be a fused root molar. Easier to treat as a single root tooth. Crown fragmented upon subsampling. Roots intact.
TFP52	HP8083	AT9	Priene	Soft tooth. Roots and crown partially fragmented upon subsampling.
TFP53	HP8085	AT11	Priene	Did not bisect as roots were mostly gone on arrival. Bisecting would likely have fragmented tooth. Lots of dirt in hole on surface. Went in with thin drill bit.
TFP54	HP8086	AT12	Priene	Rough outer surface of roots on arrival. Roots slightly fragmented upon subsampling.
TFP55	HP8087	AT13	Priene	Soft tooth. Roots fragmented upon bisecting. Missing a lot of root on arrival but could not drill down into them (at risk of high amount of fragmentation) and had to bisect, Ball-headed drill bit yielded a lot of powder from crown.
TFP56	HP8088	AT14	Priene	Relatively harder tooth than others in site, Appears to be a fused root molar. Easier to treat as a single root tooth.
TFP57	HP8089	AT15	Priene	One root loose on arrival. Roots fragmented upon

				subsampling. Could likely subsample more from crown and roots, through may fragment further.
TFP58	HP8091	AT17	Priene	One root loose on arrival. Roots fragmented upon subsampling. Appeared strong enough to use manual tools (did not generate much powder at risk of fragmenting). Could likely subsample more from crown, through may fragment further.

Table S5.2: Overview of samples processed from the Silivri District Necropolis.

Project ID	HP Number	Original ID	Site	Notes
BFP01	HP7935	AS1	Silivri District Necropolis (BOTAŞ Excavation)	Easy to bisect. Could go deeper into roots and crown at risk of fragmenting.
BFP02	HP7936	AS2	Silivri District Necropolis (BOTAŞ Excavation)	Very easy to bisect. Could go deeper into roots at risk of fragmenting.
BFP03	HP7937	AS3	Silivri District Necropolis (BOTAŞ Excavation)	Easy to bisect. Could go deeper into roots and crown at risk of fragmenting.
BFP04	HP7938	AS4	Silivri District Necropolis (BOTAŞ Excavation)	One root chipped off on arrival. Roots fragmented upon bisecting, chalk-like. Crown stronger and could be subsampled again at risk of fragmenting.
BFP05	HP7939	AS5	Silivri District Necropolis (BOTAŞ Excavation)	One root fragmented upon drilling. Could possibly further subsample crown.
BFP06	HP7940	AS6	Silivri District Necropolis (BOTAŞ Excavation)	Cracks in tooth on arrival, though surprisingly strong. Did not go to deep into roots as it seemed they would fragment. Could possible further subsample crown.
BFP07	HP7941	AS7	Silivri District Necropolis (BOTAŞ Excavation)	Easy to bisect. No fragmenting. Could possibly subsample further at risk of fragmenting.
BFP08	HP7942	AS8	Silivri District Necropolis (BOTAŞ Excavation)	One root fragmented upon bisecting. Roots further fragmented on drilling. Could possibly further subsample crown.
BFP09	HP7943	AS9	Silivri District Necropolis (BOTAŞ Excavation)	Possible juvenile tooth. Crown fragmented upon drilling. Could possibly subsample further at high risk of further fragmentation.
BFP10	HP7944	AS10	Silivri District Necropolis (BOTAŞ Excavation)	One root split upon drilling. High risk of fragmentation if further subsampled.
BFP11	HP7945	AS11	Silivri District Necropolis (BOTAŞ Excavation)	Surprisingly strong tooth. Shallow crown, no fragmenting.
BFP12	HP7947	AS13	Silivri District Necropolis (BOTAŞ Excavation)	Surprisingly strong tooth. Light fragmentation when gripping tooth with tweezers. Further subsampling will result in fragmentation. Very chalky tooth.
BFP13	HP7948	AS14	Silivri District Necropolis (BOTAŞ Excavation)	Multi-root tooth split upon bisecting. Thin cemento-enamel junction. Mostly drilled into crown to prevent fragmenting of the thin roots.
BFP14	HP7949	AS15	Silivri District Necropolis (BOTAŞ Excavation)	No fragmenting. Could not drill deeper into roots at risk of fragmenting them entirely. Most of the pulp powder from crown.
BFP15	HP7950	AS16	Silivri District Necropolis (BOTAŞ Excavation)	Single root tooth (likely incisor). Crown split upon drilling. Possible dental calculus on outer surface. Could not drill too deep into roots at risk of fragmenting.
BFP16	HP7951	AS17	Silivri District Necropolis (BOTAŞ Excavation)	Roots fragmented upon drilling. Dark red pulp cavity. Crown had soil fragments in it, likely due to the small holes present at the end of the roots on arrival.
BFP17	HP7952	AS18	Silivri District Necropolis (BOTAŞ Excavation)	Surprisingly strong tooth. No fragmenting. Chalky. Could go further into crown if re-subsampling. Most pulp powder from roots.
BFP18	HP7953	AS19	Silivri District Necropolis (BOTAŞ Excavation)	Crown fragmented on bisecting. Possible abscess inside tooth, solidified. Sanded down. Could possibly re-subsample roots if needed, though fragile. Notable odour. Large indent on outer surface of teeth covered in soil on arrival.
BFP19	HP7954	AS20	Silivri District Necropolis (BOTAŞ Excavation)	Roots fragmented upon drilling. Could possibly further subsample crown. Chalky tooth, Piece of mandible wedged between roots on arrival.
BFP20	HP7955	AS21	Silivri District Necropolis (BOTAŞ Excavation)	Piece of mandible stuck between roots. Easy bisection. Relatively stronger than other teeth in set, yet still chalky. Could further subsample crown. Could drill deeper into roots at high risk of fragmentation.
BFP21	HP7956	AS22	Silivri District Necropolis (BOTAŞ Excavation)	Multi-root tooth. Roots fragmented on drilling. Could re-subsample crown.
BFP22	HP7957	AS23	Silivri District Necropolis (BOTAŞ Excavation)	Chose single root tooth since multi-root tooth had very thin roots. Strong tooth, no fragmenting.
BFP23	HP7958	AS24	Silivri District Necropolis (BOTAŞ Excavation)	Lucky bisection. Surprisingly strong tooth. Could possibly drill deeper into roots at risk of fragmenting.

BFP24	HP7959	AS25	Silivri District Necropolis (BOTAŞ Excavation)	Crack in root on arrival. Roots fragmented on drilling. Shard of dentin from root present in subsample. Could possibly re-subsample crown. Re-subsampling roots would certainly fragment them further.
BFP25	HP7960	AS26	Silivri District Necropolis (BOTAŞ Excavation)	Fused root. Surprisingly strong even with cracks on arrival.
BFP26	HP7961	AS27	Silivri District Necropolis (BOTAŞ Excavation)	Fused root. Roots fragmented upon drilling. Surprisingly strong even with cracks on arrival.
BFP27	HP7962	AS28	Silivri District Necropolis (BOTAŞ Excavation)	Roots split upon bisecting. Could possibly further subsample them at risk of complete fragmentation. Could re-subsample crown at less risk.
BFP28	HP7963	AS29	Silivri District Necropolis (BOTAŞ Excavation)	No fragmenting, surprisingly strong tooth and roots. Could not drill deeper into roots at risk of fragmenting.
BFP29	HP7964	AS30	Silivri District Necropolis (BOTAŞ Excavation)	No fragmenting. Did not drill deeper into roots at risk of fragmenting them, though could try as it is a relatively strong tooth.
BFP30	HP7965	AS31	Silivri District Necropolis (BOTAŞ Excavation)	Root chipped during drilling but did not completely fragment. Strong roots and crown. Could further subsample at risk of fragmenting. Did generate powder easily, but less chalky or fragile than others in set.
BFP31	HP7966	AS32	Silivri District Necropolis (BOTAŞ Excavation)	Roots split upon bisecting. Could possibly further subsample them at risk of complete fragmentation. Dark red interior. Could re-subsample crown at less risk.
BFP32	HP7967	AS33	Silivri District Necropolis (BOTAŞ Excavation)	No fragmenting. Did not drill deeper into roots at risk of fragmenting them, though could try as it is a relatively strong tooth.
BFP33	HP7968	AS34	Silivri District Necropolis (BOTAŞ Excavation)	No fragmenting. Did not drill deeper into thinner roots at risk of fragmenting them.
BFP34	HP7969	AS35	Silivri District Necropolis (BOTAŞ Excavation)	Piece of mandible stuck between roots. Easy bisection. Relatively stronger than other teeth in set, yet still chalky. Could drill deeper into roots at risk of fragmentation. Dark brown-ish interior. One root chipped on arrival.
BFP35	HP7970	AS36	Silivri District Necropolis (BOTAŞ Excavation)	Light fragmentation. Piece of mandible between roots. Dark purple-red interior.
BFP36	HP7971	AS37	Silivri District Necropolis (BOTAŞ Excavation)	Crown split upon bisection. Roots lightly fragmented on drilling. Could possible further subsample roots with high risk of fragmenting. Pinkish red interior.
BFP37	HP7972	AS38	Silivri District Necropolis (BOTAŞ Excavation)	Thin roots. Roots split upon bisection, nearly completely fragmented upon drilling. Two subsamples as chips of dentin included in tubes. Proceed with high degree of caution if further subsampling.
BFP38	HP7973	AS39	Silivri District Necropolis (BOTAŞ Excavation)	Possible piece of mandible between roots, covered in dirt. No fragmenting Could possibly further subsample roots at high risk of fragmentation.
BFP39	HP7974	AS40	Silivri District Necropolis (BOTAŞ Excavation)	Possible juvenile tooth. Very small, thin roots. Surprisingly did not fragment. Be highly cautious if re-subsampling.
BFP40	HP7975	AS41	Silivri District Necropolis (BOTAŞ Excavation)	Root split upon drilling. Could possibly further subsample roots at high risk of fragmenting, less risk for crown.
BFP41	HP7976	AS42	Silivri District Necropolis (BOTAŞ Excavation)	No fragmenting. Most pulp powder generated from crown, did not drill too deep into roots due to fragility. Could further subsample roots at risk of fragmenting.
BFP42	HP7977	AS43	Silivri District Necropolis (BOTAŞ Excavation)	Root split upon drilling. Could possibly further subsample roots at high risk of fragmenting, less risk for crown. Enamel still shiny on outer surface of tooth.
BFP43	HP7978	AS44	Silivri District Necropolis (BOTAŞ Excavation)	Crown split upon bisection, further fragmented upon drilling. Did not drill deeper into roots due to fragility but could possibly in the future with caution. Greyish colour inside root hole may be due to drilling/heating.
BFP44	HP7979	AS45	Silivri District Necropolis (BOTAŞ Excavation)	Indent at cemento-enamel junction. Large piece of calculus(?) along outer surface which made it very difficult to bisect. Roots fragmented on bisecting, and further on drilling.
BFP45	HP7980	AS46	Silivri District Necropolis (BOTAŞ Excavation)	Slight fragmenting of roots included small pieces of fragments in sample. Dark pink interior. Surprisingly strong for size. Re-subsampling possible at risk of further fragmentation.
BFP46	HP7981	AS47	Silivri District Necropolis (BOTAŞ Excavation)	Roots fragmented on drilling. Strong crown. Re-subsampling at high risk of further fragmentation.
BFP47	HP7982	AS48	Silivri District Necropolis (BOTAŞ Excavation)	Roots split on drilling. Re-subsampling roots will result in fragmenting, lower chance for strong crown.
BFP48	HP7983	AS49	Silivri District Necropolis (BOTAŞ Excavation)	Piece of mandible stuck in roots on arrival. Roots split (bisected) on drilling. Strong crown. Further sanding down roots possible at risk of fragmenting.

BFP49	HP7984	AS50	Silivri District Necropolis (BOTAŞ Excavation)	Crown fragmented on bisecting. Sanded down. Could possibly re-subsample roots if needed, though fragile. Indent on outer surface of teeth on arrival.
BFP50	HP7985	AS51	Silivri District Necropolis (BOTAŞ Excavation)	Teeth in mandible on arrival. Able to pry out both single root and multi-root tooth, chose multi-root to subsample. Possible blood vessel or piece of tissue stuck on root upon prying. Slight fragmentation of roots, otherwise all intact upon bisecting and drilling. Could further subsample roots at risk of fragmentation. Relatively strong overall.
BFP51	HP7986	AS52	Silivri District Necropolis (BOTAŞ Excavation)	Very skinny roots. No fragmenting. Could possibly re-subsample roots at high risk of fragmentation.
BFP52	HP7987	AS53	Silivri District Necropolis (BOTAŞ Excavation)	Small piece of mandible wedged in roots. Relatively larger tooth. No fragmenting, but some cracks visible upon drilling. Use caution if re-subsampling.
BFP53	HP7988	AS54	Silivri District Necropolis (BOTAŞ Excavation)	Clubbing on one of the roots. Strong tooth. Rather difficult to bisect. Possible solidified abscess in center of tooth. Could re-subsample roots with caution. Piece of mandible stuck between roots.
BFP54	HP7989	AS55	Silivri District Necropolis (BOTAŞ Excavation)	One root split upon drilling. High risk of fragmentation if further subsampled.
BFP55	HP7990	AS56	Silivri District Necropolis (BOTAŞ Excavation)	Very dirty on arrival. Piece of mandible wedged between roots.
BFP56	HP7991	AS57	Silivri District Necropolis (BOTAŞ Excavation)	Very small tooth. Light fragmenting of roots upon drilling. Further subsampling would need high degree of caution.
BFP57	HP7992	AS58	Silivri District Necropolis (BOTAŞ Excavation)	Seemingly fused roots. Roots fragmented on bisecting. Sanded down interior of one root. Could possibly subsample other root at high risk of fragmentation.
BFP58	HP7993	AS59	Silivri District Necropolis (BOTAŞ Excavation)	Dirty on arrival. Piece of mandible wedged in roots along with a lot of dirt. No fragmenting. Relatively strong tooth. Could further subsample roots with caution. Possible small pulp stones inside.
BFP59	HP7994	AS60	Silivri District Necropolis (BOTAŞ Excavation)	Small indent on outer surface of tooth covered in dirt. Relatively skinny roots but surprisingly strong. Crown split on bisecting. Could possibly re-subsample at risk of fragmentation.
BFP60	HP7995	AS61	Silivri District Necropolis (BOTAŞ Excavation)	Clean and lucky bisection Strong tooth. Could possibly drill deeper into roots at risk of fragmenting.
BFP61	HP7996	AS62	Silivri District Necropolis (BOTAŞ Excavation)	Single root tooth. Slight fragmentation on drilling, though relatively durable. High risk of further fragmentation if further subsampling.
BFP62	HP7997	AS63	Silivri District Necropolis (BOTAŞ Excavation)	Nearly completely covered in soil on arrival. Piece of mandible wedged between roots. Relatively strong. Could further subsample at medium risk of fragmentation.
BFP63	HP7998	AS64	Silivri District Necropolis (BOTAŞ Excavation)	Piece of mandible wedged between roots. Crown fragmented on drilling. Roots could be further subsampled with caution as they are relatively strong.
BFP64	HP8000	AS66	Silivri District Necropolis (BOTAŞ Excavation)	Small but surprisingly strong tooth. No fragmenting. Further re-subsampling of roots requires extreme caution.
BFP65	HP8001	AS67	Silivri District Necropolis (BOTAŞ Excavation)	Piece of mandible stuck in roots. Slight chipping of roots on drilling, otherwise relatively strong tooth. Could further subsample with caution.
BFP66	HP8002	AS68	Silivri District Necropolis (BOTAŞ Excavation)	Tooth in mandible with another tooth on arrival. Relatively easy to pry out of mandible with minimal chipping. Very small tooth, possibly juvenile. Two out of three roots split on drilling. Manually scraped some reddish flakes off roots.
BFP67	HP8003	AS69	Silivri District Necropolis (BOTAŞ Excavation)	Roots chipped on arrival. Surprisingly did not fragment on drilling. Proceed with caution if re-subsampling.
BFP68	HP8004	AS70	Silivri District Necropolis (BOTAŞ Excavation)	Single root tooth. Cracks in tooth root on arrival. Surprisingly strong, only light fragmenting.
BFP69	HP8005	AS71	Silivri District Necropolis (BOTAŞ Excavation)	Roots lost and covered in soil on arrival. Roots all but completely fragmented. Crown remained intact. Tried to sand down root fragments. Would not recommend re-subsampling roots, might be able to re-subsample crown.
BFP70	HP8006	AS72	Silivri District Necropolis (BOTAŞ Excavation)	Extremely small tooth, likely a child's tooth. Thankfully only chipped roots and did not completely fragment on bisection. Would not recommend re-subsampling at extremely high risk of complete fragmentation. Used powder from bisection to increase mass. Some other teeth from same individual in bag, though already bisected/cracked on arrival.
BFP71	HP8007	AS73	Silivri District Necropolis (BOTAŞ Excavation)	Piece of mandible stuck between roots. Slight chipping of roots. Could possible subsample further into roots with caution.

BFP72	HP8008	AS74	Silivri District Necropolis (BOTAŞ Excavation)	Strong tooth. No fragmentation. Could possibly drill deeper into roots.
BFP73	HP8009	AS75	Silivri District Necropolis (BOTAŞ Excavation)	Single root tooth. One small piece of upper root chipped off, otherwise no fragmentation. Relatively strong. Might be able to further subsample with high degree of caution.
BFP74	HP8011	AS77	Silivri District Necropolis (BOTAŞ Excavation)	No fragmentation. Reddish interior. Could re-subsample at risk of fragmenting roots.
BFP75	HP8012	AS78	Silivri District Necropolis (BOTAŞ Excavation)	Covered in soil and dark brown on arrival.
BFP76	HP8016	AS82	Silivri District Necropolis (BOTAŞ Excavation)	Yellowish abscess-like material hardened along the crown and roots. No fragmenting. Could drill deeper into thinner roots at risk of fragmenting. Relatively strong tooth, yet still chalky.

Table S5.3: Bioinformatic overview of all samples from historical sites and the Silivri District Necropolis.

Arch. ID	Project ID	Extraction Method	Total Reads (Illumina output)	# of reads mapping to hg38HM (min35, MQ30)	Mapped % (Endogenous)	# of reads mapping to <i>Y. pestis</i> (min35MQ30)	Mapped % (<i>Y. pestis</i>)	# of reads mapping to <i>M. tuberculosis</i> (min35MQ30)	Mapped % (<i>M. tuberculosis</i>)
TFP01	Z30	1	3,335,619	6193	0.1857%	1	0.0000%	159	0.0048%
TFP02	D179	1	3,156,138	64,063	2.0298%	29	0.0009%	171	0.0054%
TFP03	F49	1	3,158,391	1621	0.0513%	5	0.0002%	233	0.0074%
TFP04	L40	1	3,017,213	1135	0.0376%	3	0.0001%	256	0.0085%
TFP05	L41	1	3,108,968	18	0.0006%	2	0.0001%	113	0.0036%
TFP06	L42	1	3,001,150	49	0.0016%	4	0.0001%	218	0.0073%
TFP07	L44	1	3,531,222	164	0.0046%	0	0.0000%	202	0.0057%
TFP08	L45	1	3,651,165	618	0.0169%	14	0.0004%	454	0.0124%
TFP09	L46	1	3,488,356	204	0.0058%	3	0.0001%	404	0.0116%
TFP10	L47	1	1,845,670	553	0.0300%	2	0.0001%	125	0.0068%
TFP11	M31	1	1,539,433	1619	0.1052%	2	0.0001%	117	0.0076%
TFP12	M32	1	843,829	1655	0.1961%	1	0.0001%	43	0.0051%
TFP13	M37	1	3,445,567	237,288	6.8868%	6	0.0002%	363	0.0123%
TFP13	M37	1	5,100,280	403,855	7.9183%	3	0.0001%	486	0.010%
CS-TFP13	M37	2	4,299,994	35603	0.7825%	2	0.0000%	384	0.0089%
CS-TFP13	M37	2	10,220,838	110845	1.0845%	10	0.0001%	871	0.009%
TFP14	M38	1	2,622,048	4687	0.1788%	8	0.0003%	121	0.0046%
TFP15	M39	1	2,249,323	14816	0.6587%	4	0.0002%	177	0.0079%
TFP16	M40	1	3,365,390	2010	0.0597%	4	0.0001%	317	0.0094%
TFP17	M41	1	2,734,261	1795	0.0656%	16	0.0006%	189	0.0069%
TFP18	M44	1	1,692,295	365	0.0216%	3	0.0002%	202	0.0119%
TFP19	C49	1	2,072,222	31241	1.5076%	3	0.0001%	220	0.0106%
TFP20	C51	1	3,011,749	31	0.0010%	2	0.0001%	150	0.0050%
TFP21	C52	1	3,441,861	173	0.0050%	3	0.0001%	212	0.0062%
TFP22	C53	1	2,372,154	13	0.0005%	3	0.0001%	108	0.0046%
TFP23	C56	1	2,197,865	444	0.0202%	3	0.0003%	90	0.0041%
TFP24	C57	1	3,975,847	1301	0.0327%	11	0.0001%	148	0.0037%
TFP25	C58	1	2,627,793	56	0.0021%	3	0.0002%	112	0.0043%
TFP26	C64	1	2,380,123	2751	0.1156%	4	0.0004%	168	0.0071%
TFP27	C65	1	2,003,713	17235	0.8602%	8	0.0001%	80	0.0040%
TFP28	C66	1	3,037,852	162	0.0053%	3	0.0001%	399	0.0131%
TFP29	C67	1	3,149,682	679	0.0216%	2	0.0001%	127	0.0040%
TFP30	C68	1	3,272,182	636	0.0194%	4	0.0001%	494	0.0151%
TFP31	C69	1	5,588,273	580	0.0104%	5	0.0000%	491	0.0088%
TFP32	AK53	1	2,067,953	267	0.0129%	1	0.0002%	97	0.0047%
TFP33	AK54	1	3,837,644	97	0.0025%	7	0.0002%	219	0.0057%
TFP34	AK56	1	2,385,241	51	0.0021%	5	0.0002%	132	0.0055%
TFP35	AK58	1	3,117,714	147	0.0047%	7	0.0001%	210	0.0067%
TFP36	AK59	1	5,015,771	2331	0.0465%	5	0.0002%	341	0.0068%
TFP37	AK60	1	2,247,748	49	0.0022%	4	0.0004%	122	0.0054%
TFP38	AK61	1	2,204,735	108824	4.9359%	8	0.0002%	98	0.0044%
TFP39	AK62	1	2,168,954	910	0.0420%	4	0.0002%	124	0.0057%
TFP39	AK62	1	8,943,130	3428	0.0383%	16	0.0002%	504	0.0006%
TFP40	AK63	1	2,398,659	156	0.0065%	5	0.0002%	127	0.0053%
TFP41	AK64	1	2,748,369	1187	0.0432%	2	0.0001%	171	0.0062%
TFP42	AI4	1	3,154,261	8	0.0003%	5	0.0002%	88	0.0028%

TFP43	AI5	1	3,364,899	61	0.0018%	3	0.0001%	82	0.0024%
TFP44	AI6	1	1,841,470	410	0.0223%	3	0.0002%	87	0.0047%
TFP45	AI7	1	2,162,073	23	0.0011%	6	0.0003%	72	0.0033%
TFP46	AI8	1	2,300,935	102	0.0044%	2	0.0001%	58	0.0025%
TFP47	AT1	1	1,899,632	7	0.0004%	3	0.0002%	85	0.0045%
TFP48	AT2	1	2,257,288	156	0.0069%	0	0.0000%	99	0.0044%
TFP49	AT3	1	2,654,327	30	0.0011%	1	0.0000%	158	0.0060%
TFP50	AT6	1	5,480,243	38	0.0007%	5	0.0001%	494	0.0090%
TFP50	AT6	1	7,018,139	29	0.0004%	3	0.0000%	438	0.0062%
TFP51	AT7	1	2,810,954	2356	0.0838%	3	0.0001%	400	0.0142%
TFP52	AT9	1	5,359,253	65	0.0012%	5	0.0001%	195	0.0036%
TFP53	AT11	1	2,963,018	3602	0.1216%	5	0.0002%	327	0.0110%
CS-TFP53	AT11	2	3,324,576	3359	0.1010%	1	0.0000%	256	0.0077%
TFP54	AT12	1	3,399,531	10	0.0003%	5	0.0001%	121	0.0036%
TFP55	AT13	1	2,308,670	10	0.0004%	1	0.0000%	109	0.0047%
TFP56	AT14	1	1,059,205	67	0.0063%	0	0.0000%	89	0.0084%
TFP57	AT15	1	4,123,250	20	0.0005%	2	0.0000%	160	0.0039%
TFP58	AT17	1	2,589,380	26	0.0010%	5	0.0002%	92	0.0036%
TB01	Ext. Blk	1	49,448	57	0.1153%	0	0.0000%	1	0.0020%
TB02	Ext. Blk	1	90,456	100	0.1106%	0	0.0000%	3	0.0033%
TB03	Ext. Blk	1	74,899	132	0.1762%	0	0.0000%	1	0.0013%
TB04	Ext. Blk	1	291,836	314	0.1076%	0	0.0000%	2	0.0007%
TB05	Ext. Blk	1	98,250	126	0.1282%	0	0.0000%	2	0.0020%
TB06	Ext. Blk	1	198,022	1256	0.6343%	0	0.0000%	1	0.0005%
TB07	Ext. Blk	1	324,324	1615	0.4980%	1	0.0003%	5	0.0015%
TB08	Ext. Blk	1	245,437	802	0.3268%	0	0.0000%	3	0.0012%
CS-TB01	Ext. Blk	2	89,777	181	0.2016%	0	0.0000%	0	0.0000%
Arch. ID	Project ID	Extraction Method	Total Reads (Illumina output)	# of reads mapping to hg38HM (min35, MQ30)	Mapped % (Endogenous)	# of reads mapping to <i>Y. pestis</i> (min35MQ30)	Mapped % (<i>Y. pestis</i>)	# of reads mapping to <i>M. tuberculosis</i> (min35MQ30)	Mapped % (<i>M. tuberculosis</i>)
BFP01	AS1	2	6,010,436	1698	0.0283%	11	0.0002%	225	0.0020%
BFP02	AS2	2	3,985,992	15891	0.3987%	33	0.0008%	111	0.0014%
BFP03	AS3	2	4,064,101	177	0.0044%	3	0.0001%	227	0.0041%
BFP04	AS4	2	3,242,554	67	0.0021%	1	0.0000%	117	0.0022%
BFP05	AS5	2	3,094,715	140	0.0045%	8	0.0003%	149	0.0016%
BFP06	AS6	2	3,014,427	103	0.0034%	5	0.0002%	145	0.0028%
BFP07	AS7	2	2,761,608	1119	0.0405%	4	0.0001%	101	0.0037%
BFP08	AS8	2	4,476,721	185	0.0041%	5	0.0001%	139	0.0028%
BFP09	AS9	2	3,178,597	18233	0.5736%	1	0.0000%	146	0.0056%
BFP10	AS10	2	4,175,151	207	0.0050%	6	0.0001%	173	0.0036%
BFP11	AS11	2	3,012,013	50	0.0017%	4	0.0001%	63	0.0048%
BFP12	AS13	2	3,438,067	122	0.0035%	5	0.0001%	107	0.0048%
BFP13	AS14	2	2,704,664	30498	1.1276%	5	0.0002%	237	0.0037%
BFP14	AS15	2	3,926,053	3759	0.0957%	9	0.0002%	177	0.0031%
BFP15	AS16	2	4,772,437	649	0.0136%	3	0.0001%	208	0.0046%
BFP16	AS17	2	4,318,559	185	0.0043%	2	0.0000%	167	0.0041%
BFP17	AS18	2	6,794,628	1486	0.0219%	4	0.0001%	221	0.0021%
BFP18	AS19	2	3,851,194	567	0.0147%	5	0.0001%	374	0.0031%
BFP19	AS20	2	4,197,971	25	0.0006%	5	0.0001%	111	0.0088%
BFP20	AS21	2	2,492,513	19	0.0008%	4	0.0002%	84	0.0045%
BFP21	AS22	2	3,548,223	146	0.0041%	11	0.0003%	134	0.0044%
BFP22	AS23	2	5,271,001	396	0.0075%	3	0.0001%	175	0.0039%
BFP23	AS24	2	2,711,968	5861	0.2161%	3	0.0001%	87	0.0033%
BFP24	AS25	2	3,600,407	739	0.0205%	5	0.0001%	133	0.0097%
BFP25	AS26	2	2,035,372	29911	1.4696%	2	0.0001%	63	0.0026%
BFP26	AS27	2	3,160,353	67	0.0021%	6	0.0002%	179	0.0034%
BFP27	AS28	2	2,814,676	1871	0.0665%	7	0.0002%	151	0.0038%
BFP28	AS29	2	3,682,032	704	0.0191%	3	0.0001%	278	0.0033%
BFP29	AS30	2	5,021,971	1425	0.0284%	9	0.0002%	364	0.0032%
BFP30	AS31	2	3,105,921	52	0.0017%	2	0.0001%	160	0.0037%
BFP31	AS32	2	3,179,976	41	0.0013%	3	0.0001%	115	0.0031%
BFP32	AS33	2	2,446,050	1700	0.0695%	1	0.0000%	106	0.0057%
BFP33	AS34	2	2,984,233	122	0.0041%	4	0.0001%	92	0.0054%
BFP34	AS35	2	3,004,000	20	0.0007%	4	0.0001%	136	0.0076%
BFP35	AS36	2	3,994,903	997	0.0250%	3	0.0001%	137	0.0072%

BFP36	AS37	2	3,904,355	27787	0.7117%	8	0.0002%	116	0.0052%
BFP37	AS38	2	3,437,511	310	0.0090%	2	0.0001%	105	0.0036%
BFP38	AS39	2	3,576,458	777	0.0217%	5	0.0001%	174	0.0043%
CS-BFP39	AS40	2	16,597,968	13668	0.0823%	57	0.0003%	645	0.0039%
ME-BFP39	AS40	1	15,815,438	45345	0.2867%	68	0.0004%	549	0.0035%
BFP40	AS41	2	3,003,758	317	0.0024%	5	0.0002%	97	0.0032%
BFP41	AS42	2	3,162,725	281	0.0100%	13	0.0002%	123	0.0039%
BFP42	AS43	2	3,249,108	1698	0.0086%	4	0.0002%	85	0.0026%
BFP43	AS44	2	3,493,153	280	0.0080%	8	0.0003%	139	0.0040%
BFP44	AS45	2	3,138,818	2577	0.0821%	6	0.0004%	94	0.0030%
BFP45	AS46	2	2,503,359	1514	0.0605%	6	0.0001%	106	0.0042%
BFP46	AS47	2	2,304,871	143	0.0062%	6	0.0003%	67	0.0029%
BFP47	AS48	2	2,547,408	9	0.0004%	9	0.0002%	102	0.0040%
BFP48	AS49	2	2,162,654	2709	0.1253%	3	0.0002%	77	0.0036%
BFP49	AS50	2	3,050,959	619	0.0203%	8	0.0002%	122	0.0040%
BFP50	AS51	2	4,997,943	64	0.0013%	9	0.0002%	138	0.0028%
BFP51	AS52	2	3,754,240	764	0.0204%	7	0.0000%	140	0.0037%
BFP52	AS53	2	4,702,005	19	0.0004%	10	0.0003%	144	0.0031%
BFP53	AS54	2	3,417,460	9851	0.2883%	6	0.0002%	174	0.0051%
BFP54	AS55	2	2,999,985	32	0.0011%	1	0.0001%	194	0.0065%
BFP55	AS56	2	3,414,310	295425	8.6526%	10	0.0001%	181	0.0053%
BFP56	AS57	2	3,082,209	117	0.0038%	7	0.0001%	84	0.0027%
BFP57	AS58	2	2,310,813	34	0.0015%	2	0.0002%	72	0.0031%
BFP58	AS59	2	3,234,908	645	0.0199%	4	0.0001%	287	0.0089%
BFP59	AS60	2	3,845,305	1880	0.0489%	5	0.0010%	172	0.0045%
BFP60	AS61	2	3,724,101	881	0.0237%	8	0.0002%	233	0.0063%
BFP61	AS62	2	7,795,613	339206	4.3512%	7	0.0006%	506	0.0065%
BFP62	AS63	2	2,732,153	144952	5.3054%	26	0.0001%	154	0.0056%
BFP63	AS64	2	3,388,773	972	0.0287%	8	0.0006%	242	0.0071%
BFP64	AS66	2	4,618,912	69	0.0015%	30	0.0001%	158	0.0034%
BFP65	AS67	2	3,658,114	28	0.0008%	5	0.0008%	126	0.0034%
BFP66	AS68	2	1,980,866	59	0.0030%	12	0.0004%	40	0.0020%
BFP67	AS69	2	3,664,954	4364	0.1191%	5	0.0002%	92	0.0025%
BFP68	AS70	2	2,888,552	33485	1.1592%	22	0.0001%	193	0.0067%
BFP69	AS71	2	1,926,966	408	0.0212%	8	0.0006%	55	0.0029%
BFP70	AS72	2	6,716,970	449	0.0067%	15	0.0002%	246	0.0037%
BFP71	AS73	2	4,181,961	472	0.0113%	6	0.0000%	158	0.0038%
BFP72	AS74	2	2,447,603	28	0.0011%	15	0.0001%	50	0.0020%
BFP73	AS75	2	4,174,360	233	0.0056%	7	0.0002%	153	0.0037%
BFP74	AS77	2	520,832	4	0.0008%	0	0.0002%	24	0.0046%
BFP75	AS78	2	3,854,992	46	0.0012%	3	0.0002%	92	0.0024%
BFP76	AS82	2	2,453,566	774	0.0315%	5	0.0002%	180	0.0073%
CS-BB01	Ext. Blk	2	196,099	1480	0.7547%	1	0.0005%	4	0.0020%
CS-BB02	Ext. Blk	2	147,343	1493	1.0133%	0	0.0000%	2	0.0014%
CS-BB03	Ext. Blk	2	313,962	3237	1.0310%	0	0.0000%	13	0.0041%
CS-BB04	Ext. Blk	2	277,471	4548	1.6391%	0	0.0000%	6	0.0022%
CS-BB05	Ext. Blk	2	512,666	24340	4.7477%	1	0.0002%	8	0.0016%
CS-BB06	Ext. Blk	2	574,562	6533	1.1370%	2	0.0003%	16	0.0028%
CS-BB07	Ext. Blk	2	1,332,809	462	0.0347%	0	0.0000%	3	0.0002%
CS-BB08	Ext. Blk	2	578,543	257	0.0444%	1	0.0002%	8	0.0014%
CS-BB09	Ext. Blk	2	891,245	461	0.0517%	0	0.0000%	0	0.0000%
CS-BB10	Ext. Blk	2	1,028,998	342	0.0332%	2	0.0002%	5	0.0005%
CS-BB11	Ext. Blk	2	1,333,788	267	0.0200%	2	0.0001%	4	0.0003%

Table S5.4: Endogenous content of remains from second pandemic Denmark.

Sample (Second pandemic Denmark, Eaton <i>et al.</i> , 2023)	Shotgun clusters	# of reads mapping to hg38HM (min35, MQ30)	Mapped % (Endogenous)
D24	946,213	5,197	0.5
D51	872,087	5,969	0.7
D62	845,921	9,677	1.1
D71	1,496,705	90,539	6.0
D72	1,325,886	174,404	13.2
D75	1,010,003	45,365	4.5
R21	1,810,523	15,640	0.9
R36	1,116,614	95,342	8.5
P187	974547	6,645	0.7

P212	1660940	20,122	1.2
P246	397829	106	0.0
P384	1384975	531	0.0
P377	946,213	1,497	0.2
Sample (Second pandemic Denmark, unpublished)	Shotgun clusters	# of reads mapping to hg38HM (min35, MQ30)	Mapped % (Endogenous)
LD104a	4,010,391	963152	24.0
LD57a	3,312,309	697413	21.1
LD12a	4,653,751	958502	20.6
LP389	4639524	904291	19.5
LP157	3556966	537805	15.1
LP165	4913104	686849	14.0
LD109a	6378291	768357	12.0
LP372	3115228	366619	11.8
LP138	4322914	432245	10.0
LP148	5479734	533211	9.7
LP142	3965725	198875	5.0
LP164	5334594	195615	3.7
LP147	4952375	42147	0.9
LP178	5191643	1192104	23.0
LP182	4984884	638410	12.8
LP208	4254032	527551	12.4
LP181	3630848	327375	9.0
LP179	6805607	360543	5.3
LD50a	2620658	118292	4.5
LP176	5307538	203673	3.8
LP177	3956298	132804	3.4
LP219	5613904	93300	1.7
LP172	6680311	59917	0.9
LP174	3711735	31548	0.8
LP373	5380484	25978	0.5
LD23a	4069007	760928	18.7
LD49a	4305261	786587	18.3
LD66a	3999237	663759	16.6
LP247	4406604	486617	11.0
LD21a	4389998	465054	10.6
LP249	4369066	239383	5.5
LP381	5504599	231982	4.2
LP236	5091088	141540	2.8
LD45a	2565621	68376	2.7
LP238	2271175	48744	2.1
LD93a	4757589	100742	2.1
LD120a	2682013	26818	1.0

Table S5.5: Endogenous content of remains from second pandemic UK.

Sample (Second pandemic UK, unpublished)	Shotgun clusters	# of reads mapping to hg38HM (min35, MQ30)	Mapped % (Endogenous)
LM73r	6099417	1564320	25.6
LM79r	4350673	1102942	25.4
LM78r	4278817	613291	14.3
LM56r	3161	301	9.5
LM97r	4985755	461711	9.3
LM51r	6563434	372119	5.7
LM88r	2803169	83700	3.0
LM76r	2596629	67625	2.6
LM80r	2131949	26926	1.3
LM72r	4635130	46592	1.0
LM84r	4703932	42467	0.9
LM101r	3302171	28677	0.9
LE133r	3327260	402026	12.1
LE103r	3,897,686	390673	10.0
LE08r	3,813,986	278033	7.3
LE02r	3,397,012	247213	7.3

LE132r	5495382	376390	6.8
LE150r	3318441	212141	6.4
LE140r	5074274	311104	6.1
LE143r	2716343	150443	5.5
LE07r	3,380,102	170426	5.0
LE117r	7217178	230582	3.2
LE137r	2874771	89335	3.1
LE142r	3210261	85644	2.7
LE16r	5740484	113787	2.0
LG22r	3793269	1025719	27.0
LM61r	3997185	1032766	25.8
LG21r	4481086	1079186	24.1
LM21r	6783361	1435808	21.2
LM47r	5847336	1185840	20.3
LM26r	3874428	776768	20.0
LG28r	2866385	402773	14.1
LG07r	3479491	485760	14.0
LM23r	3659908	470232	12.8
LG40r	2652750	102397	3.9
LM34r	3284012	71687	2.2
LG02r	4451355	75589	1.7
LM03a	3457251	58695	1.7

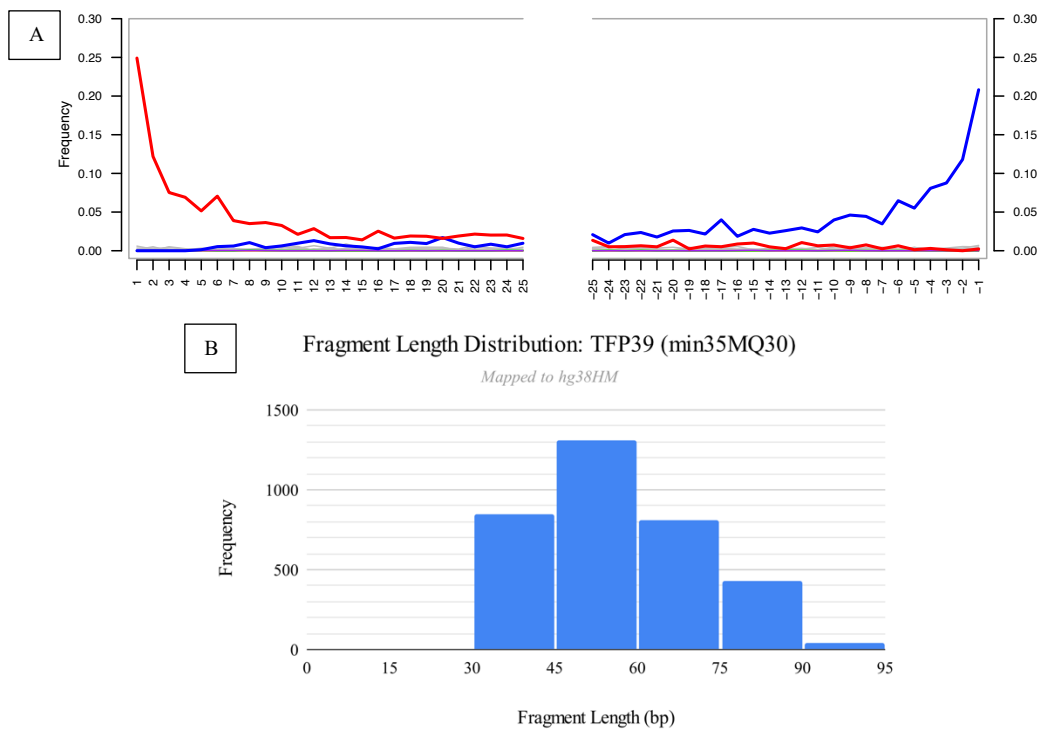


Figure S5.1: TFP39 mapped to the masked human reference genome hg38 (min35, MQ30). a) ancient DNA authentication using mapDamage. b) Fragment length distribution. c) Plot of edit distances.

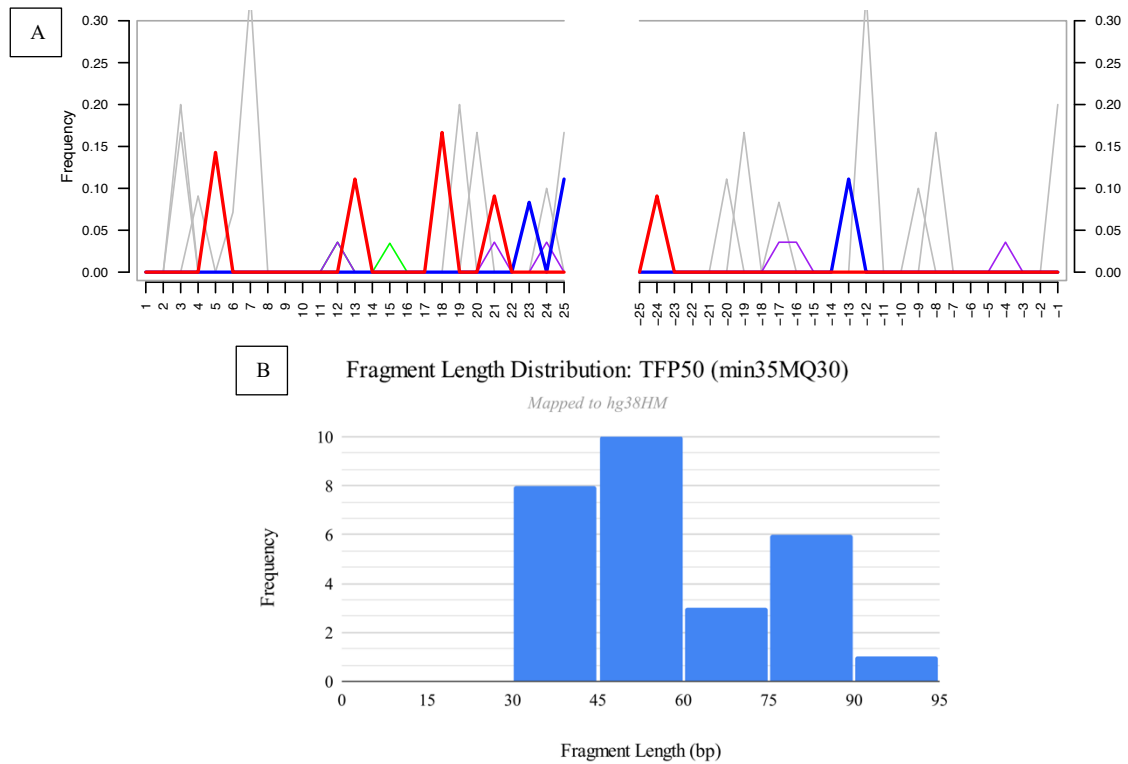


Figure S5.2: TFP50 mapped to the masked human reference genome hg38 (min35, MQ30). a) ancient DNA authentication using mapDamage. b) Fragment length distribution.

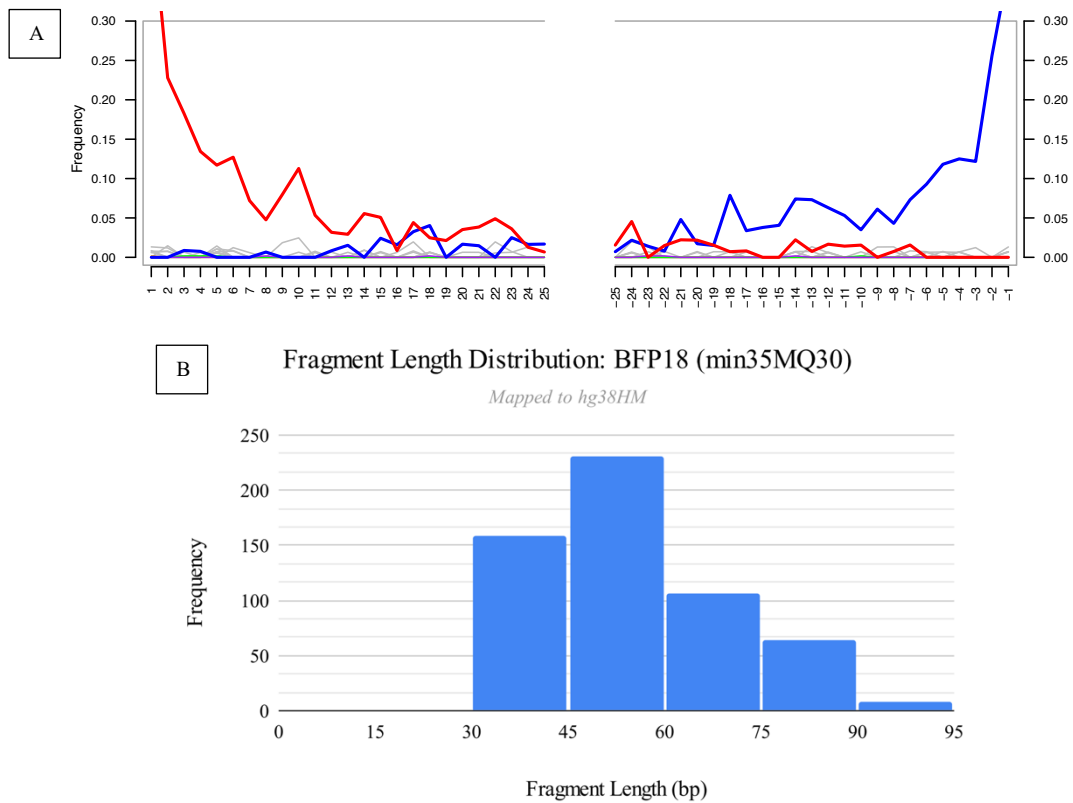


Figure S5.3: BFP18 mapped to the masked human reference genome hg38 (min35, MQ30). a) ancient DNA authentication using mapDamage. b) Fragment length distribution.

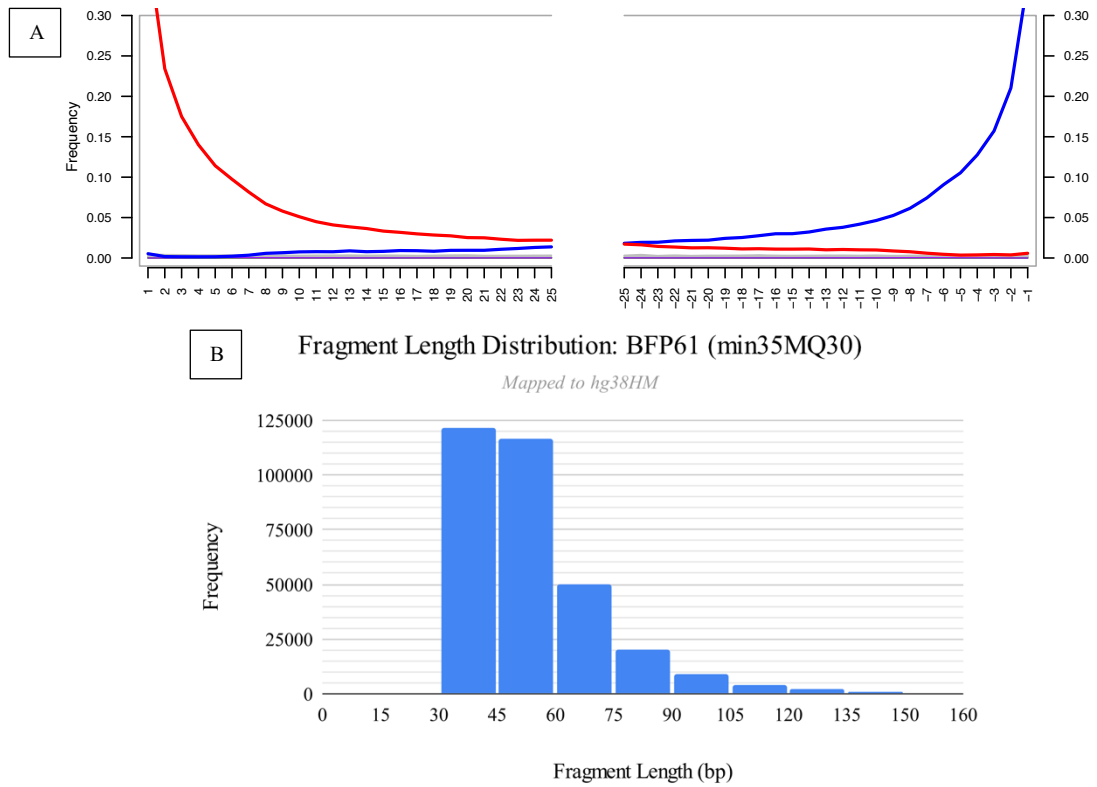


Figure S5.4: BFP61 mapped to the masked human reference genome hg38 (min35, MQ30). a) ancient DNA authentication using mapDamage. b) Fragment length distribution.

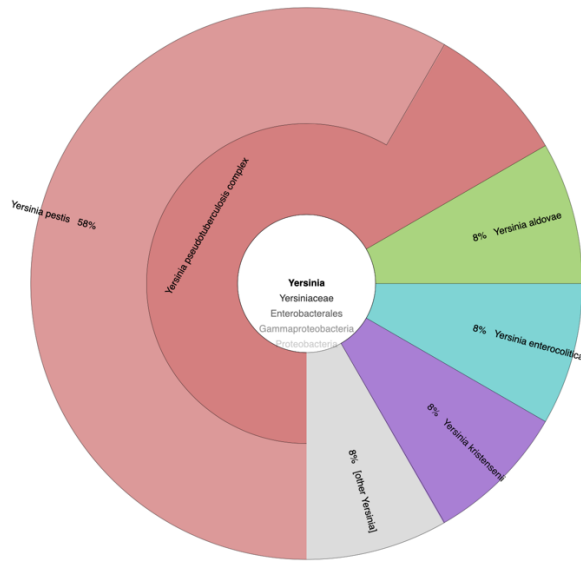


Figure S5.5: Krona plot of TFP14 showing the proportion of reads in the *Yersinia* genus. A total of 12 reads were classified as belonging to the *Yersinia* genus using Kraken 2. Of those reads, 7 were classified as *Y. pestis*, the most of any sample from the Historical Sites sample set. The 7 reads classified by Kraken 2 comprised 0.0003% of the total mapped reads in the sample.

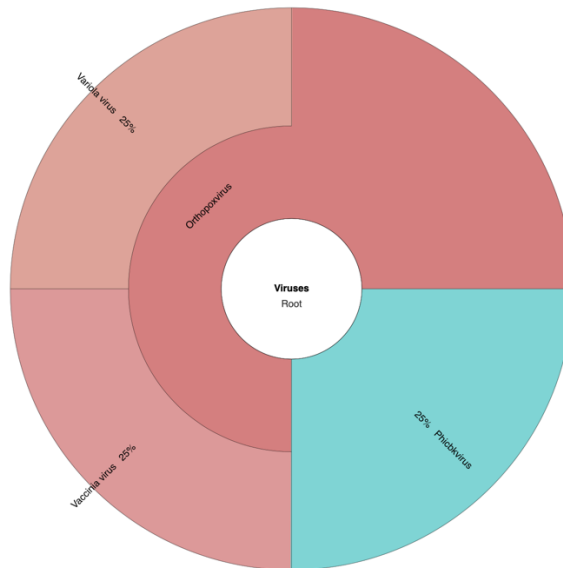


Figure S5.6: Krona plot of TFP58 showing the proportion of virus reads. A total of 3 reads were classified as belonging to the *Orthopoxvirus* genus using Kraken 2. Of those reads, 1 was classified as variola virus and another was classified as vaccinia virus. The 3 *Orthopoxvirus* reads classified by Kraken 2 comprised 0.0001% of the total mapped reads in the sample.

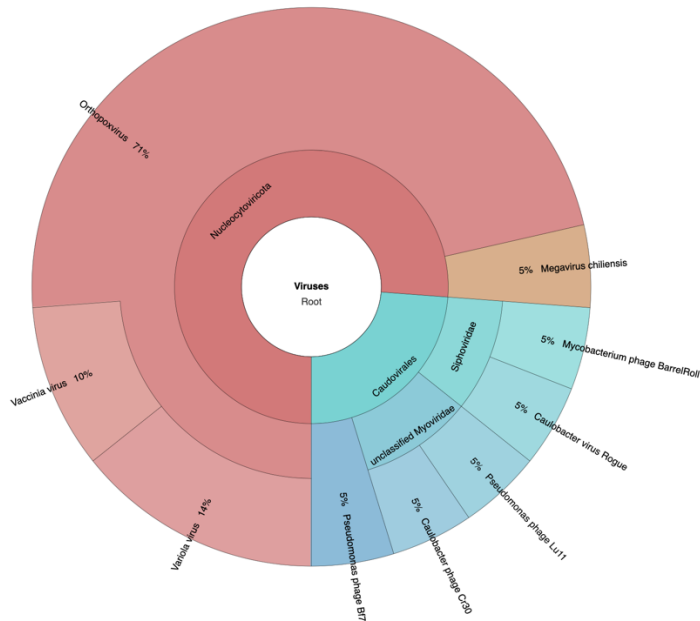


Figure S5.7: Krona plot of TFP06 showing the proportion of virus reads. A total of 15 reads were classified as belonging to the *Orthopoxvirus* genus using Kraken 2. Of those reads, 3 were classified as variola virus and 2 were classified as vaccinia virus. The 15 *Orthopoxvirus* reads classified by Kraken 2 comprised 0.0006% of the total mapped reads in the sample.

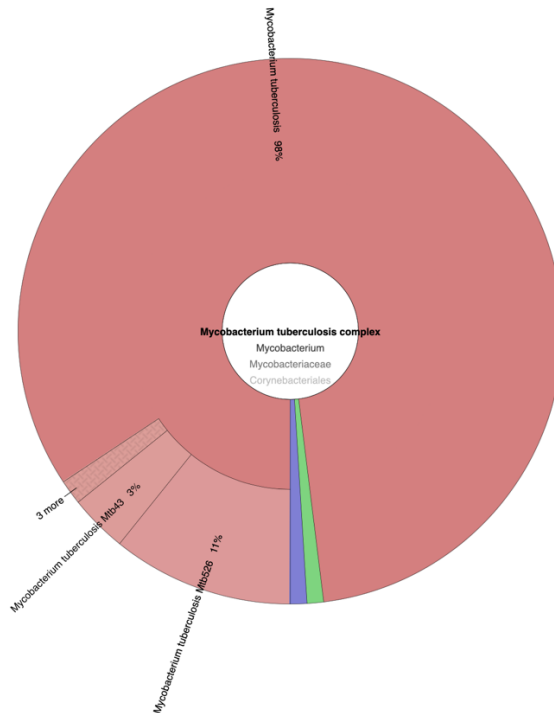


Figure S5.8: Krona plot of TFP13 showing proportion of reads in the *M. tuberculosis* complex. A total of 204 reads were classified as belonging to the complex using Kraken 2. Of those reads, 200 were classified as *M. tuberculosis*. These 200 reads classified by Kraken 2 comprised 0.005% of the total mapped reads in the sample.

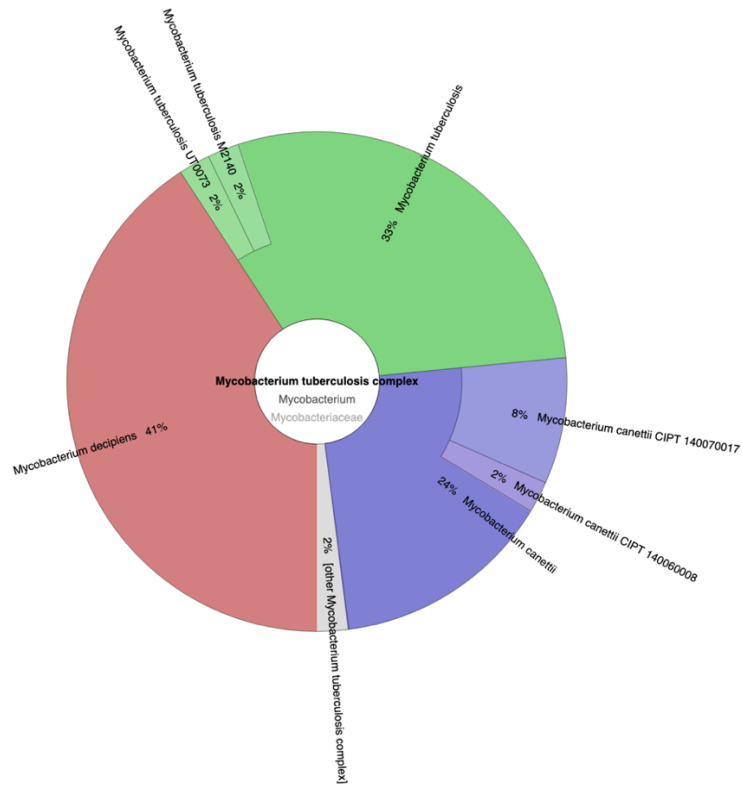


Figure S5.9: Krona plot of TFP50 showing proportion of reads in the *M. tuberculosis* complex. A total of 33 reads were classified as belonging to the complex using Kraken 2. Of those reads, 7 were classified as *M. tuberculosis*. These 7 reads classified by Kraken 2 comprised 0.0001% of the total mapped reads in the sample.

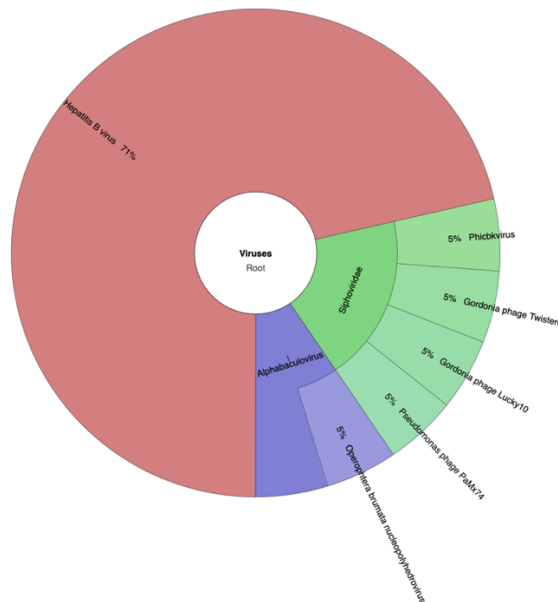


Figure S5.10: Krona plot of TFP39 showing proportion of virus reads. A total of 15 reads were classified as hepatitis B virus using Kraken 2. These 15 reads classified by Kraken 2 comprised 0.0002% of the total mapped reads in the sample.

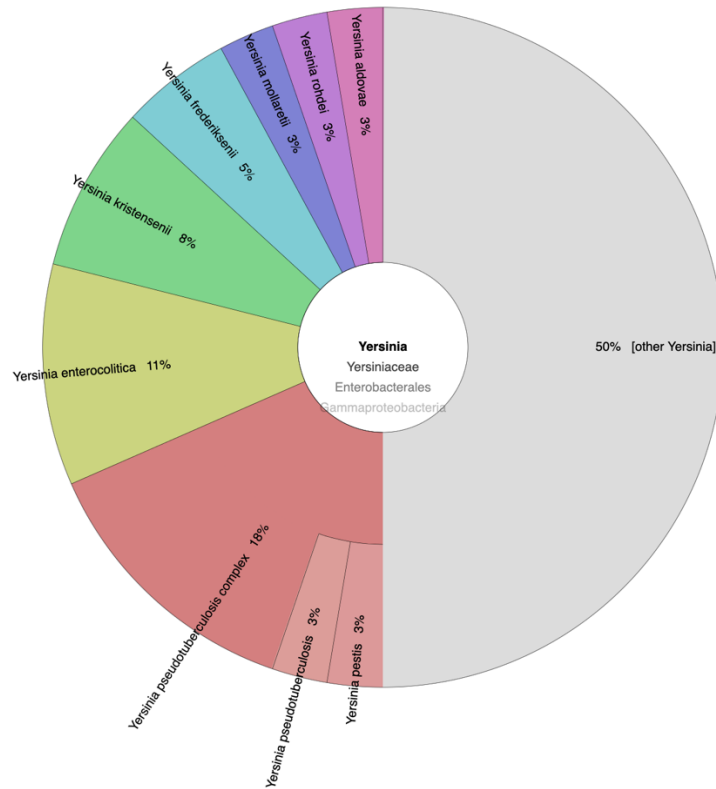


Figure S5.11: Krona plot of CS-BFP39 showing proportion of reads in the *Yersinia* genus. A total of 38 reads were classified as belonging to the *Yersinia* genus using Kraken 2. Of those reads, 1 was classified as *Y. pestis*. The reads classified as belonging to the *Yersinia* genus by Kraken 2 comprised 0.0003% of the total mapped reads in the sample.

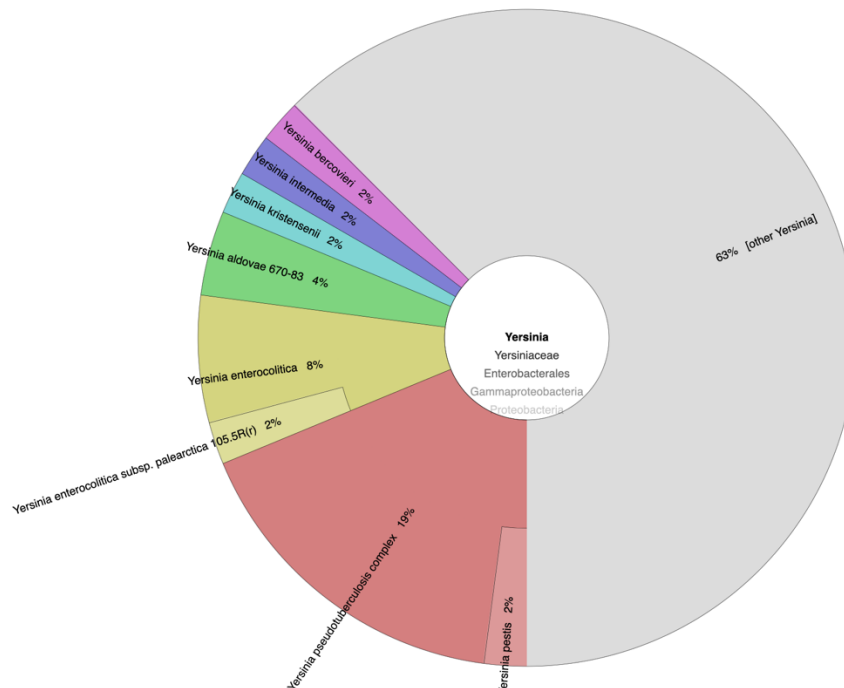


Figure S5.12: Krona plot of ME-BFP39 showing proportion of reads in the *Yersinia* genus. A total of 48 reads were classified as belonging to the *Yersinia* genus using Kraken 2. Of those reads, 1 was classified as *Y. pestis*. The reads classified as belonging to the *Yersinia* genus by Kraken 2 comprised 0.0005% of the total mapped reads in the sample.

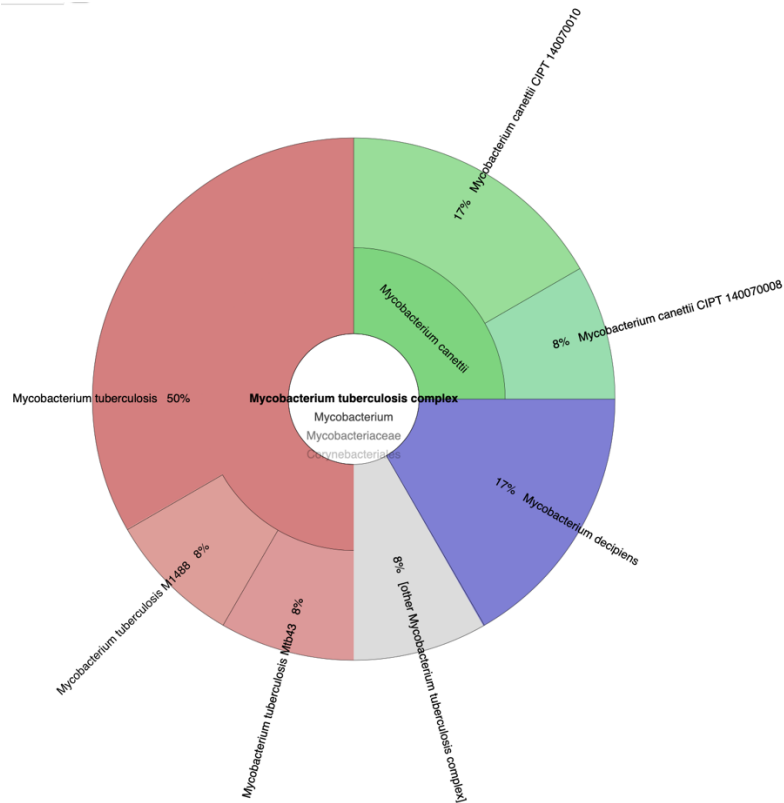


Figure S5.13: Krona plot of BFP18 showing proportion of reads in the *M. tuberculosis* complex. A total of 12 reads were classified as belonging to the complex using Kraken 2. Of those reads, 6 were classified as *M. tuberculosis*. These 6 reads classified by Kraken 2 comprised 0.002% of the total mapped reads in the sample.

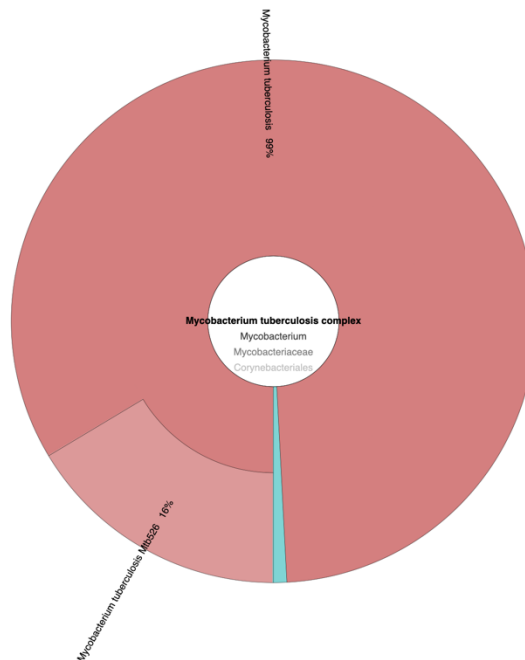


Figure S5.14: Krona plot of BFP55 showing proportion of reads in the *M. tuberculosis* complex. A total of 122 reads were classified as belonging to the complex using Kraken 2. Of those reads, 121 were classified as *M. tuberculosis*. These 121 reads classified by Kraken 2 comprised 0.006% of the total mapped reads in the sample.

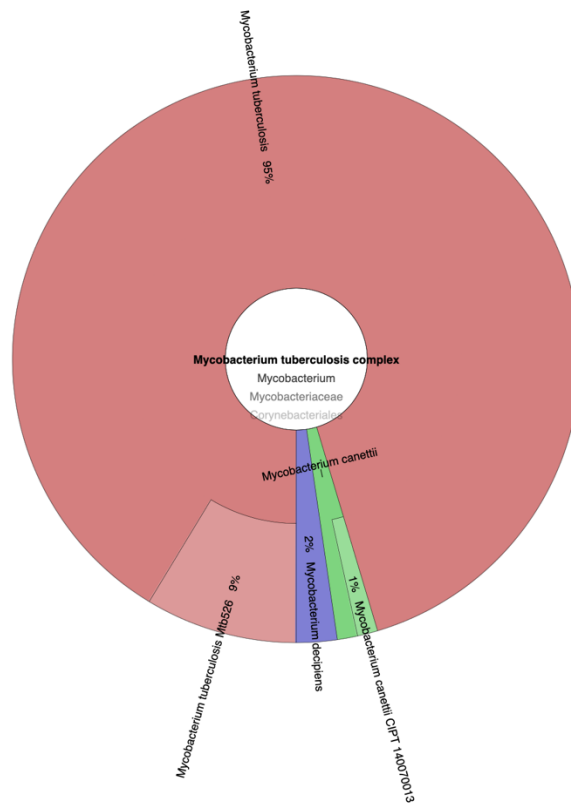


Figure S5.15: Krona plot of BFP61 showing proportion of reads in the *M. tuberculosis* complex. A total of 173 reads were classified as belonging to the complex using Kraken 2. Of those reads, 165 were classified as *M. tuberculosis*. These 165 reads classified by Kraken 2 comprised 0.003% of the total mapped reads in the sample.